ALMA MATER STUDIORUM – UNIVERSITY OF BOLOGNA

CAMPUS OF CESENA

DEPARTMENT OF ELECTRICAL, ELECTRONIC, AND INFORMATION ENGINEERING "GUGLIELMO MARCONI" – DEI

SECOND CYCLE DEGREE IN
BIOMEDICAL ENGINEERING FOR NEUROSCIENCE

POSTURE EVALUATION AND REHABILITATION IN PERSONS WITH PARKINSON'S DISEASE USING WEARABLE SENSORS

Graduation thesis in
Ageing and Rehabilitation Engineering

Supervisor

Prof. Lorenzo Chiari

Candidate

Giorgia Faggi

Co-Supervisor

Luca Palmerini

Ilaria D'Ascanio

Giovanna Lopane

Silvia Imbesi

Session III

Academic Year 2022-2023

CONTENTS

THESIS STRUCTURE

The first chapter of the thesis introduces two fundamental topics: Parkinson's disease and inertial sensors. It outlines the nature of Parkinson's disease along with motor and non-motor symptoms, as well as pharmacological treatments and deep brain stimulation. The patient evaluation process in the clinical environment is also addressed, using scales such as Hoehn and Yahr or MDS-UPDRS, highlighting the subjectivity of this clinical rating scales and the importance of using wearable devices to obtain a more objective evaluation. Moreover, the chapter provides a detailed analysis of wearable inertial sensors, and their main components. Finally, it defines the purpose of this thesis work.

In the second chapter, the use of wearables in clinical evaluation is addressed. It outlines the procedures for assessing the posture of Parkinson's patients in clinical settings, with particular focus on the motor protocol performed before deep brain stimulation surgery (pre-DBS monitoring). Among the various tasks included in the pre-DBS protocol, the study is specifically focused on the task of quiet standing which analyses postural oscillations (sway). The chapter concludes by presenting the results related to posture parameters extracted by a single inertial sensor placed on the lower back during 30 sec quiet standing performed before and after levodopa intake.

The third chapter focuses on the use of biofeedback rehabilitation systems individuals with postural problems (e.g., Pisa syndrome). An explanation of the biofeedback system and its components is provided. In addition, the state of the art of biofeedback system used in rehabilitation is outlined. The bibliographical research considers the analysis of several case studies, including healthy subjects, Parkinson's patients, and amputees. In addition, the previous project PASSO was presented which deals with rehabilitation training for subjects affected by the syndrome of PISA and camptocormia. Specifically, this thesis starts from the PASSO project to make an improved version to be used both in the clinic settings and as a home training program.

To evaluate the effectiveness of rehabilitation using wearable sensors, the following activities were carried out in collaboration with Chiara Pirini (master student):

- Development of an application prototype called "myPosture" that allows subjects to perform a training program outside clinical settings while clinician can configure specific parameters for the treatment and monitor their progress later.
- Creation of a complementary filter-based algorithm to process real-time subject inclinations.

- Validation of the developed algorithm using a stereophotogrammetric system as reference. Several tests were conducted to determine the optimal position of the sensor.
- Test of the system recruiting three subjects to receive feedback about the device and the training program.

In the fourth chapter, the conclusions and future development are discussed.

CHAPTER 1- INTRODUCTION

Impaired postural control is common in Parkinson's disease (PD) and worsens with disease progression, despite drug treatments. This postural instability is one of the most debilitating features of the PD and leads to difficulties in postural transitions, the initiation of movements, gait disorders and independence in daily life, as well as the main cause of falls. Clinical assessment scales, commonly used to assess PD-associated equilibrium disorders, are known to be subject to subjective bias, poor reliability, and insensitivity. The use of new technologies and protocols using inertial wearable sensors has contributed greatly to the clinical analysis of these patients, and in recent years such devices have also been used for rehabilitation purposes.

1.1 Introduction to Parkinson's disease

In 1817, James Parkinson first described Parkinson's disease (PD) by publishing his "Essay on the Shaking Palsy" in which he described six patients who displayed the clinical features of what we now recognize as PD. PD is the second most common neurodegenerative disease after Alzheimer's disease (AD), with a prevalence of approximately 0.5–1% among those 65–69 years of age, rising to 1–3% among persons 80 years of age and older [1], [2], [3].

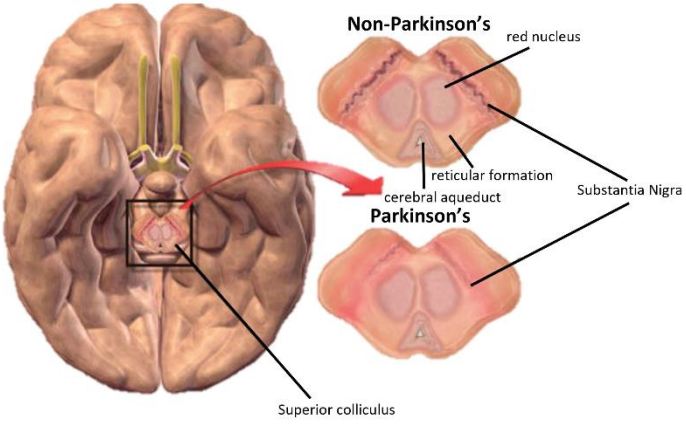

Figure 1 How Parkinson's disease originates. Figure from [4]

PD is a multi-systemic neurodegenerative disorder that affects the human nervous system, specifically the hallmark is the decline of dopamine-producing ("dopaminergic") neurons in the substantia nigra region of the midbrain [1]. Approximately 50 percent of neurons are lost before patients manifest first motor symptoms [1]. Dopamine is essential for sending messages to control and coordinate movement. It acts as a messenger between the substantia nigra and the striatum, an area of the brain responsible to control smooth movements [1], [4]. Neurodegeneration is not limited only to the nigral dopaminergic neurons but also involves cells located in other regions of the neural network [3]. Such a widespread pathology makes PD a very disorder with heterogeneous symptoms manifestation. A reliable diagnostic test for it is not yet available [3].

Parkinson's disease is a common neurological disorder with a significant impact on society, individuals, and families. PD is a multifactorial disease, with both genetic and environmental factors playing a role [3].

Age is the biggest risk factor for PD, although it can manifest at any age; it is unusual in person under 30 years, only 10% of cases start before 40 and the median age of onset being 60 years of age [3], [5].

Globally, the incident number of PD was $1{,}081.72 \times 10^3$ in 2019, and it increased with an annual average of 0.61% from 1990 to 2019 [6]. Ray et al. in 2018 applied worldwide prevalence data from 2014 meta-analysis to projections of the world's future PD population and the incidence is about 12,9 million people that will be affected by 2040 [7].

Compared to female patients, male patients had a larger incident number, and a higher increasing trend in ASIR (EAPC = 0.80, 95% CI: 0.75–0.85) [6]. Among the age groups, the high incidence numbers of PD were observed in the patients aged over 65 years, and the largest increasing percentage occurred in the age group of over 80 years (221.67%) [6]. Additionally, there are cross-cultural variations, with higher prevalence reported in Europe, North America, and South America compared with African, Asian, and Arabic countries [3].

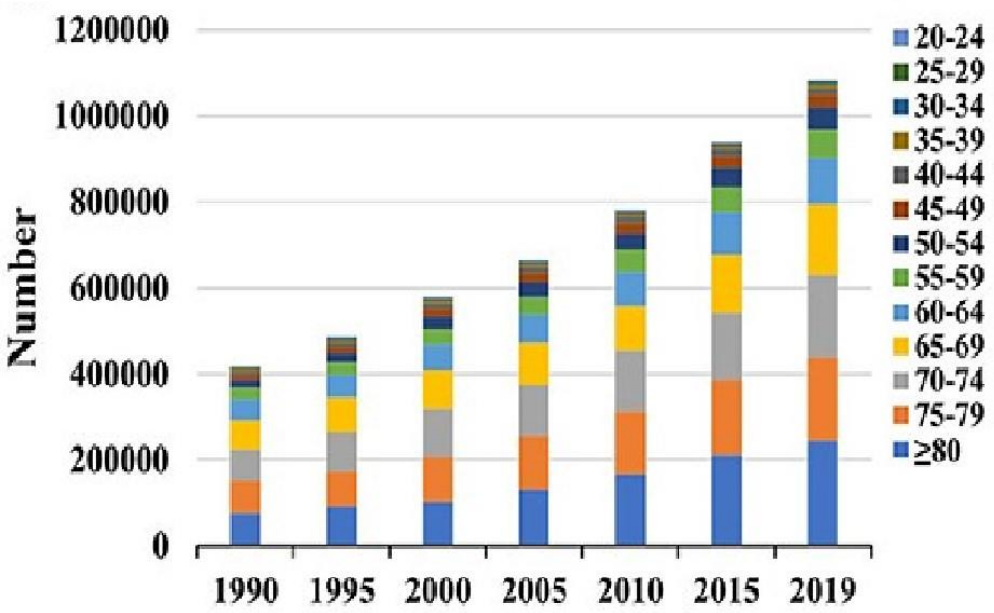

Figure 2 The distribution of Parkinson's disease incidence number in age groups, regions from 1990 to 2019 [6].

1.2 Parkinson's symptoms

Parkinson's disease is a complex progressive neurodegenerative syndrome affecting movement and gait function in early to mid-stages of the disease, and cognitive function in the later years of the disease [1], [3]. As illustrated in Figure 3, the motor symptoms can be manifest 10-20 years before the actual clinical diagnosis.

Many of the motor symptoms can be treated with medications and procedures that active dopamine receptors within the brain [1]. As treatments for PD have advanced and people are living longer with the condition, there is a greater awareness of the long-term treatment complications, and the "non-motor" symptoms can arise [1].

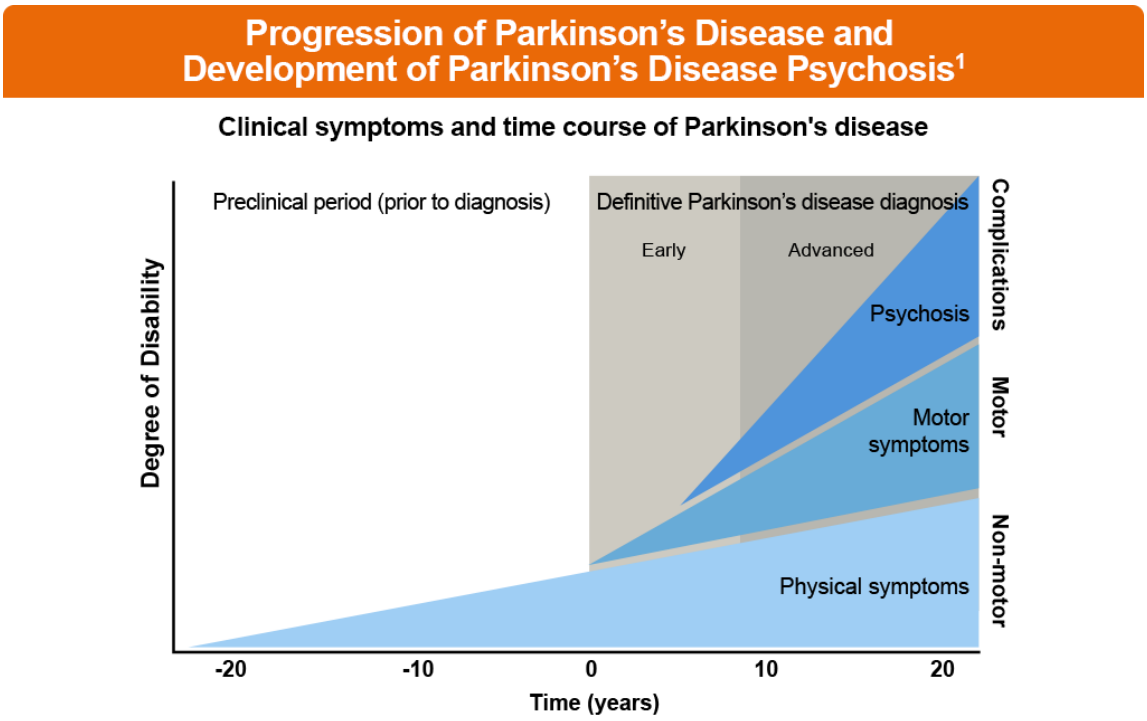

Figure 3 Representation of the different symptoms during the disease evolution. [8]

1.2.1 Motor-related symptoms

The cardinal clinical features of PD are tremor at rest, rigidity, bradykinesia and postural instability [9]. In addition, flexed posture and freezing (motor blocks) have been included among classic features of parkinsonism, with PD as the most common form [1], [9].

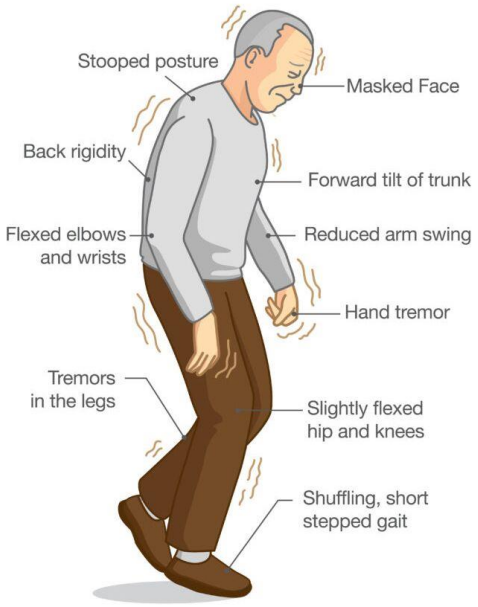

Figure 4 Representation of the motor symptoms in PD subjects [10]

- *Resting Tremor*

Rest tremor is the first symptoms in 70% of Parkinson's disease patients and an easily recognised symptom of PD [11]. Tremors are unilateral (asymmetric) at disease onset and worsen with anxiety, contralateral motor activity [[11]. It occurs at a frequency between 4 and 6 Hz, and almost always is prominent in the distal part of an extremity (e.g hand). Resting foot tremor is much less common than hand tremor [9], [11].

- *Rigidity*

Rigidity is one of the most frequent initial manifestations of PD [9]. The body posture becomes stooped, there is axial and limb rigidity. The tendency to a shuffling gait and lack of arm swing while walking may sometimes be accompanied by the cogwheel phenomenon [12]. Increased rigid resistance is also noticeable during the passive joint movement that is uniform throughout the whole motion range. Rigidity may also radiate proximally such as onto neck, shoulders, hips and distally onto wrists and ankles. It can even be enhanced by contralateral motor activity or mental task performance [9], [11].

- *Bradykinesia*

The term bradykinesia literally means “slowness of movement” [1] and it is the most disabling symptom of early Parkinson's disease [11]. It is a combination of slow movements that are of small amplitude and the absence of movement in expected situations (reduced arm swing while walking). It initially manifests by difficulties with fine tasks (e.g. handwriting) [1], [11]. The examples of bradykinesia include fascial masking, hypophonic speech, decreased eye-blink frequency, lack of hand-gesturing when speaking and changes in gait such as dragging a leg, or diminished arm swing [1].

- *P*ostural instability

Postural instability, due to loss of postural reflexes, and gait abnormalities are rarely prominent early in the course of Parkinson’s disease [9], [11].

Gait becomes slower, with shuffling, and turning is characterized by stiffness [11]. Postural instability, along with freezing of gait (e.g. difficulty initiating gait, gait hesitation on turning, or arriving at a real or perceive obstacle), is the most common cause of falls and contributes significantly to the risk of hip fractures [9], [11]. Several other factors (parkinsonian symptoms) also influence the occurrence of postural instability in patients with PD, such as orthostatic hypotension, age related sensory changes, ability to integrate visual, vestibular and proprioceptive sensory input (kinaesthesia) [9].

- *Pisa syndrome*

In function of the progression of the motor symptoms, the patient with PD may present abnormalities such as camptocormia and Syndrome of Pisa [13]. Pisa syndrome is defined as a lateral flexion of the trunk of more than 15° that increases during walking; it can be associated or not with rotation, which can be almost completely corrected with passive mobilization or in the supine position [13], [14]. The lateral deviation of the spine with a corresponding tendency to lean to one side, is one of the most common postural deformities. The lateral flexion of the trunk is also known as “scoliosis of parkinsonism” [14]. The medical treatment for truncal postural abnormalities, like camptocormia and Pisa syndrome, is often difficult [15].

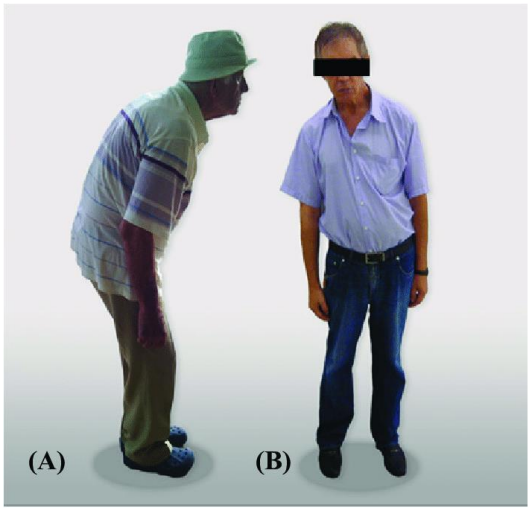

Figure 5 Patient with Parkinson's disease and presence of Camptocormia (A) and Pisa Syndrome on the right (B). (Photos published with patients' consent) [13] .

- *Secondary motor symptoms*

Patients with PD may exhibit a number of secondary motor symptoms that may impact on their daily living at home, at work and while driving [1], [9].

- The freezing of gait (FOG), it is a motor block where an intended movements fails which prevents the patient from walking or moving for seconds to minutes;
- Micrograph, contraction of the patient's fist;
- Lack of facial expression;
- Festination is when subjects starts an uncontrollable acceleration in the march in order to maintain their equilibrium.

1.2.2 Non-Motor Symptoms

Patients with PD may have a wide variety of non-motor symptoms, they are a common in early stage and underappreciated feature of the disease [1], [3], [9]. The non-motor symptoms are categorized into disturbances in autonomic function, sleep disturbances, cognitive and psychiatric disturbances, and sensory symptoms [12]. Moreover, non-motor symptoms contribute significantly to overall disability and quality of life for patients with PD [1].

- Neuropsychiatric non-motor symptoms/Mood disorder

The mood disorders include depression, anxiety, and apathy [1]. The depression and anxiety are other common symptoms in PD [12]; depression has a prevalence of approximately 35%, although higher rates are often seen in later disease stages [1]. Depression and anxiety may relate to several factors, including advancing disease severity. Anxiety and depression may disappear with dopaminergic treatment but may be persistent or recur in the long clinical course of the disease [12].

- Cognitive impairment

Cognitive deterioration and dementia are common in PD and may occur early or at a later stage [12]. Cognitive impairment in Parkinson's disease may affect any number of cognitive domains, particularly executive function, psychomotor speed, memory, visuospatial processing, and attention [1]. Progression of the dementia shows a correlation with spread of the neuropathological changes to cortical brain structures. Age has been associated with incident dementia in PD [12].

- Sensory abnormalities

Sensory symptoms such as olfactory dysfunction, pain, paresthesia, pain-associated restlessness (akathisia), oral pain and genital pain are frequent but are often not recognised as parkinsonian symptoms. Olfactory dysfunction (hyposmia) may be an early marker of PD, it is related to either neuronal loss in the corticomedial amygdala or to decreased dopaminergic neurons in the olfactory bulb [9], [12]. Pain is reported by 40–85% of patients, the most common is the limb pain and it may be the presenting symptom and misdiagnosed as a frozen shoulder or degenerative spine disease [12].

- Sleep disorder

Sleep-related disorders are frequently experienced by PD patients. They may be primary related to the disease or secondary to medication [1]. A variety of sleep disorders may appear with approximately two third of patients affected, such as periodic limb movement disorder (PLMD), rapid eye movement (REM) behaviour disorder, restless legs syndrome and excessive daytime

sleeping [1], [16] [12]. Insomnia, particularly sleep fragmentation, is also frequent (>50% prevalence), but the occurrence is highly variable among patients [9].

- Autonomic non-motor symptoms

Autonomic dysfunction may present prior to the diagnosis or become apparent with disease progression or be induced by medication [12]. The autonomic failure may be the presenting different features, that include orthostatic hypotension, sweating dysfunction, sphincter dysfunction and erectile dysfunction [9].

The othostatic hypotension affects 30-40% of patients, it is defined as a dall in systolic blood pressure or in dyastolic one. Assuming the upright posture, hypotension-induced hypoperfusion of the brain can result in dizziness, visual disturbances and impaired cognition that may precede loss of consciousness [12].

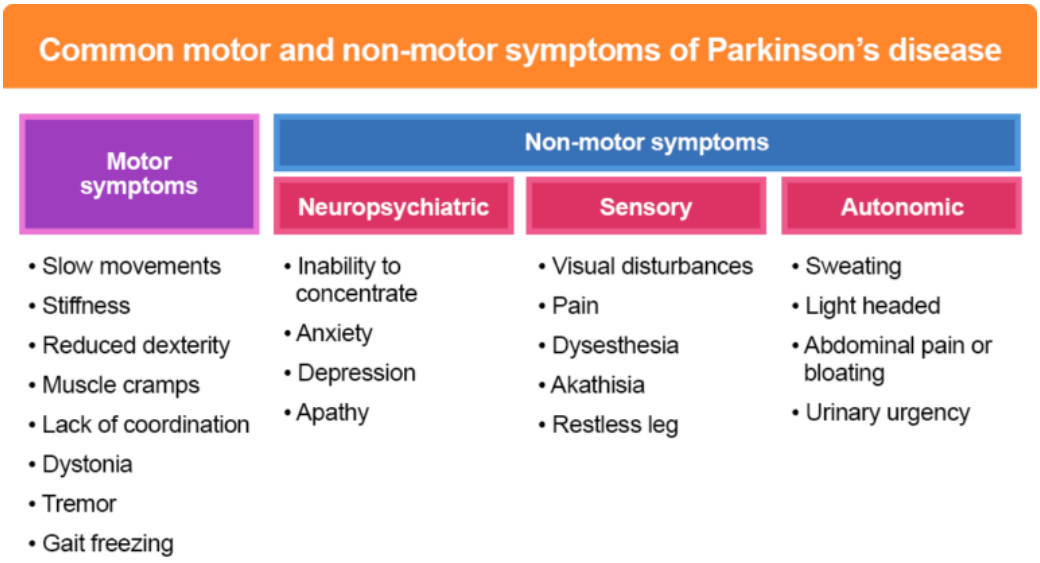

Figure 6 Scheme of the common motor and non-motor symptoms of Parkinson's disease [8].

1.3 Medical treatment

Parkinson’s disease is the only neurodegenerative disorder for which a meaningful treatment exists [1].

The decision to initiate treatment for early PD is made in collaboration with the patient. When symptoms affect the quality of life, the ability to work or socialize, treatment is started [1], [17]. When motor symptoms limit everyday activities, treatment is necessary to maintain a desired level of function [1]. Unlike other neurodegenerative diseases, idiopathic Parkinson's disease has effective treatments that mitigate symptoms. Medications can improve day-to-day function and, in cases where medication does not give a sustained benefit or has significant side effects, treatments like deep brain stimulation result in improved quality of life [17].

1.3.1 Pharmacological treatment

Levodopa

Levodopa became the primary treatment for Parkinson's disease in the early 1960s [17]. It has been, and still is, considerably the golden standard therapy for PD especially in the early stages in treating motor symptoms of PD [1], [18]. L-Dopa (LD), is the direct precursor of dopamine (DA) and is a suitable prodrug as it facilitates CNS penetration and delivers DA [18].

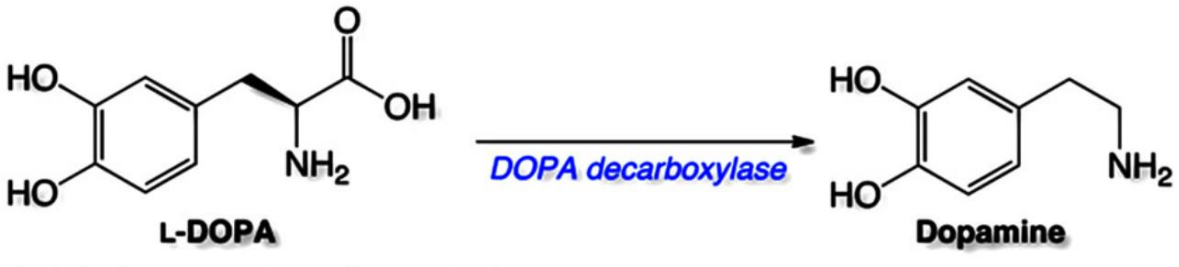

Figure 7 L-dopa is a dopamine precursor that can be converted in the CNS to dopamine [19].

It is converted within the brain to dopamine by DOPA decarboxylase. Levodopa is usually combined with carbidopa to prevent its conversion to dopamine outside of the central nervous system, attenuating the side effects of nausea and hypotension and reducing the total amount of levodopa needed to produce symptom relief [1]. Nevertheless, chronic long-term treatment with LD causes motor complications (on-off phenomenon) in most patients. In addition, dyskinesia and dystonia may occur due to excess dopaminergic tone [18]:

- The dyskinesia is one of the most debilitating effects of levodopa therapy [20]. Dyskinesias are the intrusions of unwanted, involuntary movements and exist in two primary forms: choreiform dyskinesias (or simply as dyskinesia) and dystonic posturing [1]. The dyskinesias consist of random, curvilinear movements that affect the limbs, head and neck, or trunk [1]. They tend to momentarily intensify when the patient attempts to speak or move, also anxiety may also heighten the effect [1].
- As well as dyskinesia, also dystonia is another important motor symptom in PD which depends on levodopa therapy. It is the state when a limb or body part assumes a particular posture due to the involuntary co-contraction of antagonistic muscles frequently accompanied by abnormal movements, postures or both. [1], [12]. This may rarely be a prediagnostic symptom in PD, but dystonic symptoms are mostly related to treatment [12]. In particular, the dystonia is typically a low-dose effect, often presenting as a morning phenomenon with foot inversion and toe flexion upon awakening [1].

The main Parkinson's motor symptoms, bradykinesia, rigidity, and tremor are generally improved by assuming levodopa treatment (or other dopaminergic medications) multiple times during waking hours. Typically, the daytime of a Parkinson's subject is subdivided in two conditions: ON and OFF. During ON periods the motor functions are improved, the symptoms are relieved, while during OFF periods the Parkinson's symptoms re-emerge and the motor abilities decline. Transitions between ON and OFF periods are referred to as *motor fluctuations*. The beneficial effects of levodopa are usually assessed by testing subject's motor performance in two different conditions: without medication (MED OFF) and with medication (MED ON) [21], [22]. Generally, patients with PD tolerate carbidopa/levodopa well [1].

Dopamine agonists

Dopamine agonists (e.g. pramipexole, ropinirole) stimulate dopaminergic receptors in the central nervous system, which alleviate symptoms of Parkinson [17]. They provide a viable alternative or adjunct to levodopa therapy in Parkinson's disease and are associated with fewer motor complications and dyskinesia; many clinicians choose a dopamine receptor agonist as first-line monotherapy, particularly in patients with a younger age of PD onset [23]. Dopamine agonists have the potential to cause the following adverse effects: nausea, somnolence, compulsive behaviours, hallucinations, orthostatic hypotension, and peripheral oedema.

Comt and mao-b inhibitors

COMT inhibitors are an alternative to increasing levodopa doses or adding dopamine agonists to reduce "off" time and enhance motor function in fluctuating PD patients [24]. COMT mediates peripheral catabolism of levodopa. Therefore, agents that block COMT, such as tolcapone and entacapone, increase the elimination half-life of levodopa [25].

1.3.2 Deep Brain Stimulation

The management of advancing Parkinson's disease has been dramatically changed since the introduction of deep brain stimulation surgery in 1987 [1]. Its efficacy and safety have been demonstrated in numerous controlled trials; the effects are sustained over time and are superior to those from medication alone [1].

The DBS system is a permanent, surgically implanted system with three main components: an implanted pulse generator (IPG) that is sometimes called a "neurostimulator" or "battery", a stimulation electrode leads implanted into the brain target, and a lead extension that connects the two [1].

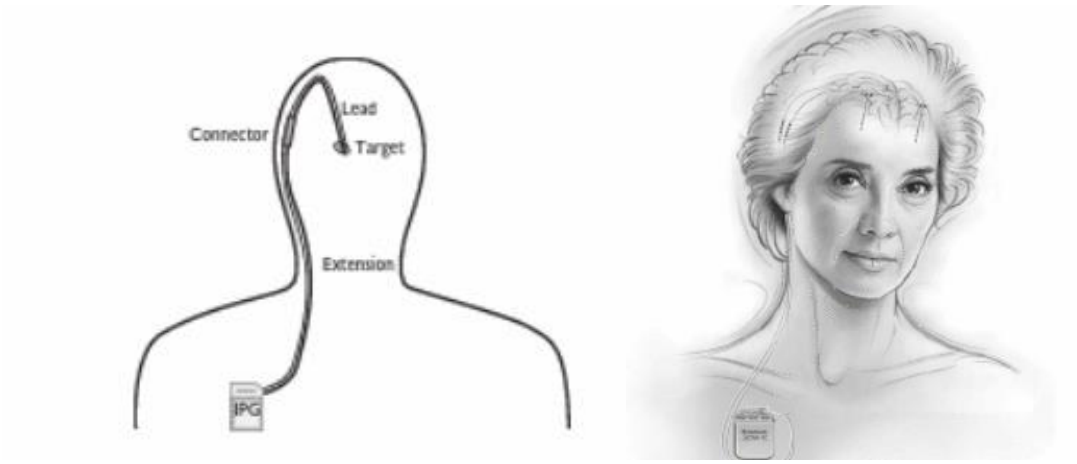

Figure 8 DBS system components: lead, connector, extension, and IPG (implanted pulse generator) [1]

The central lead is implanted into a target, typically the subthalamic nucleus or the globus pallidus interna, the extension is tunnelled underneath the scalp's skin from the lead's proximal end anchored to the external surface of the skull to the IPG, which is implanted subcutaneously, most commonly in the subclavicular region [1].

DBS can improve the cardinal motor features of PD such as rigidity, bradykinesia, tremor, decrease "off" times, increase "on" time, reduce medication-related motor fluctuations as well as PD-associated dyskinesias and dystonia [1]. The system may even reduce of medication. Although it provides little improvement in motor functioning, it increases the "on" time without involuntary movements which see an implementation from 25% to 65-75%.

Also, rigidity and tremor improve approximately of 50-75%. In order to have it employed effectively, patients must be selected carefully [1].

The ideal DBS patient is relatively young (under 70-75), has been treated for 5-10 years with a clear response to levodopa, has developed motor fluctuations that compromise functioning, may spend a significant portion of the day in an "off" state, does not have severe comorbid medical conditions, is cognitively intact, and does not suffer from poorly controlled depression or anxiety [1].

1.4 Clinical evaluation

The severity of illness and disability in Parkinson's disease (PD) is due to the presence of both motor and non-motor symptoms [26]. There is strong evidence that motor and non-motor symptoms in persons with PD restrict their independence and social participation, leading to a low quality of life (QoL) for both patients and their caregivers [26]. Therefore, information about the QoL of those with PD as well as studies on the relationship between QoL and severity of disease are necessary for both research and clinical practice, to make informed health care and rehabilitation decisions [26].

1.4.1 Clinical rating scales for Parkinson's disease

To standardize clinical diagnosis for Parkinson's disease due to the variability with which the syndrome develops, different rating scales exist. There are different kinds of rating scales for evaluating the impairments and disabilities faced by PD patients, the most widely used are: Hoehn & Yahr (H&Y) and Movement Disorder Scale-Undefined Parkinson's Disease Rating (MDS-UPDRS) [26], [27], [28], [29], [30].

Hoehn and Yahr Scale

Hoehn and Yahr Scale was published in 1967 in the journal Neurology by Melvin Yahr and Margaret Hoehn [27].

Stages	H&Y	Modified H&Y
0	-	No signs of disease
1	Unilateral involvement only usually with minimal or no functional disability	Unilateral disease
1.5	-	Unilateral plus axial movement
2	Bilateral or midline involvement, without impairment of balance	Bilateral disease, without balance impairment
2.5	-	Mild bilateral with recovery on pull test
3	Mild to moderate bilateral disease; some postural instability; physically independent	Mild to moderate bilateral disease; some postural instability; physically independent
4	Severe disability; still able to walk or stand unassisted	Severe disability; still able to walk or stand unassisted
5	Wheelchair-bound or bedridden unless aided	Wheelchair-bound or bedridden unless aided

Figure 9 Hoehn & Yahr (H&Y) scale to rate PD disability level [29].

The H&Y is a scale compiled by neurologists based on the signs and symptoms that the patient reports. In evaluating the results of therapy, it is essential to consider not only the type of parkinsonism and its chief manifestations but also the extent of disability at the time of treatment and the rate of progression before and after the treatment. Each case is rated on an arbitrary scale (stages 0-5) based on the level of clinical disability [26], [30].

The stage 0 corresponds to no signs and no symptoms of the disease, first stage corresponds to a patient who is still autonomous in activities of daily living (ADL) and has a tremor or/and bradykinesia or/and rigidity on only one side of the body [26], [29]. Stage 5, on the other hand, corresponds to a dependent patient in all ADL and who is in bed or in a wheelchair [26], [29].

Movement Disorders Society-Unified Parkinson's Disease Rating Scale

The standard scale to evaluate the neurological state of the patients is the Movement Disorders Society-Unified Parkinson's Disease Rating Scale (MDS-UPDRS) [31].

The MDS-UPDRS structure is composed by four sections:

- Part I: Nonmotor Experiences of Daily Living

It consists of 4 items, assessing cognitive symptoms, mood, motivation, and the presence or absence of a thought disorder. Although helpful as a general screen, these items are inadequate to estimate the severity of dementia or depression.

- Part II: Motor Experiences of Daily Living

It is composed of 13 items, describing difficulties in performance of a number of activities of daily living such as bathing, dressing, using utensils, as well as any interference in functioning from impairments in walking as a result of tremor or of sensory symptoms. A limitation is the functional performance may change during “on” and “off” states. Because patients commonly perform certain daily activities during certain times or only during “on” periods, rating functional performance only during “on” or “off” states may be artificial and difficult for patients to answer accurately.

- Part III: Motor Examination

It made up of 14-item rating of motor signs based largely on items in the Columbia Disability scale. In addition to ratings of tremor and an assessment of facial and generalized bradykinesia, performance of several tasks is used to rate disease severity, including slowness noted while the patient is repeatedly tapping the index finger against the thumb, clenching and unclenching a fist, rising from a chair, and other tasks. The definitions of impairment with each task are straightforward, and the scale is reproducible. However, this motor scale does not consider any interference from dyskinesias or dystonias, which may downgrade motor performance in some patients.

- Part IV: Motor Complications

The last part rates complications of therapy. This includes questions about the duration, severity, and timing of dyskinesias and motor fluctuations and the presence or absence of anorexia, sleep disturbance, or orhostatic hypotension [32].

Each items have five response options with uniform anchors of 0 = normal, 1 = slight, 2 = mild, 3 = moderate, and 4 = severe (Table 1). Several questions in Part I and all of Part II are written as a patient/caregiver questionnaire, so that the total rater time should remain approximately 30 minutes [33].

Patient Name or Subject ID	Site ID	Assessment Date (mm-dd-yyyy)	Investigator's Initials
_____	___ ___ ___	_____ - _____ - _____	___ ___ ___

MDS UPDRS Score Sheet

1.A	Source of information	☐ Patient ☐ Caregiver ☐ Patient + Caregiver	3.3b	Rigidity– RUE	
			3.3c	Rigidity– LUE	
Part I			3.3d	Rigidity– RLE	
1.1	Cognitive impairment		3.3e	Rigidity– LLE	
1.2	Hallucinations and psychosis		3.4a	Finger tapping– Right hand	
1.3	Depressed mood		3.4b	Finger tapping– Left hand	
1.4	Anxious mood		3.5a	Hand movements– Right hand	
1.5	Apathy		3.5b	Hand movements– Left hand	
1.6	Features of DDS		3.6a	Pronation- supination movements– Right hand	
1.6a	Who is filling out questionnaire	☐ Patient ☐ Caregiver ☐ Patient + Caregiver	3.6b	Pronation- supination movements– Left hand	
			3.7a	Toe tapping– Right foot	
1.7	Sleep problems		3.7b	Toe tapping– Left foot	
1.8	Daytime sleepiness		3.8a	Leg agility– Right leg	
1.9	Pain and other sensations		3.8b	Leg agility– Left leg	
1.10	Urinary problems		3.9	Arising from chair	
1.11	Constipation problems		3.10	Gait	
1.12	Light headedness on standing		3.11	Freezing of gait	
1.13	Fatigue		3.12	Postural stability	
Part II			3.13	Posture	
2.1	Speech		3.14	Global spontaneity of movement	
2.2	Saliva and drooling		3.15a	Postural tremor– Right hand	
2.3	Chewing and swallowing		3.15b	Postural tremor– Left hand	
2.4	Eating tasks		3.16a	Kinetic tremor– Right hand	
2.5	Dressing		3.16b	Kinetic tremor– Left hand	
2.6	Hygiene		3.17a	Rest tremor amplitude– RUE	
2.7	Handwriting		3.17b	Rest tremor amplitude– LUE	
2.8	Doing hobbies and other activities		3.17c	Rest tremor amplitude– RLE	
2.9	Turning in bed		3.17d	Rest tremor amplitude– LLE	
2.10	Tremor		3.17e	Rest tremor amplitude– Lip/jaw	
2.11	Getting out of bed		3.18	Constancy of rest	
2.12	Walking and balance			Were dyskinesias present?	☐ No ☐ Yes
2.13	Freezing			Did these movements interfere with ratings?	☐ No ☐ Yes
3a	Is the patient on medication?	☐ No ☐ Yes		Hoehn and Yahr Stage	
3b	Patient's clinical state	☐ Off ☐ On	**Part IV**		
3c	Is the patient on Levodopa?	☐ No ☐ Yes	4.1	Time spent with dyskinesias	
3.C1	If yes, minutes since last dose:		4.2	Functional impact of dyskinesias	
Part III			4.3	Time spent in the OFF state	
3.1	Speech		4.4	Functional impact of fluctuations	
3.2	Facial expression		4.5	Complexity of motor fluctuations	
3.3a	Rigidity– Neck		4.6	Painful OFF-state dystonia	

Table 1 Movement Disorder Society–Unified Parkinson's Disease Rating Scale (MDS–UPDRS)

1.4.2 Quantitative evaluation using wearable inertial sensors

Clinical gait assessment is generally performed by examiner's observational impression or patient self-reporting. This visual observation and self-reporting suffers from subjectivity and imprecision [34], [35], [36]. For a quantitative assessment of gait and motor impairment, assessments take place in a 3-dimensional computerized gait laboratory [35]. Furthermore, the clinical evaluations (normally performed in a hospital, clinic, or physician's office) cannot capture the entire spectrum of a patient's symptomatology and not accurately reflect functional capacity in daily-life environments [37], [38]. The ideal mobility evaluation of Parkinson's disease should be instrumented and based on a continuous monitoring approach, that follows patients also in real-life conditions [38]. A promising solution for real-time monitoring is the use of wearable sensors [34]. Devices like wearable inertial sensors, force plates, insole pressure sensors, and portable electromyography (EMG) support the acquisition of gait signals that can be further processed and analysed for disease monitoring [34]. In this way, ambulatory monitors are used to quantify the daily walking and overall mobility in daily-life [35].

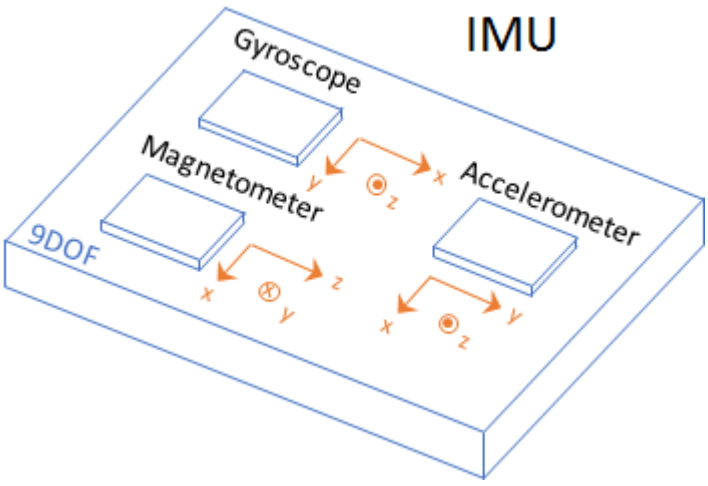

Figure 10 An IMU is an electronic device mounted on a platform. IMUs combine multiple sensors, which can include accelerometers, gyroscopes, and magnetometers. Axes orientation in Inertial Measurement Unit [39].

Recently, the healthcare system is trending towards early discharge to monitor and train patients in their own environment and provide personalized and patient-centric solutions [40], [41].

Inertial measurement unit (IMU) sensors are used in different aspects of human movement analysis, due to their small size, robustness and accuracy.

IMU systems are used to collect movement data in a more flexible and user-friendly manner, thanks to their easily deployed and the extended battery life. Moreover, they provide a lot of information and accurate 3D acquisition [42].

IMU sensors can be useful for people with Parkinson's disease, who particularly suffer balance and gait impairments that contribute to the increased risk of falls. The balance impairment affects both static and dynamic equilibrium. For PD individuals, it results crucial to assess their balance and gait impairments and monitor their changes after the treatment (pharmacological or surgical) [43]. For this purpose, the Timed Up and Go (TUG) test is usually performed during clinical monitoring. It is a clinical test to assess mobility in Parkinson's disease, that involves a series of tasks such as rising from a chair, walking 3 meters, turning, and sitting; the most used clinical outcome is the total duration. The instrumented TUG (iTUG) is usually performed using a single IMU, worn on the lower back. It records acceleration and angular velocity reached during the test, from which different quantitative motor parameters are extracted [44].

1.5 Motion Capture Systems

Human movement analysis aims at collecting quantitative information about the mechanics of the musculo-skeletal system during the execution of a motor task [45]. This analysis helps to identify the cause of altered movement patterns, assisting with prevention, identification, and rehabilitation of a wide range of diseases, disabilities, and injuries. Early identification plays an important role in combating disease progression, facilitating interventions, and it also improve rehabilitation using precise measurements of small changes in movement characteristics [46].

In motion analysis, three types of data can be measured:

- kinematic data: movement of body related to the position in space, speed, and acceleration of the body. These data are obtained using Motion Capture systems.
- dynamic data: forces and moments that generate the movement. This information is measured with the help of force plates.

- electromyographic data: electrical signals related to the activation of the muscles involved in the execution of a motor task. These data are recorded through electromyography (EMG).

Motion capture, or mocap, is an important method for studies in biomechanics and has traditionally been used to diagnose the patho-mechanics related to musculoskeletal diseases [47]. It is the process of recording a live motion event and translating it to usable mathematical terms by tracking several points in space over time [48].

As shown in Figure 11, motion capture systems are divided into two main categories [49]:

- The optical system (stereo-photogrammetry) operates without direct contact between the instrument and skin of subject. It consists of a set of calibrated and fixed cameras focused on the scene where the subject is moving. The subject's movements are calculated by processing the data acquired by the video cameras. The optical systems are divided into two types: marker-based and in marker-less [49].
- In contrast, the non-optical systems operate with direct contact between the sensor and subject skin, and they do not use the set of cameras. These systems are further differentiated in electromagnetic, electromechanical, and inertial mechanism [49].

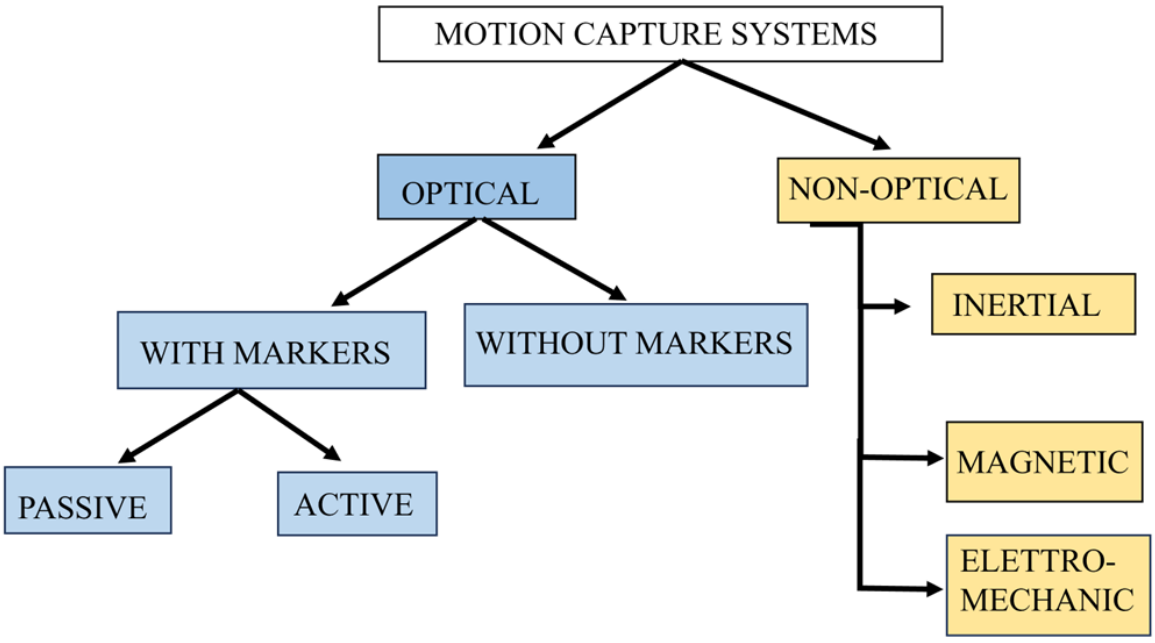

Figure 11 Diagram of motion capture system systems [49]

Several measuring instruments are currently available to accurately assess human motor performance. Video-motion sensing is the most important technology used to detect and track body motion using an external source (e.g., optical, magnetic, or acoustic) to determine position and orientation information of the moving object of interest. These sources are effective only over a relatively small working space; therefore, dedicated laboratory setups are necessary for the application of externally referenced sensing techniques [50]. Although these systems provide accurate position information with errors approximately 1mm, there are some drawbacks: the high costs and restricted measurement volume. The use of a dedicated laboratory with fixed equipment impedes many applications, like monitoring of daily life activities or assessment of workload in ergonomic studies [40].

Emerging inertial sensing and communication technologies are driving the innovation of a various application fields, such as fitness, healthcare, and rehabilitation therapy [41]. The capability of inertial sensors to detect their own motion without external source feature. Body-mounted sensors make it possible to determine position and orientation information based on the measurement of physical quantities (acceleration, angular velocity), which are directly related to the motion of the body part where they are placed. Inertial sensors are internally referenced, inertial sensors can detect and track body motion and orientation over an unlimited working space [37]. Given the capabilities of inertial sensors and in alignment with the thesis's project to collect movement data from Parkinson's subjects, the focus will be on wearable inertial sensors and their components.

1.5.1 Wearable inertial sensor

An Inertial Measurement Unit (IMU) quantify linear and angular motion in the three-dimensional space without external references. Using IMU data outputs, an Inertial Navigation System (INS) evaluates a body's position and orientation, in connection with a gravitational field model and the operation of a reference clock [37]. Recent progress in Micro-Electro-Mechanic Systems (MEMS) technologies have led to the development of a new generation of inertial sensors. These sensors are suitable for the application in biomedical field, thanks to their specifications in terms of dimension, robustness, power consumption, measuring performance and cost [37].

The main problem of inertial systems is that position and orientation are found by time-integrating signals from accelerometers and gyroscopes, also any sensor drift and noise superimposed to them. The velocity can be derived from the integration of the time domain acceleration data.

Then, a second integration can give the displacement, as a function of time.

Also, the orientation, obtained using micromachined gyroscopes, introduce an increasing error of a few degrees per second. This integration drift is mainly due to the fluctuations of the gyroscope offset and measurement noise. In addition, inertial sensors are not well-suited for determination of absolute position and orientation. In order to be accurate, the integration process needs to be started from accurately known initial conditions, which inertial sensors are unable to provide at all (position and velocity) or can provide to just a limited extent (orientation). So, the use of inertial systems is most efficacy in those applications which involve relative motion [50], [51].

Accelerometer

In the 1950s, the use of accelerometers to assess human body movement was proposed. These devices were expensive, bulky, and unreliable, therefore, unsuitable for ambulatory monitoring. In the last decade, has been occurred a revolutionary progression in accelerometers production, in terms of designed to satisfy the extremely stringent quality and reliability requirements of that industry, in addition to satisfying the demand for high-volume, low-cost manufacturing [52].

Accelerometers can measure both static (e.g. gravity) and dynamic (e.g. vibration) acceleration of the body or object they are attached to [52], [53]. Three accelerometers can be incorporated into a single device providing information on three-dimensional movement, known as a tri-axial accelerometer [52].

The basic principle of accelerometers is based on the detection of a mass's inertia when subjected to an acceleration. The configuration of seismic mass accelerometers for uniaxial measurements is represented in Figure 1. Inside sensor case, there is a mass connected to the base via an elastic element (characterized by an elastic constant k) and a damping element (with damping coefficient μ). Further, there is a sensor measuring the displacement of the mass relative to the case (referred to mass-case displacement). The case is rigidly fastened to the body whose acceleration has be measured [54].

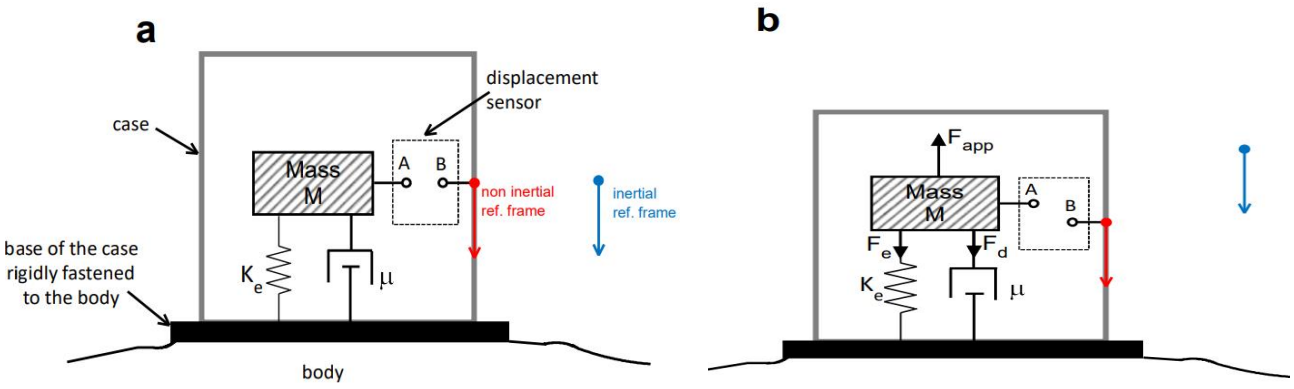

Figure 12 Configuration and principle of functioning of seismic-mass accelerometers. Panel a: Initial state with the system at rest and the mass M not displaced relative to the case. Panel b: The body (and the case rigidly attached to the body) is accelerating downward (positive direction) at acceleration $\ddot{x} = a$ relative to an external observer in the inertial reference frame. The mass M is displaced upward relative to the case, causing an elongation of the spring and damper by x. In the non-inertial reference frame (attached to the case), the fictitious force Fapp acting on the mass M appears, together with the actual forces Fe (elastic force) and Fd (viscous force) [54].

We can assume the system starts in a rest state (Figure 12a). In the Figure 12, the blue axis represents the uniaxial space coordinate in an inertial reference frame (Earth-fixed coordinate). Otherwise, the red axis representing the uniaxial space coordinate in a reference frame attached to the case of the accelerometer. When the body accelerates, the reference frame accelerates with it.

In the initial state, the body and the accelerometer are at rest, and the mass (M) is at rest relative to the case. In a subsequent state, the body and the attached case are accelerating in positive direction ($\ddot{x}\mathrm{i} = a\mathrm{i}$). Due to the inertia of the mass (M), it is subjected to a displacement relative to the case in the opposite direction to the acceleration of the body ($-x$). Hence, the mass M subjected to acceleration $-\ddot{x}$. For the non-inertial frame, of the motion M, the Newton's second law is applied.

To this aim, it is introduced an additional force called fictitious force (inertial forces). The fictitious forces (Fapp) acting on mass M is equal to $F\mathrm{app} = -Ma\mathrm{i} = -M\ddot{x}\mathrm{i}$. Of course, due to the displacement of the mass M relative to the case, also actual forces act on the mass, generated by the elastic and damping elements. Hence, we have:

$$Fe + Fd + Fapp = -M\ddot{x}$$

where $Fe = k_e x$ is the elastic force and $Fd = \mu\dot{x}$ is the viscous force acting on the mass.

$k_e x+\mu\dot{x}-M\ddot{x}_i=-M\ddot{x}$

$M\ddot{x}+\mu\dot{x}+k_e x=M\ddot{x}_i$

A single axis accelerometer allows the movement in one direction, that represent its sensitive axis. In order to measure the acceleration in all three spatial axes, three single-axis accelerometers are combined to form a tri-axial accelerometer. Otherwise, a 3D accelerometer can be constructed using a single mass., based on only one mass with three translational degrees of freedom [51].

The accelerometers can be categorized according to the physical principle that is used to detect the displacement of the moving inertial mass with respect to the fixed mass of the sensor. The most common devices are: piezoresistive, piezoelectric and variable capacitance [55], [56]. Within these, capacitive sensors are the most used for motion analysis.

Gyroscope

Gyroscopes are devices that measure angular motion of the body they are attached to. The construction of angular rate sensors is based on different designs including spinning rotor gyroscopes, laser gyroscopes and vibrating mass gyroscopes (Figure 13). In the human movement field, the most common design of gyroscope is the vibrating type. This type of gyroscope is small, inexpensive and have low power requirement [37], [51]. Different geometries are utilized, but each one is based on the principle of a vibrating mass undergoing an additional vibration due to the Coriolis effect [51].

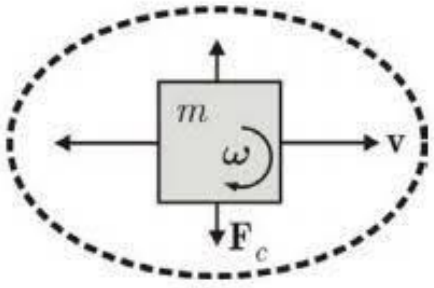

Figure 13 Vibrating mass gyroscope [55].

In the absence of rotation, the vibrating element embedded in the sensor vibrates continuously in a plane. In the presence of a rotation about an axis perpendicular to the vibration plane, the vibrating element deviates from its plane of vibration due to the Coriolis acceleration effect. The magnitude out of plane vibration is proportional to the rate of rotation [37].

The Coriolis force is an apparent force, perceived by an observer within the rotating reference system, where the principle of inertia does not apply. To understand the concept, imagine a rotating circular platform with angular velocity (ω) relative to an inertial reference system. When a body moves in uniform rectilinear motion from the centre to the edge of the platform, an observer attached to the inertial reference frame will see the body move in a straight way. However, when the observer was at the centre of the platform and was therefore integral with the rotating non-inertial frame of reference, the body deviating from the straight trajectory, in the opposite direction to that of rotation of the platform, as if it were subject to an external force: this force is the apparent force of Coriolis. Gyroscopes with vibrating masses exploit the inertia forces created by the motion of the sensor with respect to a non-inertial reference system [57].

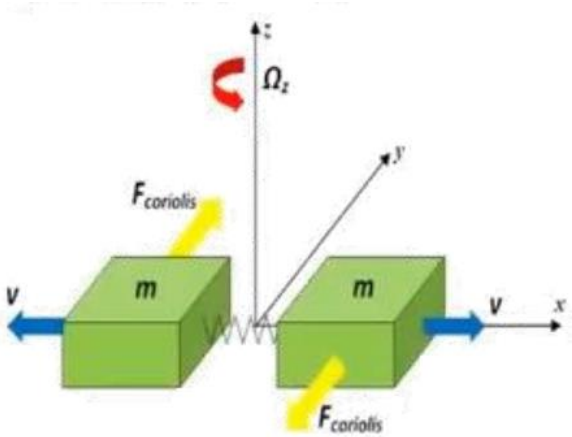

Figure 14 Vibrating mass gyroscope and the Coriolis Force. The mass m may move in the x-axis direction following a vibration imposed by the actuator. The gyroscope is rotated with an angular velocity ω along z-axis, it will experience, as a result of the Coriolis principle, a force in the direction indicated on the y-axis [53].

Therefore, the effect of the Coriolis force generates a mass displacement in perpendicular direction to the velocity of the mass itself. This displacement depends on the angular velocity ω to be measure.

The quantification of the Coriolis force allows to measure the angular velocity: a mass is implemented in the driving direction, while the angular velocity is detected in the perpendicular direction of sensing [58]. The displacement in the y direction is directly related to the angular velocity that we want to calculate.

The amplitude of the Coriolis force (Fc) depends on the vibrating mass (m), its velocity (v) and the angular velocity of the rotating frame (ω) by the following equation:

$$Fc = -2\, m\, \omega\, x\, v$$

Where m is the mass, v is momentary speed of the mass relative to the moving object to which it is attached and ω the angular velocity of that object.

Magnetometer

The magnetometer is the measure sensor of the Earth's magnetic field. Most of magnetic sensors are based on the Hall effect. The Hall element is a conductor, so the sensors rely on the production of an electric field across a material through which an electric current is flowing and where a magnetic field is acting. The force applied to the charge carriers by the electric field exactly balances a force from the magnetic field called the Lorentz force:

$$F = q\, v\, B$$

Where q is the electron charge, v is the speed of electron and B is the magnetic field [53], [59].

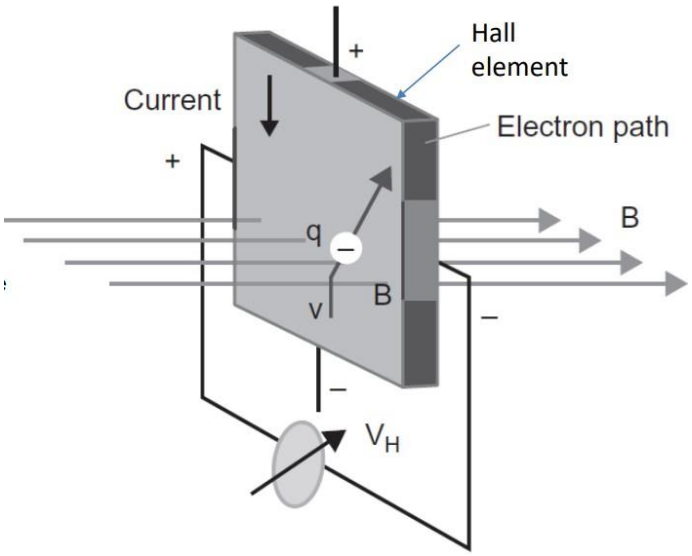

Figure 15 Magnetometer representation [53].

Other ways to sense magnetic fields use optical sensors that rely on the magneto-optical effect.

In recent years, magnetometers have been extensively used in a wide range of applications, including biomedical, automotive industry, robotics, and non-destructive material testing. In addition, the significant improvement in the performance of magnetic sensors, such as excellent sensitivity, high resolution, minimum detectable magnetic field, low power consumption, high stability, wide bandwidth, small size, low cost, and excellent linearity [60].

1.6 Aim

The aim of this thesis is to examine the posture of patients affected by Parkinson's disease. The thesis is structured into two distinct sections:

1) The primary objective concerns the posture analysis of individual with PD. To achieve this, data are recorded from Parkinsonian patients with wearable sensors. Specifically, the study focuses on assessing sway during the Quiet Standing task to observe and assess sway oscillations. Then, the data acquired during this test are analysed to compare potential differences in subjects' sway before and after medication intake.

2) The second objective, conducted in collaboration with Chiara Pirini (master student), is related to the development and testing of a biofeedback system for posture rehabilitation in Parkinsonian patients with Pisa syndrome and camptocormia. A previous project (PASSO) was revisited to enhance biofeedback features, such as vibrations and bandwidth, with the aim of optimizing the device and potentially using it not only in clinical settings but also for home-training. In order to optimize the device and the biofeedback system, a bibliographic research was conducted on the state of the art of wearable sensors used for rehabilitation purposes. Moreover, an algorithm was developed to identify the inclination angle that the subject adopts during a static training. In particular, the identified angles are related to trunk flexion and lateral bending typical of subjects with postural issues. The rehabilitation objective is to provide a biofeedback (vibration) on the opposite shoulder with respect to the involuntary inclination. Different sensor positions were evaluated to determine the best accuracy. Finally, the prototype system was tested by three subjects who evaluated it through a questionnaire.

CHAPTER 2 - POSTURE EVALUATION USING WEARABLE SENSORS

Evaluating Parkinson's disease (PD) patients is a complex task to be able to detect subtle signs. The evaluation is not only about the movements themselves but also about the effects of drugs and non-motors aspects [1]. Nowadays in the clinic, sensors are used to monitor mobility and extract quantitative gait parameters. These sensors integrate clinical rating scales (e.g., UPDRS), which provides an objective method for assessing the efficacy of treatment and the disease progression compared to clinical assessment. The use wearable of sensors offers a more precise and accurate way of evaluating the treatments (pharmacological or surgical) and the patient's motor impairment [38]. This type of analysis is a crucial in the advanced phase of the disease, such as in the evaluation of the DBS surgical procedure. In this thesis, the focus is on posture evaluation performed before the DBS surgery.

2.1 Methods

2.1.1 Clinical protocol

In order to assess if a patient is a suitable candidate for DBS, a standard clinical protocol (called pre-DBS monitoring) was defined at the "IRCCS Istituto delle Scienze Neurologiche" in Bologna (Figure 16). The ideal DBS patient is under 75 years, has been treated for 5-10 years with a clear respond to levodopa, has developed motor fluctuations that compromise functioning, may spend a significant portion of the day in an "off" state, does not have severe comorbid medical conditions, is cognitively intact, and does not suffer from poorly controlled depression or anxiety [1].

Figure 16 Description of pre-DBS monitoring, divided into two phases (MED OFF and MED ON) and the subsequent possible surgery.

Pre-DBS monitoring

The pre-DBS monitoring is subdivided into two phases, that correspond to two different medication (MED) conditions:

- MED OFF: the subject is not under the effect of dopaminergic medication that has not been taken since the previous night (12-h). The patient is evaluated in OFF state while performing some motor tasks monitored by wearable inertial sensors.
- MED ON: the subject is under the effect of dopaminergic medication. The patient is instructed to take his/her usual medication, which absorption is analysed a sequence of blood samples acquired every 15 minutes for three hours. The patient performs the same motor tasks as the previous MED OFF condition, about 60-75 min after taking the dopaminergic medication to evaluate the subject in his/her ON state.

Position Of Wearable Sensors

The clinical monitoring was conducted using 3 sensors produced by mHealth Technologies srl (Bologna, Italy), that included two IMUs attached to the subject's shoes using Velcro straps, and one IMU attached to the lower back using an elastic belt (Figure 17).

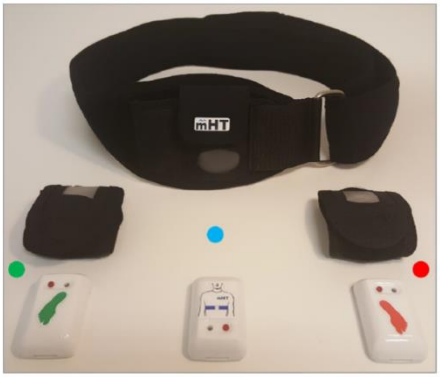

Figure 17 Set of three IMU sensors and belts were utilized during the clinical monitoring. The green and red dots represent the sensors placed on the shoes using Velcro straps, while the light blue dot represents the sensor placed on the lower back using the elastic belt.

The IMU sensors were placed before the motor tasks. Once they were positioned (Figure 18), they were connected to the dedicated smartphone application using bluetooth connection.

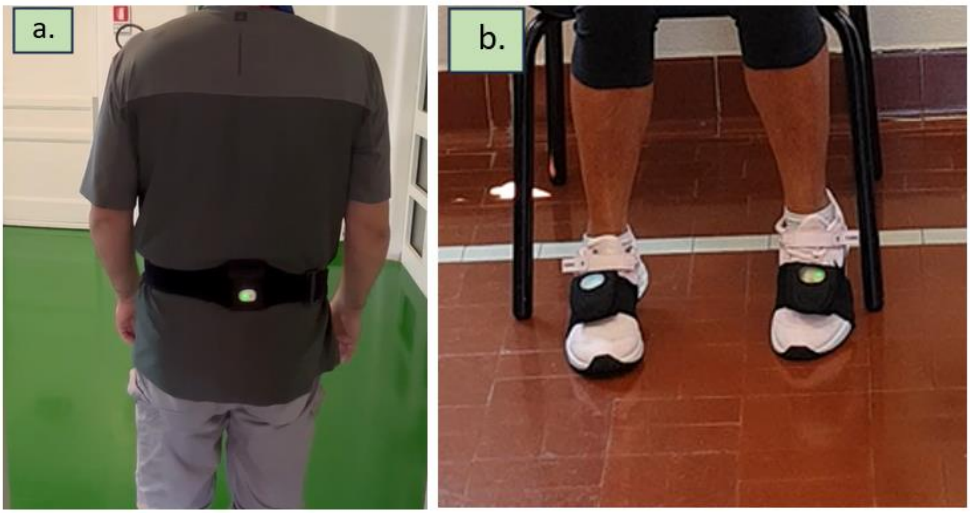

Figure 18 Inertial sensors positioning.

Motor tasks

During the clinical protocol six different motor tasks were performed in the two different medication conditions (MED OFF and MED ON):

1) Finger tapping test;
2) Timed Up & Go test;
3) Quiet standing test;
4) Full 360° turn clockwise and counterclockwise test;
5) 18 meters walking test;
6) Complex task;

Except for the finger tapping test and quiet standing test, all the motor tasks were performed in both single and dual tasks. In the single task, the subject only had to perform the motor exercise, while during the dual task condition the subject had to performs the motor exercise simultaneously with a backward count (e.g. subtraction 3 from an initial number like 50). Quiet standing was performed for 30 seconds with open and closed eyes.

1) Finger tapping test

The finger tapping test is performed using a computerized touch screen system with a dedicated app (mHealth Technologies srl, Bologna, Italy) [61]. The patient is seated on a chair in front of a table over which the tablet is placed. Two red buttons (20 cm apart) are visualized on the display (Figure 19).

The subject should press the buttons alternatively with the index finger of the most affected hand as many times as possible over a period of 60 seconds. The tap must be performed as accurately as possible.

The test result is provided as the number of taps performed in one minute. The device is also able to count the number of taps per button. This type of test has been widely utilised in neurophysiological examinations to assess upper extremity bradykinesia (slowness of movement) which is a core clinical symptom of Parkinson's disease [62].

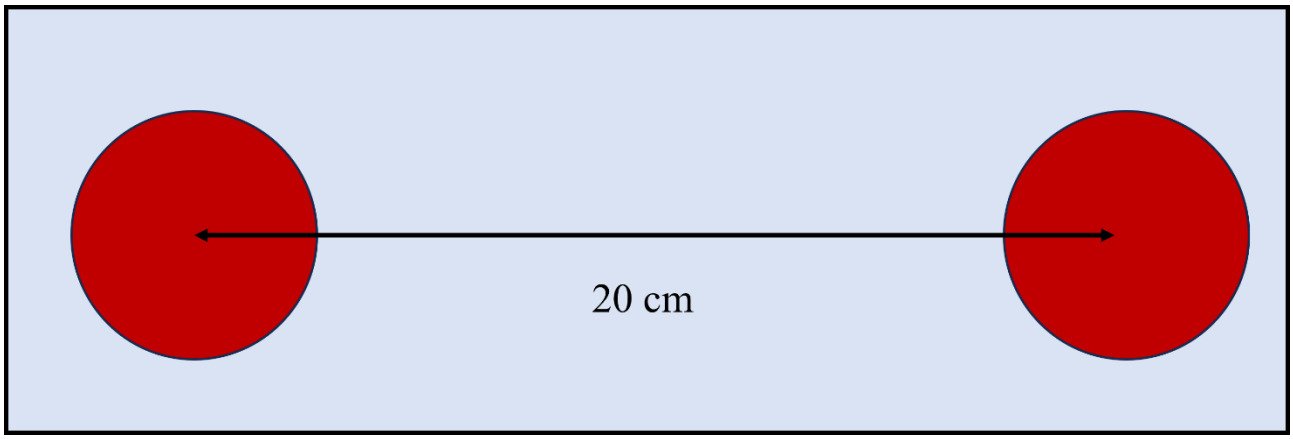

Figure 19 Tablet display configuration during the tapping test.

2) Timed Up & Go task

The Timed Up and Go (TUG) test is a clinical test to assess balance, mobility and fall risk in PD patients. It consists of rising from a chair, walking 3 metersat preferred speed, turning around, returning, and sitting (Figure 20) [44].

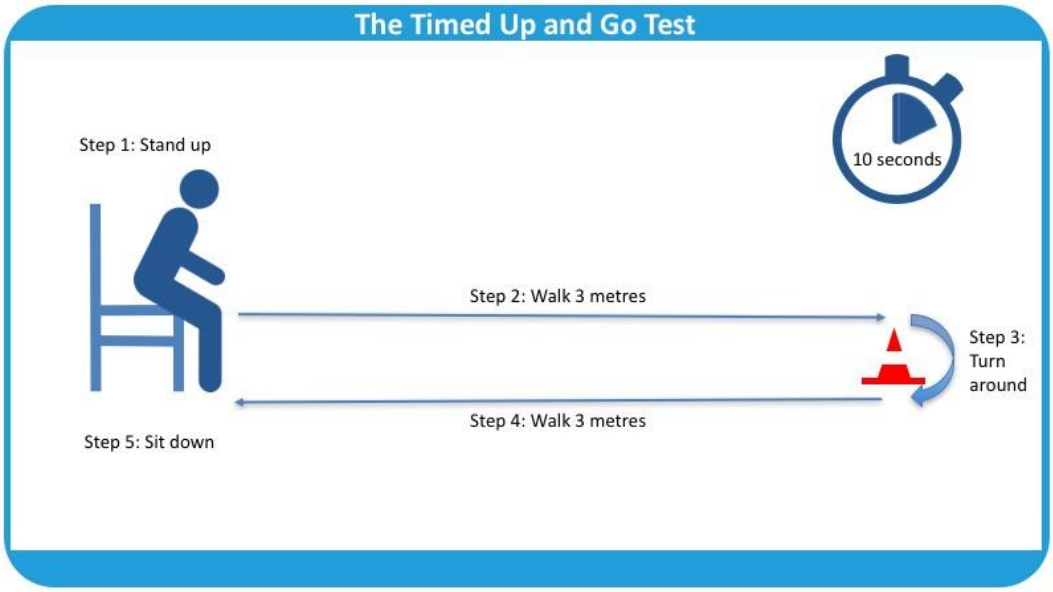

Figure 20 Representation of TUG test. https://www.frailtytoolkit.org/category/asess-tools/

It is simple and easy to perform in the clinic. The test is repeated 5 times: 3 times as single task and two times as dual task. The traditional clinical outcome of TUG test is its total duration which is usually measured by a stopwatch. However, this single measure no providing information regarding the performance in specific components of the test. Thanks to the application of wearable inertial sensors, several parameters can be extracted, providing an object evaluation of the functional performance of the patient (e.g., sit to walk duration, 180° turn duration, number of steps) [44].

3) Quiet Standing task

During the quiet standing task, the patient has to maintain the rest position and stay as still as possible for 30 seconds. The subject has to keep the arms along the body and fix the point positioned at the head height on the wall. This task is repeated four times: two times with eyes open, and two times with eyes closed (Figure 21).

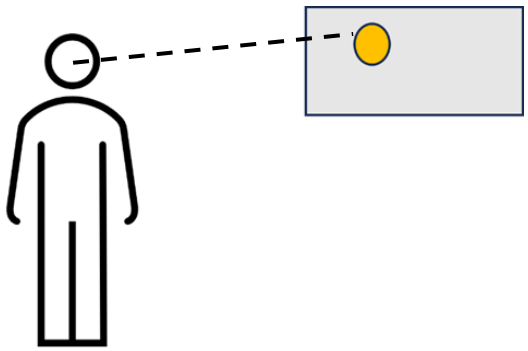

Figure 21 Performance of quiet standing task, first with open eyes and second with closed eyes.

The data acquired by wearable IMUs was analysed to evaluate the body sway displacement. The following parameters of body sway for anterior-posterior (AP) and medial-lateral (ML) directions were analysed: velocity (dividing the total body sway by the time in each direction) and root mean square (RMS; corresponding to the mean variability of the displacement in the trial). In addition, the sway area (95% of the ellipse) and nonlinear variables were analysed [63].

4) Full 360° turn

During the full 360° task, the patient performs a full clockwise turn and then a full counterclockwise (Figure 22). This task is repeated two times as single task and two times as dual task. The 360° turning in combination with a dual-task is the most important trigger for Freezing of Gait (FOG). During turning, non-freezers and controls decreased their cadence whereas freezers increased it, which may be related to FOG [64].

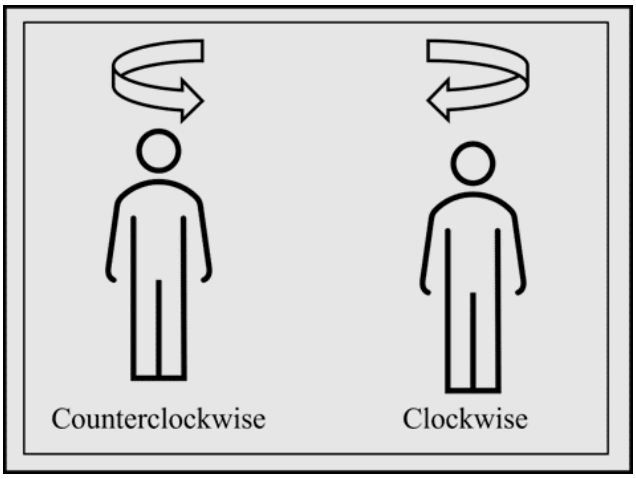

Figure 22 Representation of Full 360° clockwise and counterclockwise task.

5) 18 meters walking task

During 18 meters walk test, patients were instructed to walk straight along a corridor at a self-selected pace (Figure 23). This task was performed 3 times as single task and then repeated another 2 times as dual task. The wearable inertial sensors provide quantitative instrumental variables describing gait and postural transitions such as the gait velocity, cadence, stride length [65].

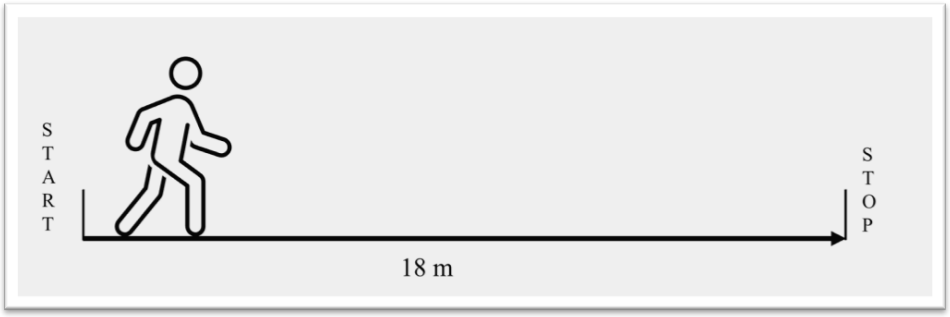

Figure 23 Representation of 18 meters walking task.

6) Complex task

In the last task, the complex task, several actions are carried out: the subject walks a few meters straight to arrive in front of a door, which he opens. The subject then has to walk 3 meters inside the room and turn 180° in a small space delimited by close walls (Figure 24). Subsequently, retrace the same path as previously defined (Figure 25). This task is performed 2 times as a single task and then repeated another 2 times as a dual task. The complex task was designed to induce freezing of gait events.

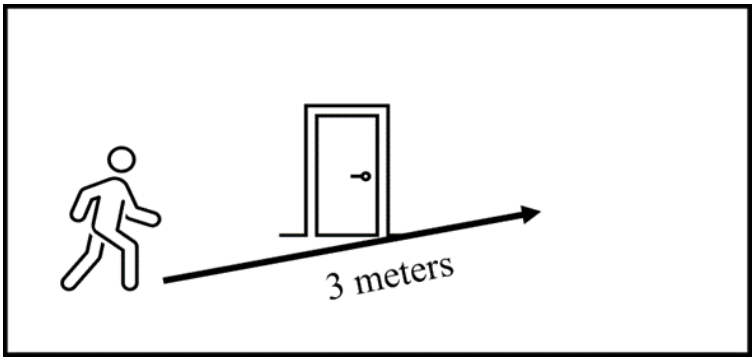

Figure 24 Representation of the first phase of complex task.

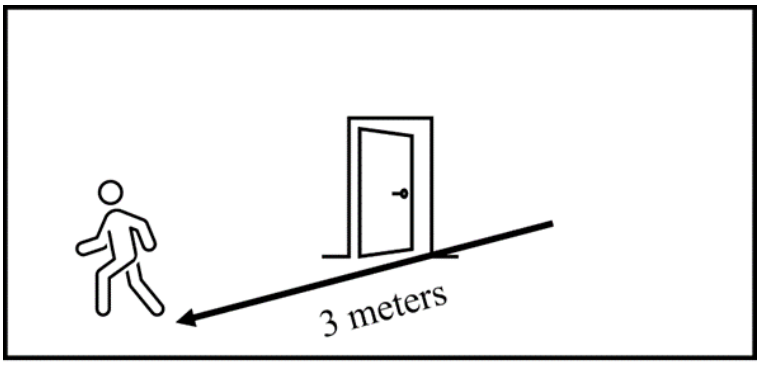

Figure 25 Representation of the second phase of complex task.

2.1.2 Participants

In this work, the focus is on Sway analysis. In particular, 46 patients were recruited to performed pre-DBS monitoring at the "IRCCS Istituto delle Scienze Neurologiche" in Bologna from January 2022 to July 2023. One participant who did not perform the MED OFF condition was discarded from the analysis.

2.1.3 Posture analysis

The two pre-DBS conditions (MED OFF and MED ON) were recorded separately, 75 minutes apart, using wearable inertial sensors. To analyse them, the unprocessed data acquired was first segmented to isolate signals for each specific task (considering the timestamp reported by the operator during the data acquisition) and then analysed using provided algorithms (mHealth Technologies srl).

In our specific case, in Figure 26 and Figure 27 are reported an example of the tri-axial acceleration and angular velocity recorded by the IMU placed on the lower back during the quiet standing task. In both figures, three signal components are shown: the mediolateral (ML), the vertical (V), and the antero-posterior (AP).

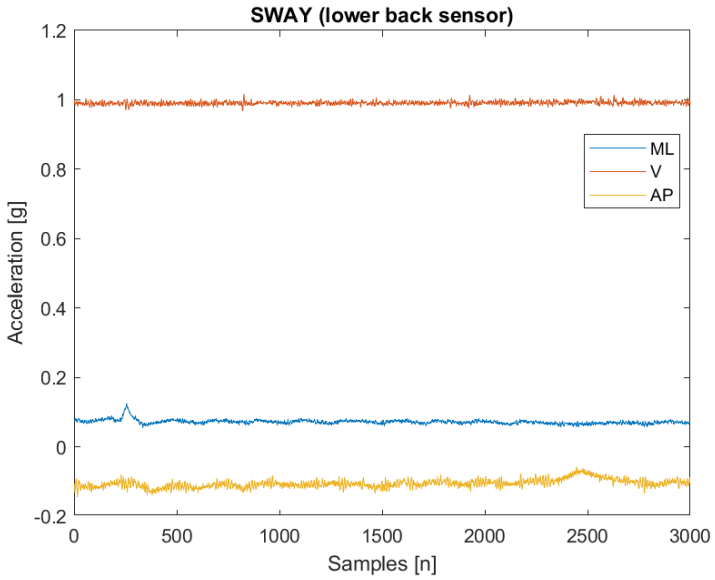

Figure 26 Graphic representation of the acceleration during the Quiet Standing task, are marked the three distinct signal components: the medio-lateral component in blue, the vertical component in red, and the posterior-anterior component in yellow.

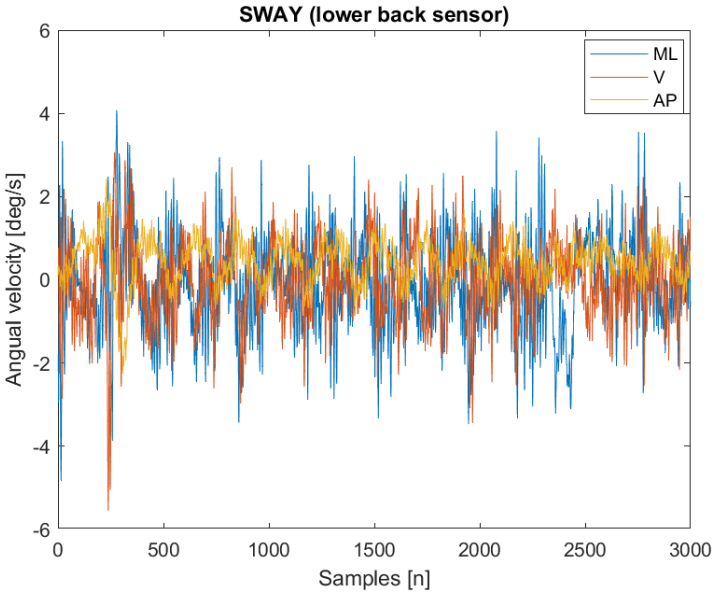

Figure 27 Graphic representation of the angular velocity during the Quiet Standing task, are marked the three distinct signal components: the medio-lateral component in blue, the vertical component in red, and the posterior-anterior component in yellow.

Once pre-processing is complete, 120 quantitative parameters were extracted. Among these, only 9 parameters were selected as the most significant for the further analysis and were computed for each test performed by the recruited patients. In particular, in accordance with the study of Moretto et al. [63], the following parameters of body sway for anterior-posterior (AP) and medial-lateral (ML) directions were analysed: velocity (dividing the total body sway by the time in each direction) and root mean square (RMS, corresponding to the mean variability of the displacement in the trial).

In addition, the sway area (95% of the ellipse) was analysed. The selected parameters for the quantitative evaluation of quiet standing task are reported in Table 6.

Root mean square of the displacement along AP axis [mm].	It represents the AP oscillation expressed as the distance (in mm) between the maximal forward and backward shift in the centre of thrust.
Root mean square of the displacement along ML axis [mm].	It represents the ML oscillation expressed as the distance (in mm) between the maximal forward and backward shift in the centre of thrust.
Sway path of the displacement along the AP axis [mm].	Length of trajectory covered by the centre of mass during postural oscillation along the AP axis.
Sway path of the displacement along the ML axis [mm].	length of trajectory travelled by the centre of mass during postural oscillation along the ML axis.
Sway path of the displacement on the horizontal plane [mm].	length of trajectory travelled by the centre of mass during the postural oscillation considering the plane formed by the AP and ML axis.
Sway area [mm^2/s].	area covered by the trajectory of displacement from the centre of mass in the unit of time
95% confidence interval ellipse area [mm^2].	area of the confidence ellipse containing, at 95% probability, the points of the trajectory on the horizontal plane (AP, ML)
Mean sway velocity along AP axis [mm/s].	average speed of the centre of mass along the AP axis
Mean sway velocity along the ML axis [mm/s].	average speed of the centre of mass along the ML axis

Table 2 The table describes the parameters used in further analysis.

For each subject included in the sway analysis, the defined parameters were extracted. Each subject performed two open-eyes trials (OE) and two closed-eyes (CE) trials during the MED OFF and MED ON conditions.

Consequently, for each parameter, the mean and the standard deviation of the trial pairs in the different conditions were computed; in this way, four average values were obtained (one for each trial). A further analysis was carried out considering, for each parameter, the median, the maximum and minimum values, of the two different medication conditions and the two different trials.

In addition, non-parametric statistical tests were applied to verify if the selected parameters have values that are significantly different among the different conditions (MED OFF vs MED ON with open eyes, MED OFF vs MED ON with closed eyes). In particular, the Wilcoxon signed rank test was applied with a significance level α=0.05.

2.2 Results

As indicated in chapter 2.1.3, nine parameters have been considered to evaluate the sway. The parameters required for the analysis were determined for each patient. Mean and standard deviation were calculated for each parameter based on the different values obtained from the considered subjects. Different studies have studied SWAY analysis with eyes open and closed, with and without Levodopa medication, to assess the effect of the disease on static postural SWAY in Parkinson's subjects.

PARAMETER	MED OFF EO	MED ON EO	MED OFF EC	MED ON EC
RMS, displacement along AP axis [mm]	0.0108± 0.0030	0.0136± 0.0044	0.0121± 0.0041	0.0138± 0.0039
RMS, displacement along ML axis [mm]	0.0038± 0.0014	0.0052± 0.0017	0.0041± 0.0016	0.0049± 0.0018
SWAY path displacement along AP axis [mm]	0.1767± 0.0383	0.2671± 0.0432	0.2229± 0.0384	0.2791± 0.0423
SWAY path displacement along ML axis [mm]	0.0831± 0.0187	0.1296± 0.0354	0.1010± 0.0211	0.1323± 0.0252

SWAY path displacement on horizontal plane [mm]	0.2133± 0.0432	0.326± 0.0607	0.2670± 0.0417	0.3380± 0.0508
SWAY area [mm^2]	2.05e-05± 9.18e-06	4.80e-05 ± 2.78e-05	2.84e-05 ± 1.50e-05	4.56e-05 ± 2.07e-05
95% confidence ellipse area [mm^2]	7.19e-04± 3.02e-04	0.0013 ± 7.10e-04	8.93e-04 ± 4.566e-04	0.0013± 5.97e-04
Mean sway velocity along AP axis [mm/s]	0.0048± 9.44e-04	0.0069± 8.645e-04	0.0061± 0.0010	0.0074± 0.0011
Mean sway velocity along ML axis [mm/s]	0.0022± 4.2067e-04	0.0029± 5.99e-04	0.0026± 5.0365e-04	0.0033± 3.39e-04

Table 3 Representations of the mean value and standard deviation in the four conditions for each parameters. Abbreviation definition: EO, stand for Eyes Open; EC, stand for Eyes Closed; MED ON, stand for the phase with medication; MED OFF, stand for the phase without medication.

The performed comparisons are MED OFF vs MED ON with open eyes and MED OFF vs MED ON with closed eyes. It was observed that for all parameters, the average was higher after levodopa intake. In agreement with Gago et al. we also found a significant increase in the displacement of sway after levodopa intake, which can be related to the fact that levodopa reduces the rigidity without improving control of posture or because subclinical dyskinesia increases body motion [66].

Parameter	Off stage	On stage	p-Value
Root mean square of displacement along AP [mm]			
EO	0.093 [3.1e-3, 0.029]	0.0114 [4e-3, 0.0469]	**3e-3**
EC	0.0112 [0.029, 0.028]	0.0127[0.058, 0.0374]	0.1579
Root mean square of displacement along ML [mm]			
EO	0.034 [6.62e-4, 9.2e-3]	0.005 [1.6e-3, 1.94e-2]	**2.8e-3**
EC	3.6e-3 [9.2e-3, 1.29e-2]	0.0044 [9.9e-4, 1.66e-2]	7.23e-2
Sway path of displacement along the AP [mm]			
EO	0.15 [0.067, 0.53]	0.2066 [0.10, 1.42]	**9.19e-4**
EC	0.193 [0.53, 0.55]	0.2328 [0.11, 1.23]	**0.0274**
Sway path of displacement along the ML [mm]			
EO	0.0636 [3.03e-2, 0.38]	0.1157 [3.55e-2, 0.46]	**1.75e-5**
EC	0.081 [0.38, 0.57]	0.1015 [3.45e-2, 0.74]	**0.011**
Sway path of displacement along the horizontal [mm]			
EO	0.18 [0.089, 0.58]	0.27 [0.12, 1.53]	**1.49e-4**
EC	0.23 [0.58, 0.76]	0.282 [0.13, 1.34]	**1.62e-2**
Sway area [mm^2]			
EO	1.27e-5 [2.83e-6, 9.28e-5]	2.78e-5[4.20e-6, 2.37e-4]	**1.27e-5**
EC	1.9e-5 [9.28e-5, 1.43e-4]	2.49e-5 [3.33e-6, 2.3e-4]	**2.22e-2**
95% confidence interval ellipse area [mm^2]			

EO EC	5.46e-4 [6.08e-5, 2.7e-3] 5.83e-4 [2.7e-3, 3.7e-3]	9.36e-4 [1.6e-4, 0.058] 9.13e-4 [9.52e-5, 4.9e-3]	**2.48e-4** **4e-2**
Mean sway velocity along AP [mm/s] EO EC	 4e-3 [1.9e-2, 1.49e-2] 0.05 [1.49e-2, 1.63e-2]	 0.049 [0.027, 0.0411] 6e-3 [2.9e-2, 3.34e-2]	 **7.5e-3** **3.67e-2**
Mean sway velocity along ML [mm/s] EO EC	 1.6e-3 [8.04e-4, 0.0125] 2.1e-3[0.0125, 0.017]	 0.022 [1e-3, 1.18e-2] 2e-3 [9.94e-4, 2.47e-2]	 **1.6e-3** **0.0291**

Table 4 Data is presented as median [minimum, maximum]. The median was calculated for each parameter considering the two conditions ("ON" and "OFF") and for each condition the two trials: eyes open (OE) and eyes closed (CE).

In agreement with the Contini's study [67], by evaluating the entire group of patients after the levodopa assumption, there was a significant increase in postural variables after administration, especially in the open-eye condition, compared to baseline values.

To observe the distribution of the quantitative parameters extracted by wearable inertial sensors, boxplots are reported below (Figure 28 – 36).

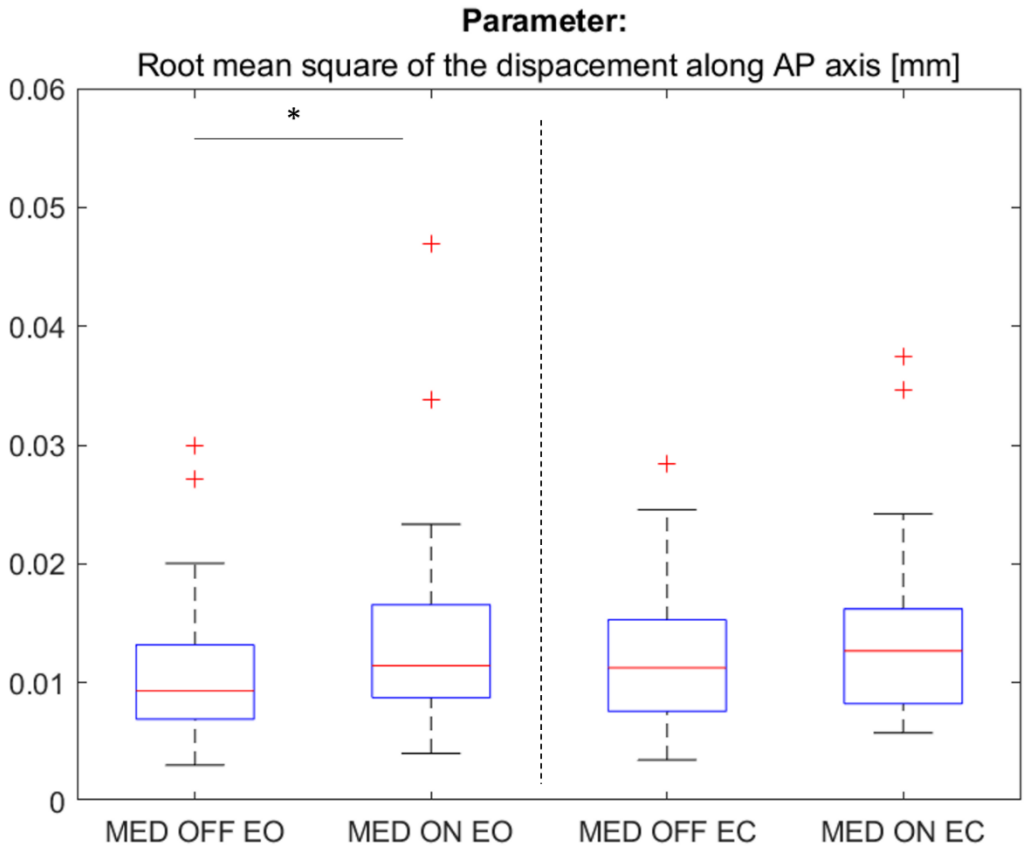

Figure 28 Boxplot graph of root mean square of the displacement along antero posterior (AP) axis.

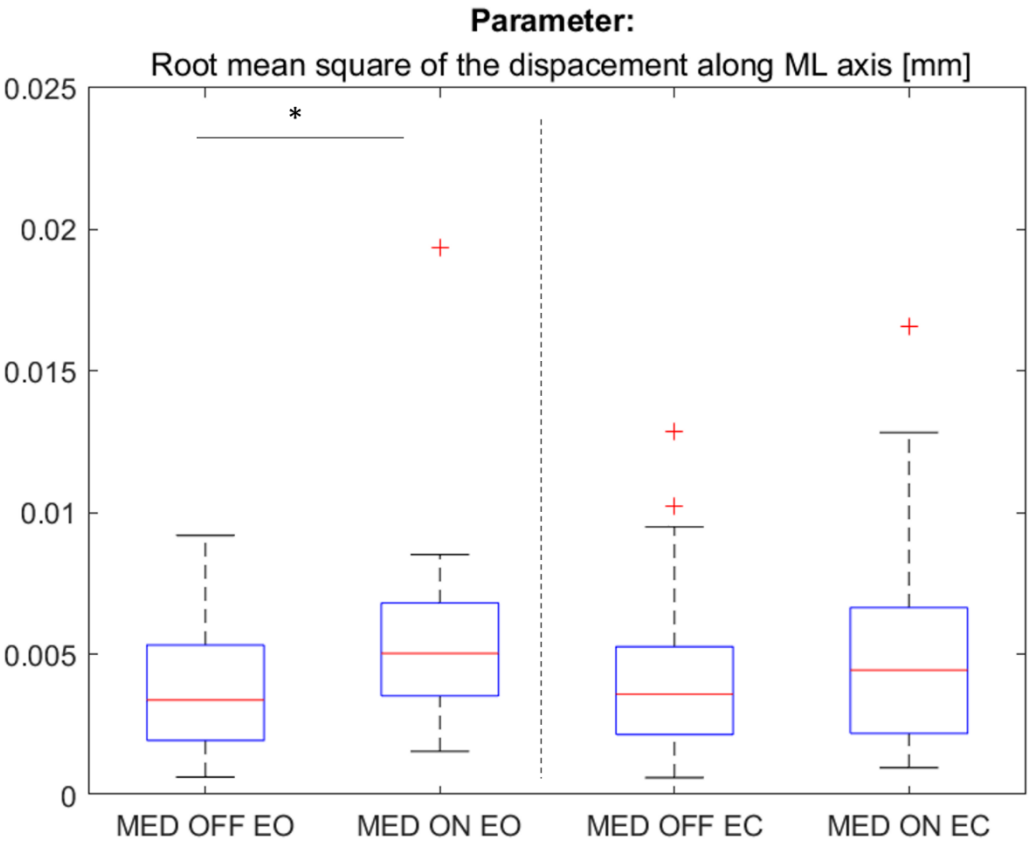

Figure 29 Boxplot graph of root mean square of the displacement along medio lateral (ML) axis.

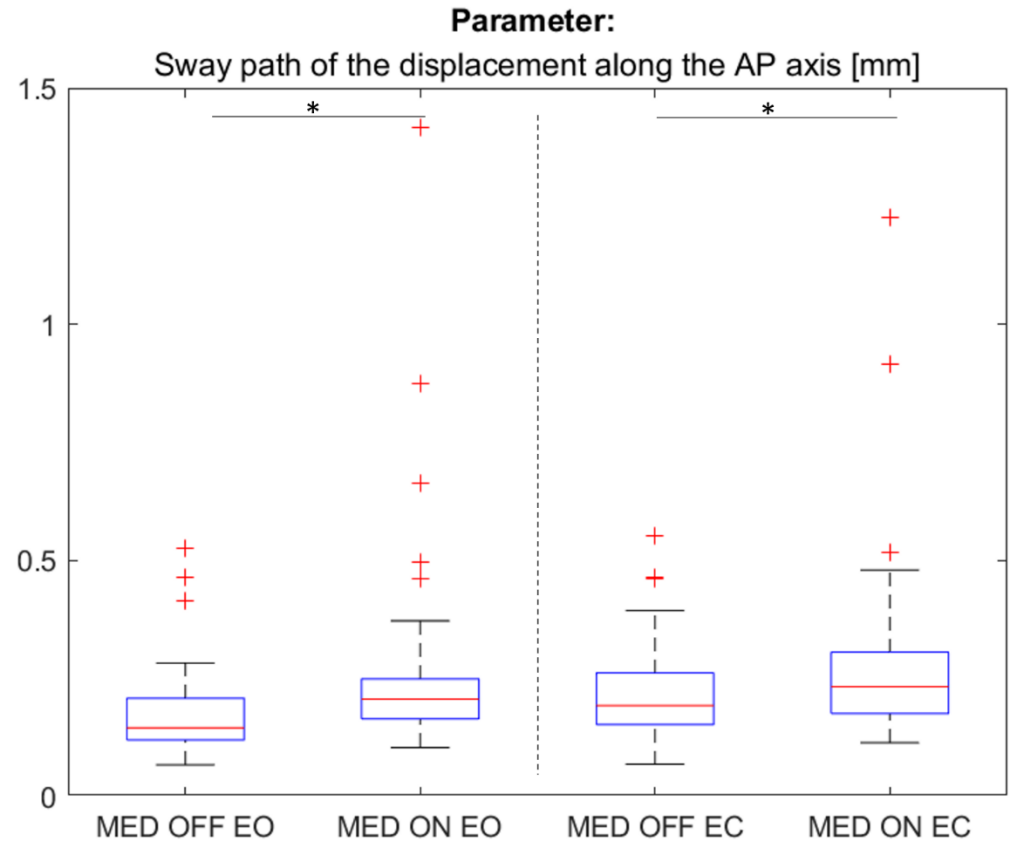

Figure 30 Boxplot graph of sway path of the displacement along antero posterior (AP) axis.

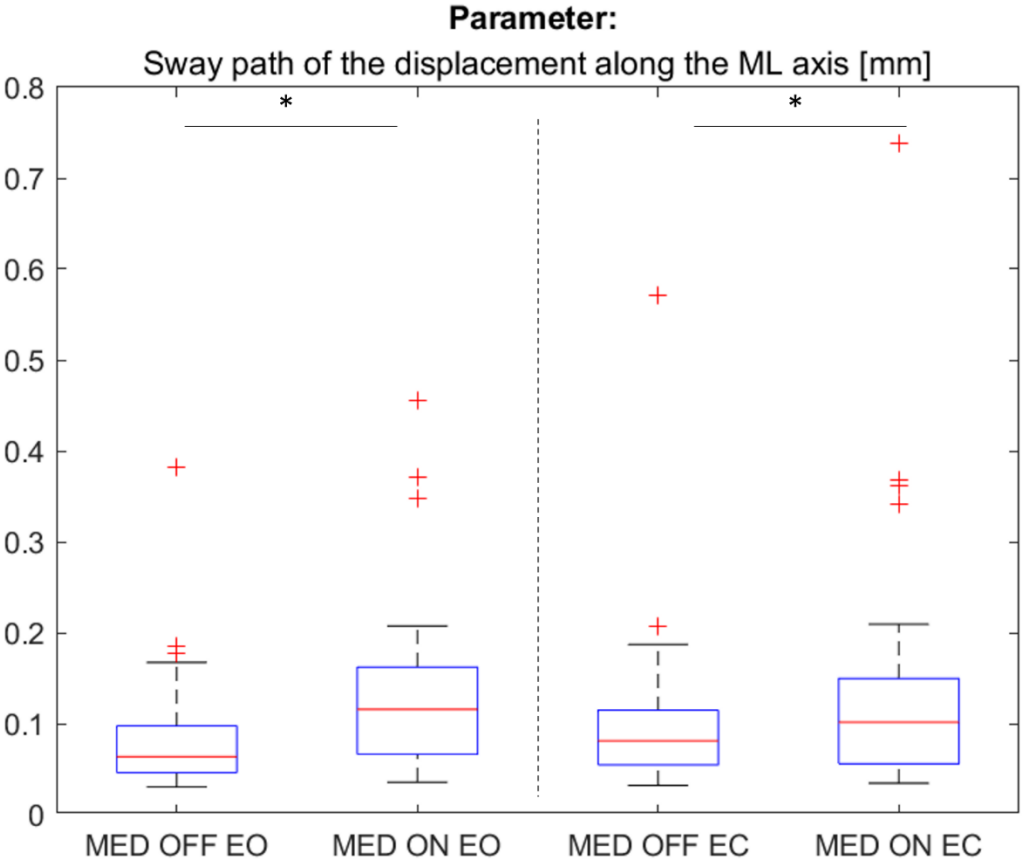

Figure 31 Boxplot graph of sway path of the displacement along medio lateral (ML) axis.

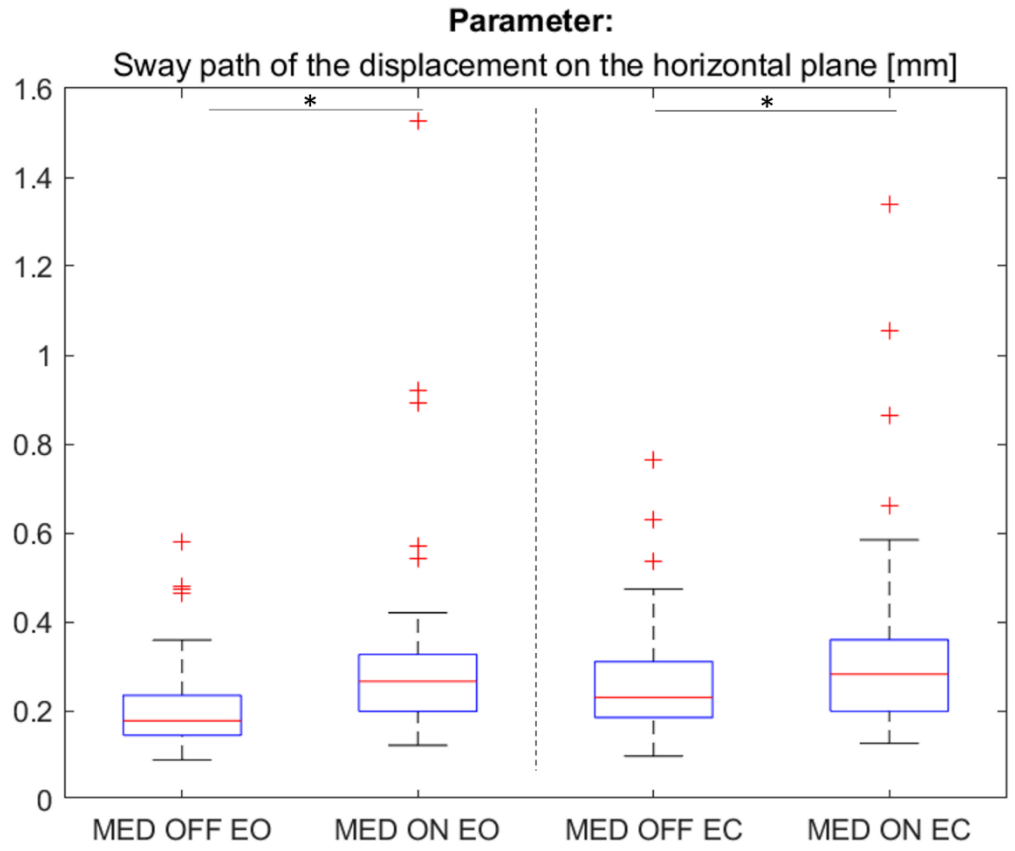

Figure 32 Boxplot graph of sway path of the displacement along horizontal plane.

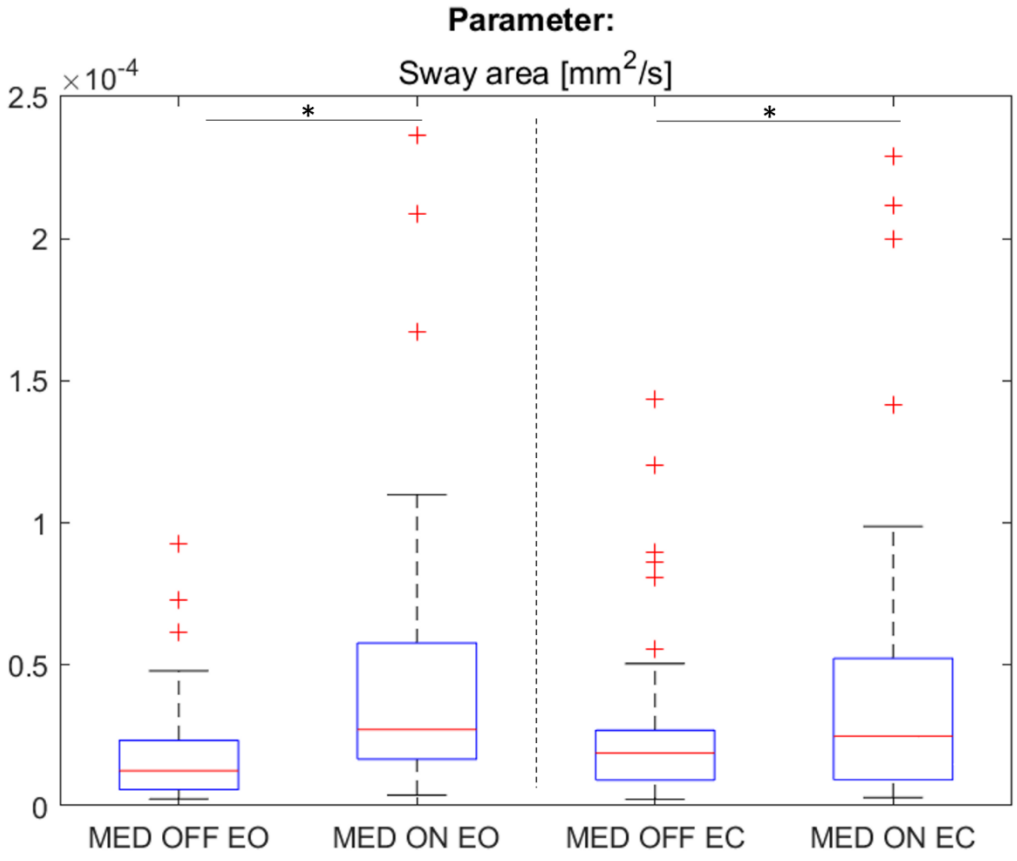

Figure 33 Boxplot graph of sway area.

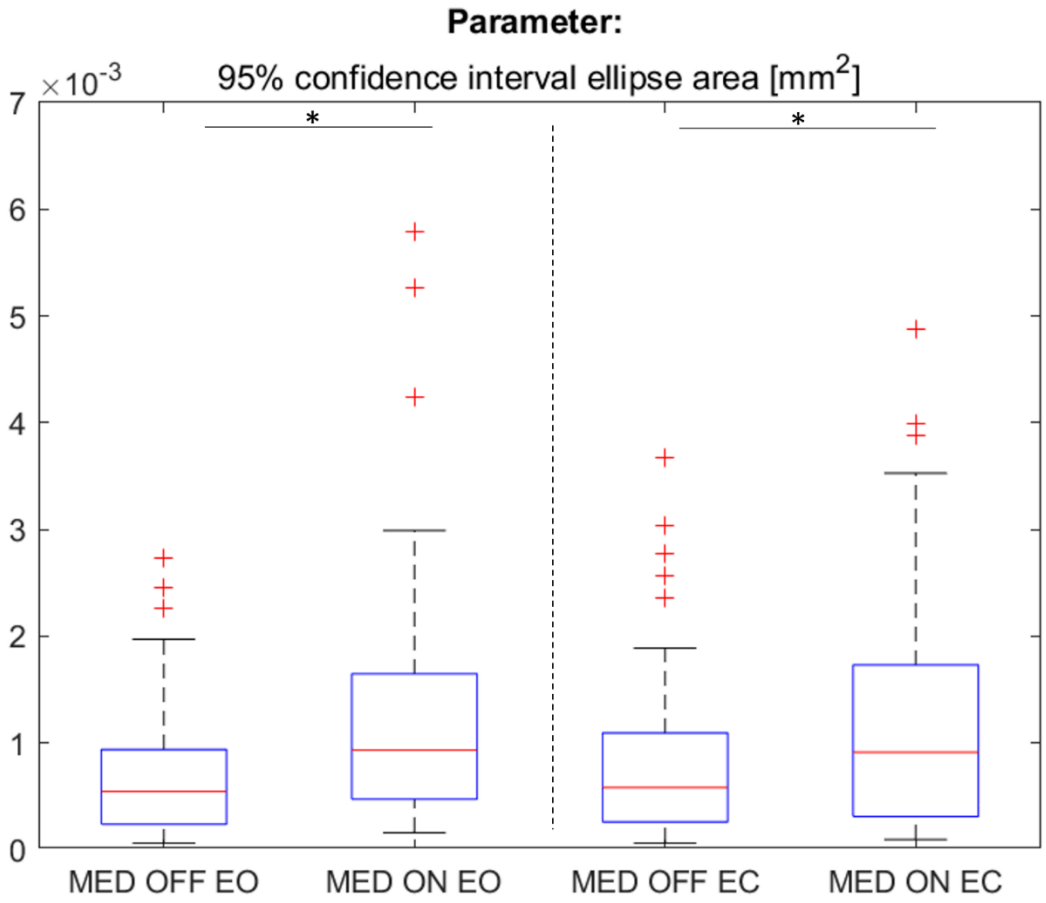

Figure 34 Boxplot graph of the 95% confidence interval ellipse area.

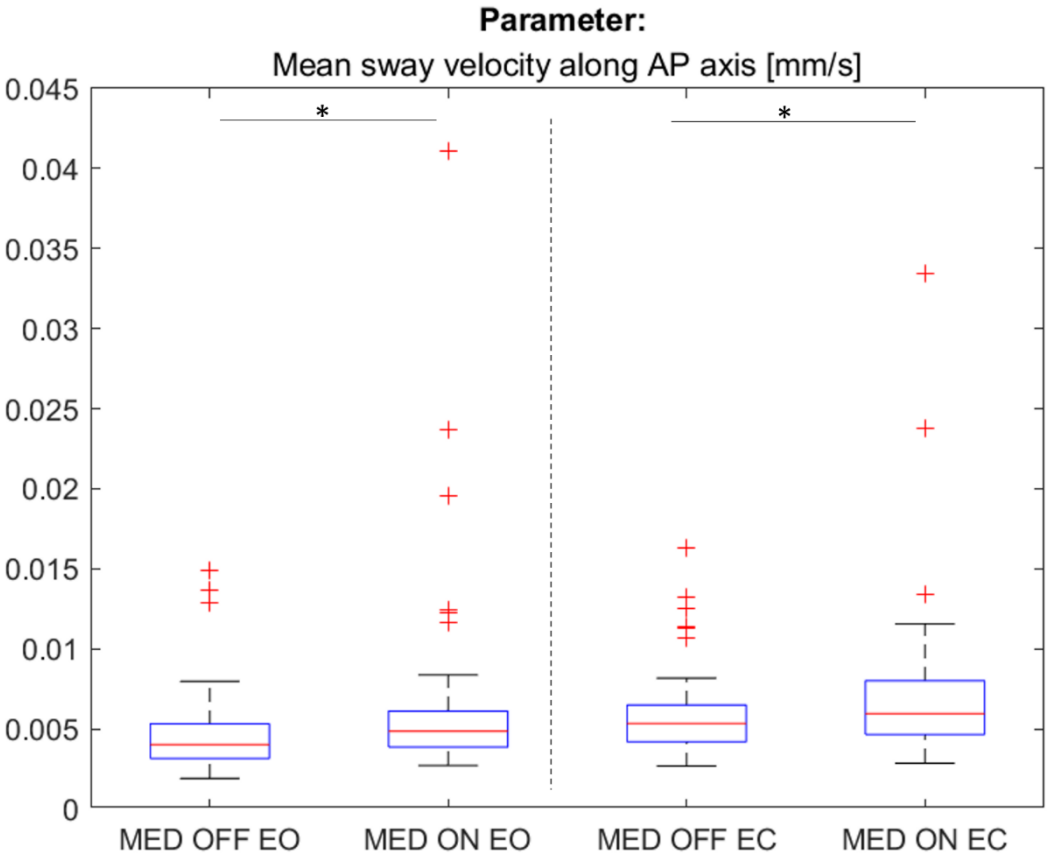

Figure 35 Boxplot graph of mean sway velocity along antero posterior (AP) axis.

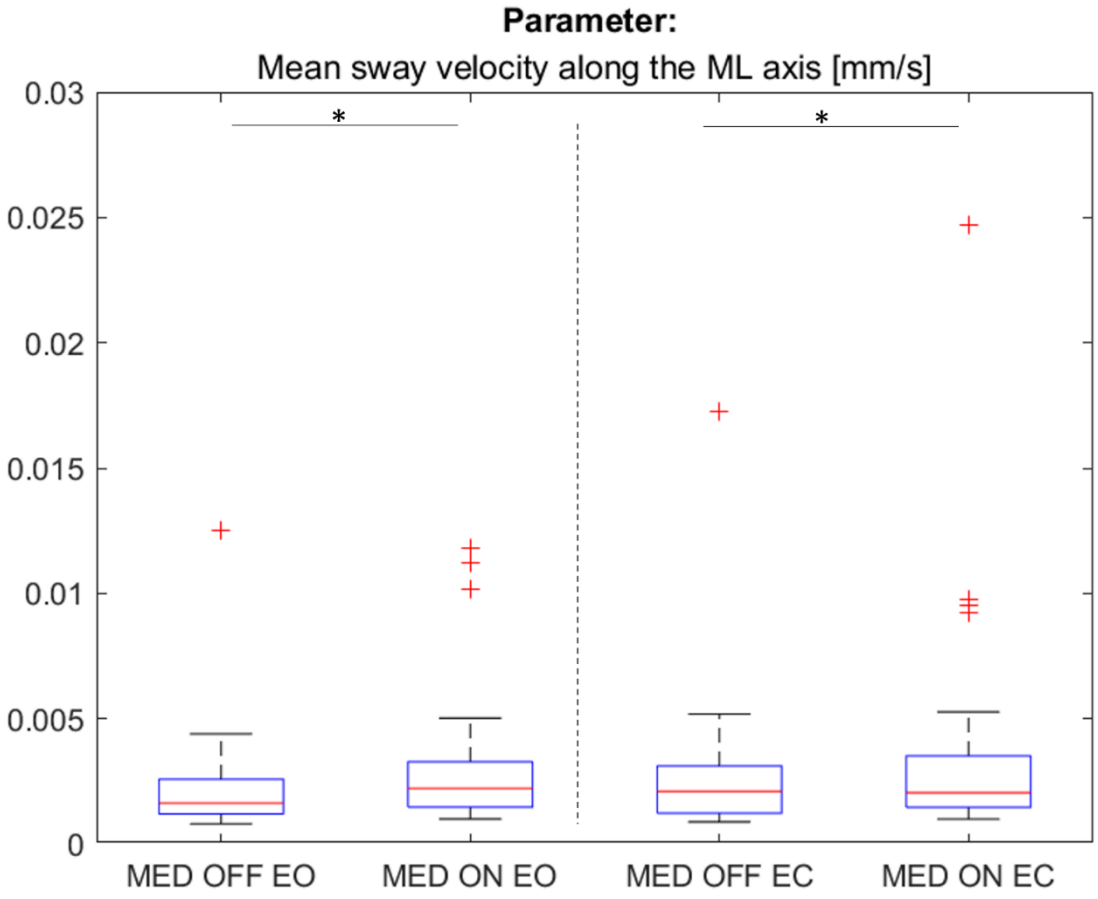

Figure 36 Boxplot graph of root mean square of the displacement along medio lateral (ML) axis.

In order to graphically summarize the changes in median posture parameters in the different conditions, a radar plot is reported in Figure 54. In particular, the state with opened eyes for both MED OFF and MED ON conditions is represented by red and green dashed lines, respectively. The closed eyes condtion is reproduced by solid lines in both MED OFF and MED ON conditions, using red and green to differenciate the medication condition described above. The radar plot reveals that MED OFF condition with open eyes (red dashed line) and MED OFF condition with eyes closed (red solid line) resulted in a lower median sway displacement, as the area covered by the curves is greater. In each condition, a bigger area covered by the curve indicates an higher displacement and a worse postural control. The reduced sway in MED OFF condition can due to the increased rigidity caused by the absence of Levodopa, which results in lower oscillation during the quiet standing test.

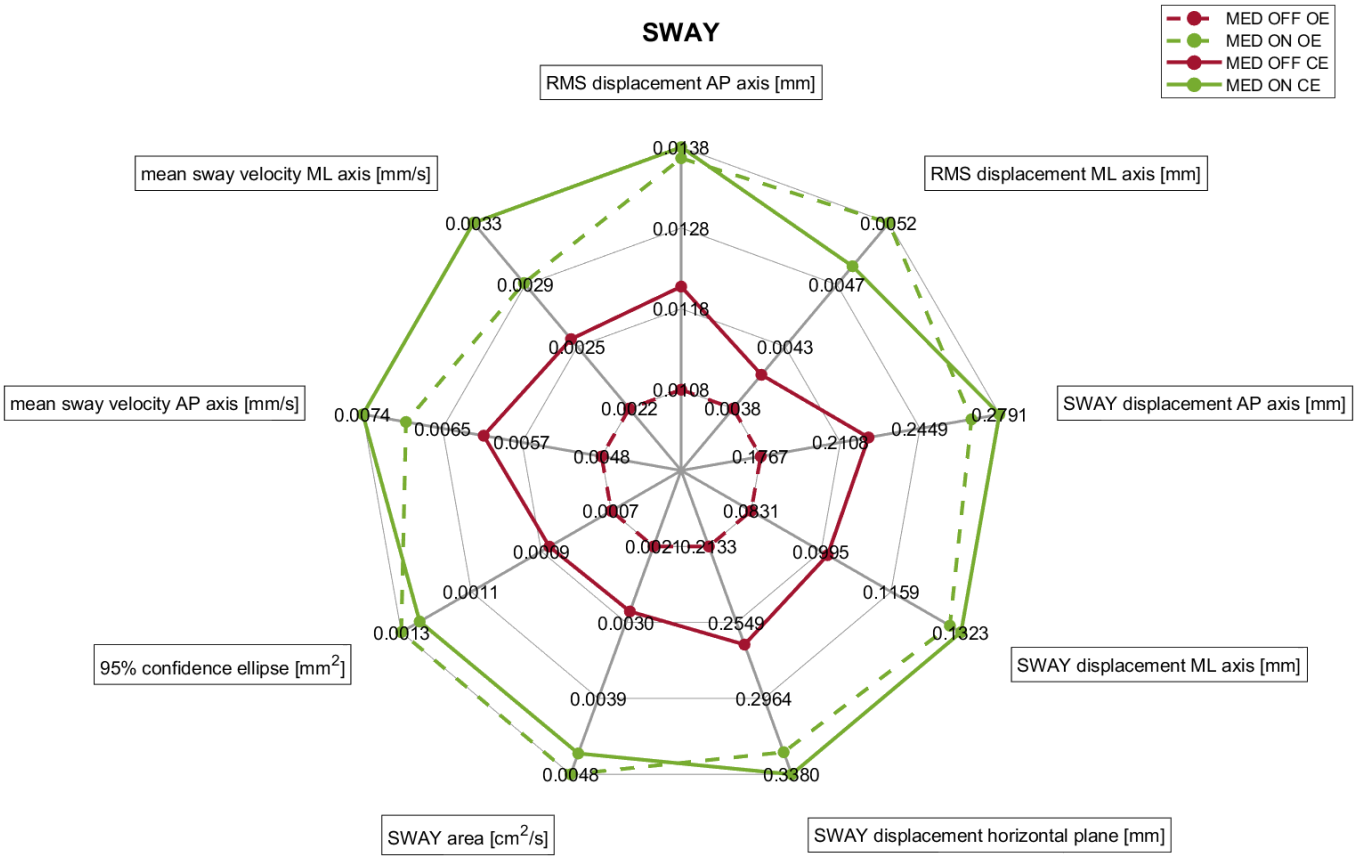

Figure 37 Radar plot about SWAY task.

As before, from the radar graph analysis it can be concluded that the subjects exhibit less sway during the MED OFF condition as compared to the evaluation after drug treatment.

CHAPTER 3 - POSTURE REHABILITATION USING WEARABLE SENSORS

Nowadays, the technological evolution generates a various number of devices that enable the implementation of biofeedback techniques. These techniques have the potential to improve quality of life and daily activities for patients as well as for elderly or injured people or subjects with balance and gait disorders that need rehabilitation and could benefit from it [68], [69].
Biofeedback systems use precise sensors to measure body functions and parameters (bio), including brainwaves, heart function, breathing, muscle activity, and skin temperature. These instruments provide promptly and accurately the information to the user ('feed-back') through one of the human senses (*i.e.*, sight, hearing, or touch). The feedback allows the person to act on the received information (biofeedback signal) to modify the body function or the parameter in the desired way. This process enables the users to learn how to change physiological activity to improve their health and performance. It provides biological information to subjects in real-time that would otherwise be unknown. This information can be defined as augmented (or extrinsic) feedback, that provides the user with additional information, beyond the information that is naturally available, in contrast to the sensory (or intrinsic) feedback that provides self-generated from various intrinsic sensory receptors [68], [42].

For over fifty years, wearable devices have been used in rehabilitation to provide biofeedback about biomechanical and/or physiological body parameters [42]. It improves different outcomes in people with neurological diseases and to facilitate normal movement patterns after an injury [42], [70].

Biofeedback usually involves measurement of a target biomedical variable and relaying it to the user using one of two strategies:

- Direct feedback regarding the measured variable, as in the case of heart rate or heart rate variability, where a numerical value is displayed on a wearable device, such as a watch.
- Transformed feedback regarding the measured variable, where the measurements are used to control an adaptive auditory signal, visual display or tactile feedback method.

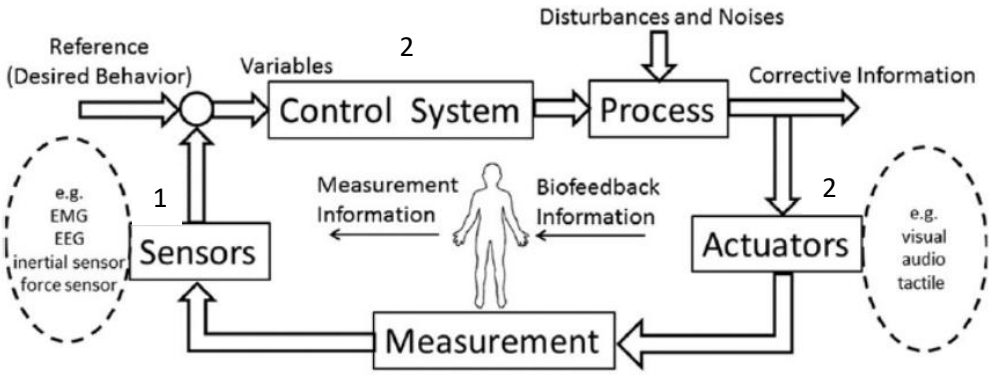

Figure 38 Architecture of a biofeedback system. All biofeedback devices are made up of three essential components: sensor(s) that is the input device, processing and control unit and actuator(s)-return unit that represent the output device. [42].

The figure above illustrates the architecture of the biofeedback system, composed of three main components:

1) SENSOR(S)

Depending on the specific deficit or pathology, different sensors can be placed in different body positions to allow the acquisition of biological signals. The signals are obtained measuring body movement, force, cardiovascular, or neurological parameters, can be categorized in two different groups: biomechanical and physiological signals [70]. The most common biological quantities include muscle activity (EMG), skin temperature, heart rate, blood pressure, breathing, skin conductivity, brain activity (EEG), movement [42].

Indeed, wearable sensors are integrated as inertial measurement units (IMU), containing accelerometers, gyroscopes, and magnetometers able to provide biofeedback about the estimated dynamics of the body centre of mass, upper- and lower-extremity movement [42], [70]. These devices give the advantage of being portable in various rehabilitation setting [42], [70].

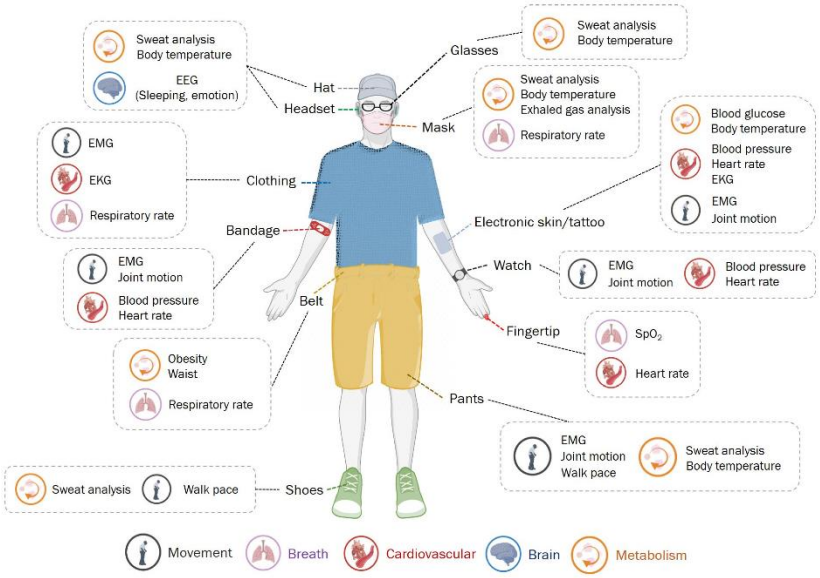

Figure 39 Representation of detectable bio-signals on human body and their wearable detection. Wearable devices are categorized by different parts of the human body and the different signal acquired.
Definition of the abbreviations: ECG is the electrocardiography, EMG is the electromyography, EEG is electroencephalography [71]

In addition, wearable sensors must have the following important attributes:

- Easy to use;
- Not invasive;
- Biological compatibility;
- Low-cost;
- Low power consumption (effective autonomy);
- Low noise level, low interference;
- Valid and accurate data respect to Gold Standard;
- Clinically data useful;
- Privacy;
- Interoperability.

2) PROCESSING AND CONTROL UNIT

A control system is an interconnection component that providing the desired outcomes to a given system. The control systems can be grouped into two categories: direct action controls (called "feedforward" or "open chain") and "feedback" or "closed chain" controls [42]. Feedback systems operate to minimise errors between the desired value of the variable to be controlled and its direct measurement [72]. It can consist of dedicated hardware or commercial devices such as PC, tablet, smartphone, or smartwatch. They must ensure efficient and effort, real-time processing of the acquired signals and timely piloting of the return devices [72].

3) ACTUATORS

The controller is a mathematical model that continuously compares the measured output variable with the desired input and modifies the actuators to reduce discrepancies [72]. The actuators are the working arms of the controller [72]. The most common solution is to allow the subjects to visualize their "performance", for example on the computer monitor. Other modalities for biofeedback include vibrotactile (haptic), acoustic. Recent applications also include the possibility to use augmented reality devices [42].

Learning model of the biofeedback

Therapies that use BFB are learning processes which can be an additional support to conventional drug therapies. Thus, undertaking a BFB training course means playing an active role and practicing a lot in order to develop the necessary skills. Therefore, BFB training involves the psychological component of the patients whose determination, conviction and willpower are crucial for the success of the therapy. Firstly, the patients should get aware of their particular pathological physical or mental condition, which will determine the actual physiological changes. Next, with the help of the therapeutic staff and BFB equipment, it is necessary for them to develop a series of strategies and behaviours to improve the whole effectiveness of the therapy [42].

In this model, the biofeedback operates as reward, reinforcing the patient's motivation to recover. The therapist's role is to explain how BFB equipment measures physiological responses and their importance to the patient's health [42].

Knowledge Of Result And Performance

Augmented feedback (AF) depends on the information provided to the learner from the external source which a sensory channel. [73]. Therefore, during the treatment, the information may be supplemented intrinsic augmented feedback.
In some cases, in which the innate feedback is strongly limited or absent (e.g., blindness, deafness, vestibular deficit) the working procedure is modified to favour a cross-modal reorganization of the cortex. These solutions can arouse the sensory prostheses or neuro-prostheses for continuous use [42].
AF can be provided as either knowledge of results (KR) or knowledge of performance (KP).
KR gives information about the outcome of the skill; it provides the outcome rather than the movement itself. In addition, KR may or may not contain a reward component.
Contrastingly, KP is process oriented, and advises the learner about their movement patterns during the execution. It can be descriptive or prescriptive, respectively: providing only information on performance and what needs to improve. It is aimed at correcting errors during the execution, it serves to refine the movements [42].

In 1972 Gentile et al. maintains that knowledge of performance (KP) is the most effective form for the acquisition of a closed skill [42].
AF can be provided to the learner through a different sources, such as video feedback of previous performances, verbal feedback on how to improve technique, and biofeedback on postural stability, and other variations. [42], [73].

3.1 State of the Art in posture rehabilitation

In order to optimize the PASSO project, bibliographic research was performed to investigate commercially available solutions and identify those that closely aligned with our objectives. This investigation allowed for the discussion of various studies and a comparison with our ideas and requirements. It provides an overview of the available options for project enhancement. This analysis contributed to a selection of approaches and technologies to be adopted in the specific work.

3.1.1 Bibliographic research

Search Strategy

The bibliographical research was carried out to know how to realize a prototype biofeedback system suitable for our project. The papers reported in the following had been found in PubMed, ScienceDirect, Google Scholar and Academic Search databases. The main key words used for the literature research were "*Parkinson" AND ("wearable sensors" OR "sensors") AND ("Biofeedback") AND ("Rehabilitation")* located in title and/or abstract.

The crucial data from the most pertinent papers have been organized into the table below. These tables consider the aim of the research, subject involved in the analysis, rehabilitation task protocols, sensor placement on the body, biofeedback stimulus, processing unit type and the connection between the processing unit and the sensor.

Inclusion criteria for the papers

The reviewed documents include experimental protocols conducted on individuals encountering specific problems (such as those with amputation or PD), as well as on healthy elderly subjects and persons that need to enhance their daily life movement, including posture. The primary focus of the analysis concerns the position of the sensor(s), the proposed biofeedback to help subjects independently improve their condition. The conducted research was categorized into two tables considering the processing unit used.

SUBJECTS	AIM	PROTOCOL	SENSOR'S POSITION	BIOFEEDBACK	PROCESSING UNIT	CONNECTION	ALGORITHM	REFERENCE
Individuals with stroke	Realize a portable gait rehabilitation biofeedback device to use outside the clinical environment	Walk	Insoles	Vibrotactile biofeedback in waist position	Computer	Bluetooth	Na	[74]
Parkinson's patients	Realize a support system forFOG episodes	Walk circuit	2 pressure sensors embedded into shoe insole 1 IMU placed on the patient's right ankle (connected with Arduino)	Vibration in right ankle position	Computer	Bluetooth	Na	[75]
Persons with lower limb amputations	Realize a system to assist lower-limb amputees to	walking on different types of terrains	16 optoelectronics sensors	Haptic belt vibrotactile, 3 actuators: 1 in spine VT1, in hip	Computing unit (Vibro Board)	Wireless	machine learning algorithm	[76]

	appreciate the floor conditions while walking and promote a more confident use of their artificial limb.		embedded in the insole	VT2 and nave VT3.			(k-nearest neighbour, KNN)	

Table 5 Bibliographic research: systems using computers as processing unit.

SUBJECT	AIM	PROTOCL	SENSOR'S POSITION	BIOFEEDBAC	PROCESSING UNIT	CONNECTION	ALGORITHM	REFERENCE
Parkinson's persons	Develop a hardware-based wireless system non-invasive for acquisition of real-time data when FOG event is present to stimulate walking progression. To prevent falls.	Walk, turns 180°, climb stairs	IMU placed near of the sural nerve of right leg	vibratory motor is at the intersection of the posterior tibial nerve and the lateral plantar nerve in both legs	Smartphone	Bluetooth	Discrete Transform Wavelet (DFT) and detects the FOG	[77]
Parkinson's patients with freezing	Monitor motor symptoms of Parkinson's disease at home.	Wearing IMU during walking hours (10 hours) for 30 days	IMU 9x3 placed in waist position	rhythmic auditory stimulation	Smartphone	Bluetooth	Na	[77]

community-dwelling healthy older adults	Home balance training	Static standing; Compliant surface standing; Weight shifting; Modified centre of gravity; Gait	2 iPods in waist position	4 actuators for vibration in waist position	iPod	Bluetooth	extended Kalman filter (EKF)	[78]
Parkinson's and healthy elderly individuals	Evaluate the dynamic wieght-shifting exercise	Dynamic weight-shifting exercises	IMU waist position	4 vibrotactile actuator placed over the front, back and right and left sides of the torso (L4/L5)	Computer	Na	Statistical analysis	[78]
Subject with musculoskeletal disorder	aimed at facilitating preventive measures by supporting	The subjects are evaluated during daily activity	IMU placed at the upper back at the level of the thoracic	2 vibration actuator units placed on sternum and	smartphone	Bluetooth	extensive complementary Kalman filter	[79]

	risk assessments, work design, and work technique training		vertebrae and placed bilaterally on the arm.	dominant upper arm				
Parkinson's patients	Two applications were used in this study: the audio-biofeedback (ABF-gait app) and the instrumented cueing for FOG-training (FOG-cue app).	gait training for 30 min, three times per week for six weeks	2 IMUs placed in shoes, when using ABF-gait app. 2 IMUs placed above their ankles when using FOG-cue app	Feedback provided via earphones	Smartphone	Bluetooth	state-of-the-art algorithms including the Kalman filter, its extended variation + recently developed complementary filters	[80]
subjects undergone microdiscectomy due to severe sciatica	Application of wearable sensor for lumbar spine kinematic	Daily activity	2 metamotion R+ positioned in L5-S1	Haptic in position L5-S1	Smatphone, Computer	Bluetooth	Number of degree of freedom (NDoF) fusion algorithm	[81]

	measurents during daily activity							
Persons with lower back pain	Use Valedo App on iOS device to reduce or preventing lower back pain	The subjects are evaluated during daily activity	1 sensor in lower back, other one positioned in upper chest	Visual and/or auditory feedback	Smartphone	Bluetooth	Na	[82]
people who want improve their posture (e.g. student, athlete and subjects with postural problems)	Upright GO 2: detect posture in real time and give you feedback to correct posture. Use upright mobile app	Sitting, walking, physical activity	2 built-in sensors	Haptic	Smartphone	Bluetooth	Na	[83]
Parkinson's persons	Patients wore the UpRight device during a baseline of	Home setting	Sensor position sternum	Vibrotactile	Smartphone	Custom matlab algorithm	Na	[84]

	1 week (no feedback), followed by an intervention period of 1 week (feedback)							

Table 6 Bibliographic research: systems using computers as processing unit.

In both tables are reported biofeedback systems with different objectives, which depend on the subjects who will use them.

It can be observed that [74], [75] and [76] employ sensors placed in the insole to acquire gait data, but depending on the subjects of study and the required stimulation, the actuator is positioned at different points (e.g. ankle, leg).

In these studies, [77], [78] and [78], the sensor is positioned at the waist. Two of them are specifically focus on subjects with Parkinson's disease.

To assess different problems related to posture the sensors are placed on the trunk [79], [81], [82], [83], [84]. Except for [84], the sensor is also the actuator, and it releases the haptic biofeedback signal.

In the market, there are two types of systems used to improve posture in healthy subject, as evidenced in the studies [82], [83]. In particular, UpRight device is used in clinical practice for home training assess the patient during their daily life [84]. The device is positioned at the level of the sternum, it provides haptic biofeedback. A different situation is presented with Valedo device, which uses visual and/or auditory feedback as biofeedback.

It is perceptible from the articles referenced in the Table 3 and Table 4 that Parkinson's disease is the most prevalent pathology. People with neurological diseases (PwND) often experience mobility disorders, including balance and gait deficits and an increased risk of falls. These conditions, consequently, impact the quality of life [85]. So, these patients' populations have specific rehabilitation needs [70]. One commonly used form of biofeedback is vibrotactile, which provide the information on correct postural alignment or the proper execution of movements.

3.1.2 Previous work

In the previous paragraph, it is possible noted that various studies have focused on cues as a smart sensory biofeedback with the most prevalent population being subjects affected by Parkinson's disease. In particular, the PASSO (Parkinson Smart Sensory cues for Older users) project aims to develop a wearable device and system that uses vibrations to enhance posture and address impairments like Pisa syndrome and camptocormia in individuals with Parkinson's disease (PD) [86]. Patients with this condition, have trouble maintaining proper posture which can affect their balance and gait. In particular, the excessive lateral movement can increase the risk of falls.

While drug therapies have limitations, alternative approaches such as deep brain stimulation and artificial biofeedback system show promise in addressing this issue [86]. The PASSO project employs a user-centered design approach to develop a smart system to transmit haptic cues [86]. This system consists of a sensor to detect inappropriate movement and an actuator to provide vibratory feedback [86]. The placement of sensor particularly on the chest or back and behind the person's shoulders, is crucial to ensure wearability and effectiveness (Figure 40) [86]. The optimal cue consists of a short vibration, from a smartwatch, was determined in collaboration with medical operators. The project aims to improve rehabilitation for PD patients in clinical settings and daily activities [86].

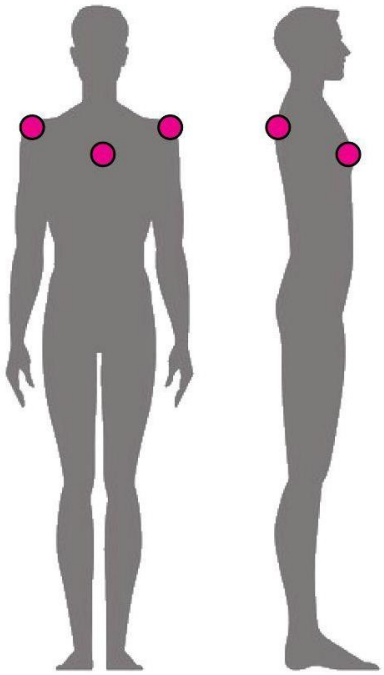

Figure 40 Choose position for actuators' location [86].

In Figure 41 shows the smart system prototype developed:

Figure 41 Data transmitted from the smartphone to the smartwatch [86].

The smartphone acts as a remote control to set different modes, is a graphical interface of the mHealth system [86]. It allows users to start and stop the training session and visualizing data reports [86]. The system's core is the smartwatch, it acts as a sensor and actuator; it returns a real-time haptic trunk-biofeedback, and it is positioned in the shoulder area for the project's aim [86].

3.2 Methods

As discussed in the previous paragraphs, wearable devices are also used in rehabilitation. In accordance with the thesis project, we will discuss the prototype developedment of biofeedback rehabilitation device for individuals with postural issues such as PISA syndrome (paragraph 3.1.2)

3.2.1 Prototype development

In the initial stage of PASSO project (chapter 3.1.2) , a smartwatch served as a sensor and actuator, but it proved unsuitable for this purpose. The vibration intensity of the smartwatch was too low, resulting in poor perception of the biofeedback. To enhance the perception of the biofeedback, the smartwatch was replaced with the Metamotion sensor (Figure 32).

Figure 42 Metamotion sensor, a wearable device that offers ***real-time and continuous monitoring of motion and environmental sensor data*** *[87].*

In particular, the model chosen is MetaMotionRL (MMRL) due to its small size (17mmx25mmx5mm). It is equipped with a rechargeable lithium-ion battery that lasts up to 14 days on a single charge [87].

The MetaMotion is a wearable device that offers a real-time and continuous monitoring of motion and environmental sensor data [87].

The sensor anlyses the data recorded by tri-axial accelerometer, gyroscope, and magnetometer to monitor movements. In particular, the sensor fusion algorithm (Bosch Kalman Filter Sensor Fusion) combines both the inertial and magnetic measurements [87].

MbientLab offers two apps (MetaBase and MetaWear), to configure MetaSensors and access the sensor data. These apps are available for free on the iOS (iOS version iOS 12 or higher is required) and Android (required Android version 10+) app stores. To use these apps, a Bluetooth connection must first be established between the smartphone and the sensor [87].

The MetaWear and MetaBase applications are both used to monitoring in the field of healthcare and research. Howeverthey have slightly different purposes and functionalities:

- MetaWear is used to configure, program and collect data from MetaWear devices; the data can be observed in real-time from the accelerometer or gyroscope; it is possible visualize angle inclination (Euler's angle or in quartenions) through Sensor Fusion. The data obtained from the recording can be saved directly on the smartphone used.
- MetaBase acts as a node for configuring and displaying data from various health monitoring devices; it offers visualization and data analysis capabilities.

The hardware and firmware components of MetaSensors are not accessible as open source, whereas the Application Programming Interface (API) and Apps are open source. This allows developers to modify the application interface according to their specific requirements and send commands to the board [87].

In this project, the MetaWear application was modified to develop a biofeedback rehabilitation app, that reflected the need of the protocol to be implemented in the PASSO project. Android Studio (version 12) is generally acknowledged as a standard tool for the application development and it is widely used by Android developers [87].

The developed application was named "myPosture". The graphical user interface has been designed focusing on simplicity and user-friendliness. The initial screen, as illustrated in Figure 33, allow the user to enter their patient identification code (ID) and corresponding password. To ensure easy of use, the first access is performed jointly with the clinician. After entering the required login credentials, the patient can access the application by clicking the "LOGIN" button located in the center of the screen.

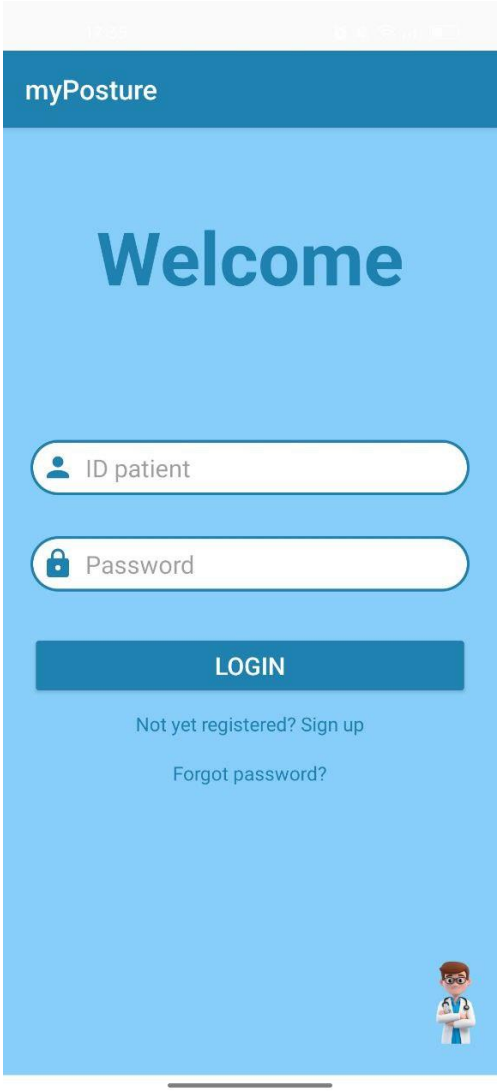

Figure 43 Login screen

Prior to logging in, the registration is mandatory for those who have not yet done it. To register, the user has to click on the option that affirm “Not yet registered? Sign up.”, located at the bottom of the Login button. In this way a new interface will appear on the screen, as shown in Figure 43.

To register, the subject (in collaboration with the clinician) has to enter the identification code (ID) and a password consisting of six numerical digits. In the subsequent field, is necessary to confirm the password. After setting the ID and the password, it is possible to proceed by clicking the “SIGN UP” button. If the user accidentally clicked “Not yet registered? Sign up”, he/she can return back by selecting “Already a user? Login”.

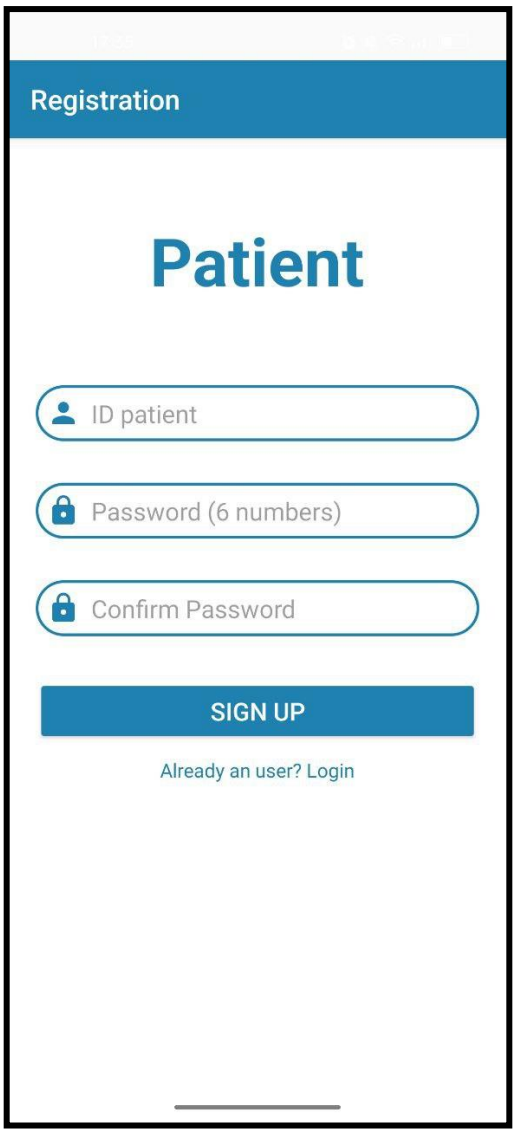

Figure 44 Registration page

In the home screen of the app MyPosture (Figure 43), there is an icon in the bottom right corner that represents a doctor. The icon operates as a button: when clicked, a distinct screen designed specifically for the clinician is displayed (Figure 45).

As the patient interface, the clinician access screen requires the entry of an identification code and password. After entering this information, it is possible to click the “LOGIN” button. As for the patient, if the clinician is not yet registered, he/she has to click the “Not yet registered? Sign up” button and a new screen is displayed (Figure 36).

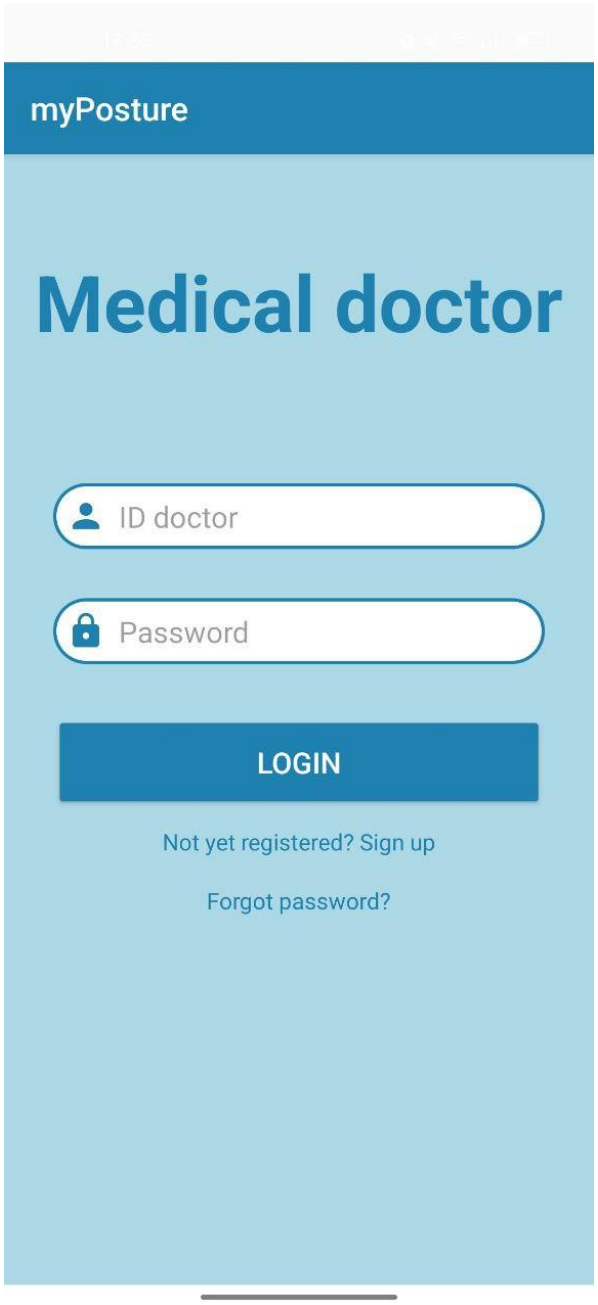

Figure 45 Medical doctor section

To register , the clinician has to enter the identification code (ID) and the password that must consist of 4 number digits. In the subsequent field, is necessary to confirm the password. Once these informations has been provided, it is possible to proceed by clicking on the “SIGN UP” button. If the clinician mistakenly clicked on “Not yet registered? Sign up”, he/she can return by selecting “Already a user? Login”.

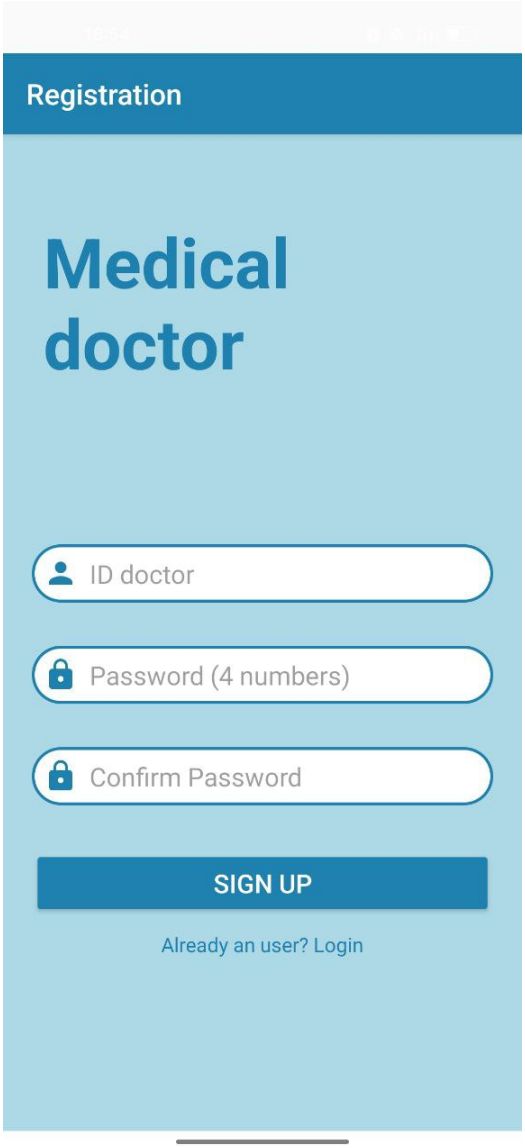

Figure 46 Medical doctor registration page

In the Login screen for both patients and clinician (Figure 43, 45), there is an option labeled “Forgot password?”. It represents a button which, when clicked, another screen will be open to recover the password (Figure 47).

In order to reset the initial password, the users have to enter their identification code (ID) in the appropriate field. Then, they can proceed by clicking on the “RESET PASSWORD” button. The same recovery procedure can be performed by the clinician, as is observerd in Figure 47.

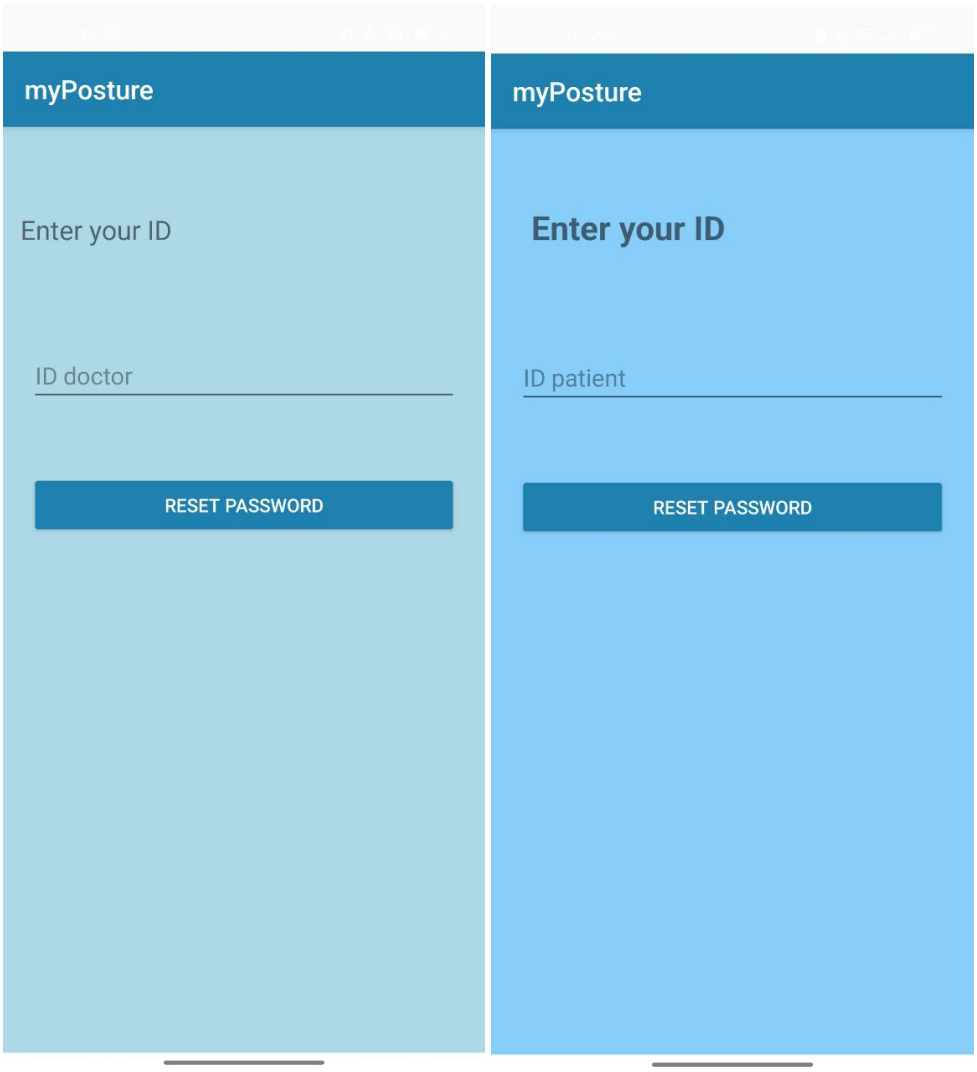

Figure 47 Reset password pages.

After the successful patient's login, the main screen (Figure 48) is displayed. The "START" button is located at the top centre of the screen and it is used to start the training session. The duration of each training session can be set from 20 to 30 minutes, with a recommended frequency of three sessions per week.

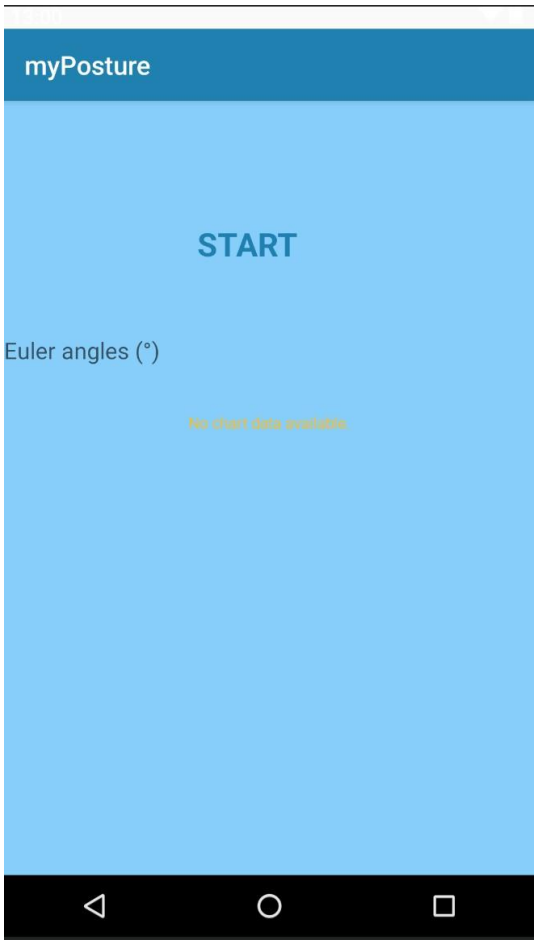

Figure 48 Main screen of initial training session.

In the application, two separate sections are designed for the clinician and the patient, due to their different target. Clinicians can monitor the output data from the wearable sensor (MetaMotion), even during real-life conditions outside the clinical setting. On the other hand, the patient can start the training session by pressing the START button, which activates the timer and sets the training duration. At the end of the training, the user receives a final evaluation of the assessment, which may include a pop-up stating "CONTINUE LIKE THIS" or "YOU CAN DO BETTER". However, it is does not provide any numerical information regarding the frequency of biofeedback occurred to assist the subjects in correcting their posture. These numerical values are accessible in the clinician page and can be used to track patient progress. The application itself has to give and augmented feedback approach to the patients, offering visual feedback of the postural training stability. It serves as a form of reinforcement, increasing the subject's motivation to improve their health. For this reason, individual training test outcomes may not be the most optimal approach for rehabilitative therapy. It is crucial for the patient to continue with rehabilitation without being discouraged by a negative result.

The patient data for training is stored in a local SQL-lite database. An identification code (ID) is assigned to each patient, recording their normal inclination while subject attempts to get into the correct position, and the degree to which the sensor must release the biofeedback vibration. Based on this information, each subject is provided with a personalized rehabilitation protocol to help them recover.

3.2.2 Prototype testing

Finally, the developed system was preliminary tested in three subjects with Parkinson's disease in order to gather information about its effectiveness, identify potential challenges, and gather user feedback. This step is crucial for further development of the prototype. To facilitate this process, a questionnaire was defined. The questionnaire consists of unequivocal questions regarding the utilised system (band and sensor). Responses are collected via binary options (YES and NO), or a rating scale from 1 to 5, where 1 represents disagreement or a lack of interest in using the device, and 5 indicates complete agreement. To ensure objectivity in the results, the test protocol was followed consistently for all the patients recruited.

QUESTIONNAIRE:

1) Would you be wearing the home training device?
    - Yes
    - No

2) How long would you use the device per day?
    - 10 minutes
    - 20 minutes
    - 30 minutes
    - More than 30 minutes

3) How many times a week?
    - 1 time
    - 2 times
    - 3 times
    - More than 3 times

4) How intense was the feedback from 1 (not perceived) to 5 (perceived with maximum intensity)?

1	2	3	4	5

5) Did vibration annoy you during the test?
    - Yes
    - No

6) If yes, how annoying was it from 1 (no hassle) to 5 (maximum annoyance)?

1	2	3	4	5

7) During the test:

- The band has guaranteed a more stable and correct posture.

  Yes O No O

- The band was comfortable (eg: not too narrow/wide)

  Yes O No O

8) Did you find the system easy to use? (1 = not at all simple, 5 = very easy)

1	2	3	4	5

9) Were you able to wear the band independently?

- Yes
- No

10) If yes, how much difficulty did you have from 1 (no difficulty) to 5 (maximum difficulty)?

1	2	3	4	5

11) If not, could you wear it with outside help?

- Yes
- No

12) There is something that would change about the design band?

a. Yes

b. No

13) If so, what would change?

_____

14) In general, do you think that the system can be helpful and applicable for posture correction in a home rehabilitation program?

- Yes
- No

15) If so, to what extent from 1 (not applicable and not aid) to 5 (highly applicable and very helpful)?

1	2	3	4	5

16) Comments and/or suggestions for possible changes

_____
_____
_____
_____
_____
_____

3.2.3 Algorithm development

The data obtained from the MetaMotion sensor had to be processed to obtain the subject's inclination as the final output. To achieve this, it was necessary to consider the data recorded from the accelerometer and gyroscope. Subsequently, a sensor fusion algorithm was developed to enhance the accuracy of information obtained by combining data from both inputs.

The majority of published sensor fusion algorithm (SFAs) can be divided into two main classes: Kalman filters (KF) and complementary filters (CF). In the last decades, numerous formulations of both groups have been proposed involving different mathematical orientation representations (such as quaternion, rotation matrix, Euler angles), also different Kalman filter formulations [88].

From a theoretical point of view, KF results to be the most appropriate filter since it can minimize signal errors. However, its implementation is challenging as it requires the assessment of noise distribution, computational load, and parameter tuning problems. For these reasons, the complementary filter was implemented in this thesis project [89], [90].

The complementary filters manage both high-pass and low-pass filters simultaneously. In particular, the low-pass filter filters high frequency signals (e.g. accelerometer data) and high-pass filter handles the low frequency signals (e.g. gyroscope drift) [90].

The analyses conducted in this thesis project are related to static condition. So, from MetaMotion sensor will consider the output from the accelerometer and gyroscope. In particular, the acquired accelerometer and gyroscope data underwent filtering to reduce noise. The gyroscope data was filtered using first-order Butterworth filter with a band-pass filtered between 0.001 Hz and 5 Hz.

On the other hand, the three-axis acceleration data was filtered using a first order low-pass Butterworth filter with a 10-Hz cutoff frequency [91].

Subsequently, using the filtered accelerometer data, Roll and Pitch angles are calculated using the following trigonometric formulas (eq. 1 and 2 respectively):

$$\theta = \arctan\left(\frac{A_x}{\sqrt{A_y^2 + A_z^2}}\right)$$

Equation 1 Pitch trigonometric formula.

$$\varphi = \arctan\left(\frac{A_y}{\sqrt{A_x^2 + A_z^2}}\right)$$

Equation 2 Roll trigonometric formula.

Then, a complementary filter was implemented to improve the orientation estimation angles. To update the roll and pitch angles, an integration cycle was used with a time-dependent weighted sum of accelerometer and gyroscope data. The weighted sum is defined by the coefficient alpha (α) [92], which is calculated as follows:

$$\alpha = \frac{dt}{\tau + dt}$$

Equation 3 Alpha coefficient definition: dt is defined as the inverse of the frequency (128Hz) and τ is the total duration of the test.

The pitch and roll angle values are defined as follows:

$$\varphi = (1 - \alpha) * roll(Gyro) + \alpha * roll(Acc)$$

$$\theta = (1 - \alpha) * pitch(Gyro) + \alpha * pitch(Acc)$$

Equation 4 Roll and Pitch formula in algorithm [92]

The sum of the filter coefficients, α and α-1 must be equal to 1, so that the output is an accurate estimate.

Showed below (Figure 49) the block diagram representing the implemented complementary filter:

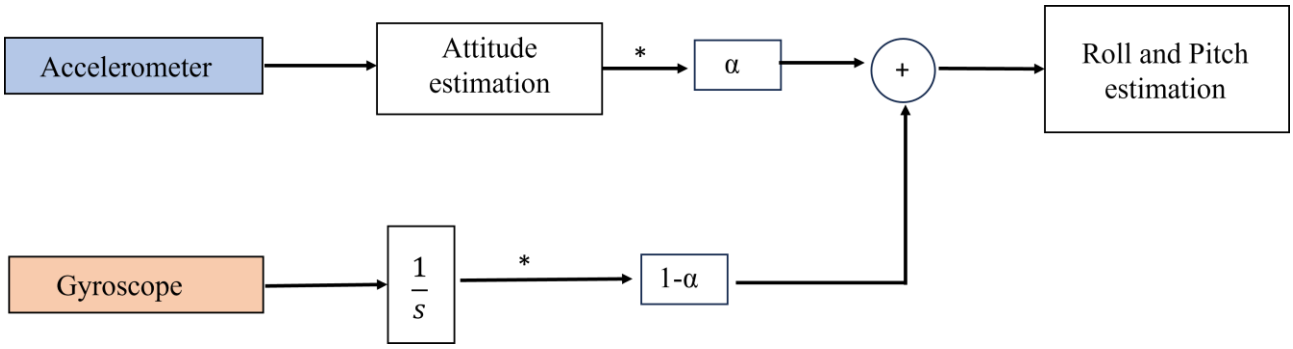

Figure 49 Block diagram of complementary filter

3.2.4 Algorithm validation

OPAL sensors vs stereophotogrammetric system

In order to validate the developed algorithm, the posture analysis parameters (roll and pitch angles respect to the vertical axis) obtained analysing the data recorded by MetaMotion sensor and computed by the developed algorithm were compared with the parameters obtained by a reference system (gold standard). In this work, the optoelectronic system from BTS Bioengineering was used as gold standard, which utilises 3D digital stereophotogrammetry to capture images of an object and reconstruct its three-dimensional coordinates. The optoelectronic system included in 7 reflective markers and 10 infrared cameras with a sampling rate of 800 Hz. In addition, four OPAL inertial measurement units were used: two placed above the shoulders (right shoulder IMU605, left shoulder IMU601), one above the back (between the two shoulders blade, IMU264), and one was utilized for the synchronization (IMU615). The sampling frequency of the OPAL sensors was 128 Hz. Opal sensors were selected for the evaluation due to their capability to synchronize multiple units, guaranteeing consistent time recording and enabling precise comparison of data collected by each unit. In addition, we had 4 Opal sensors compared to only 1 MetaMotion sensor.

Therefore, in order to assess the accuracy of the algorithm using data simultaneously collected in different positions, we used Opal sensors for the technical validation.

The protocol employed in this study was previously proposed by Bartolo et al. [93] to achieve the same purpose as ours and evaluate the lateral trunk flexion in Parkinsonian subjects.

This protocol defines the specific placement of the 7 markers on the subject as follow: right and left acromial process (AC_r, AC_l), spinous process of the 7th cervical vertebra (C_7), spinous process of the 9th thoracic vertebra (T_9), sacral prominence (S_a), and right and left anterior-superior iliac spines ($ASIS_r$, $ASIS_l$).

Figure 50 Position of the 7 markers in the correspective positions.

During the validation test, the subject performed two inclination tasks: trunk flexion and lateral bending (left and right).

Shown below (Figure 51) are reported the figures of the positioning of the Opal IMU605, IMU601 and IMU264 sensors:

Figure 51 Opal positioning.

Three different positions (Figure 52) were used to determine the optimal position of the OPAL sensors to capture the best motion data in the chosen rehabilitation context. The initial idea of PASSO project was to place the sensor on the opposite side to the subject's involuntary inclination. In this way, the patient understands the appropriate direction for executing corrective movements, assisted by sensor vibration (e.g., the bending is performed to the right side, the sensor is place on the left side).

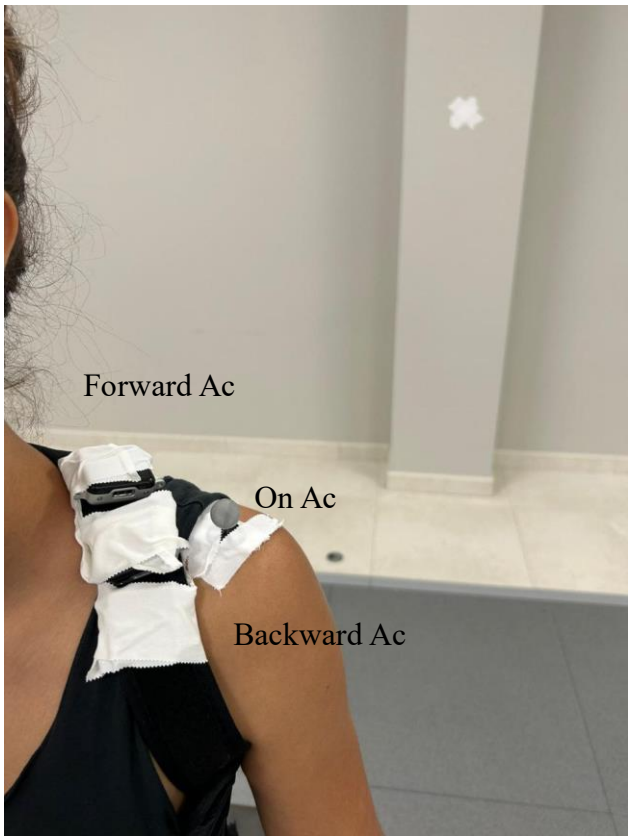

Figure 52 The three positions proposed to identify the best acquiring data. Abbreviation definition: Ac, is the acromial process.s

To perform the test, a band from the PASSO project (paragraph 3.1.2) was used. It featured a small pocket on the back, allowing for proper sensor placement. To place the sensors on the shoulder, since the provided pocket were too small for the OPAL sensors, scotch tape was used to fix them in the correct position.

Based on the placement of the sensor, the validation tests can be categorized as follows:

1) Right lateral bending, left lateral bending and forward trunk flexion with sensor positioned on acromial process;
2) Right lateral bending, left lateral bending and forward trunk flexion with sensor positioned forward acromial process;
3) Right lateral bending, left lateral bending and forward trunk flexion with sensor positioned backward acromial process.
4) Right lateral bending when three sensors positioned on the opposite left shoulder (Figure 41)

Prior to performing the test, the OPAL sensor used for the synchronization (IMU615) was placed on the BTS force plate. Three taps were then executed with a foot. to ensure the synchronization between IMU and BTS system.

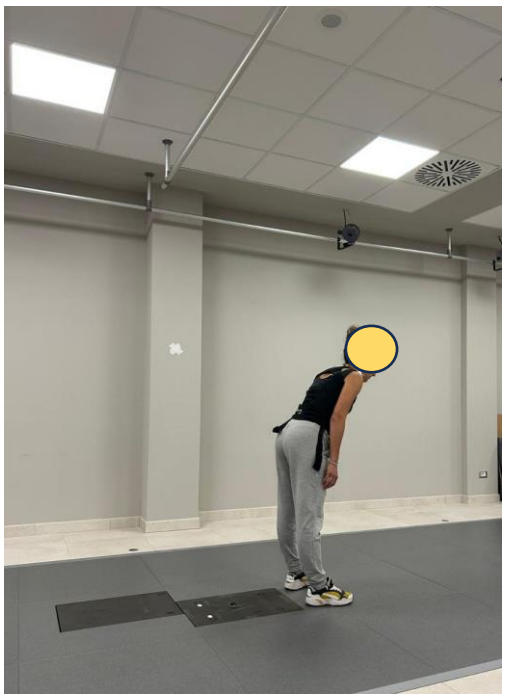

Figure 53 Forward trunk flexion test.

The test procedure for all tests, regardless of the sensor position, was conducted using the following protocol:

- Static position looking forward for 10 seconds
- 10 right lateral bending (pause for a few seconds before each inclination)
- Static position looking forward for 10 seconds
- 10 left lateral bending (pause for a few seconds before each inclination)
- Static position looking forward for 10 seconds
- 10 forward bending trunk

Numerical analyses were performed to compare the differences between the different signals in the various tests. For each inclination, the peak of the angle computed by stereophotogrammetric system

and wearable sensors (pks_stereo and pks_opal respectively) was analysed (Figure 54). The error between the detected peaks was defined as:

$$err(pks - pks) = mean(abs(pks_{stereo} - pks_{OPAL}))$$

Equation 5 Error difference between the peaks of the two analysed signals.

This formula calculates the average error between peak values obtained from stereophotogrammetry (pks_stereo) and those obtained with Opal sensors (pks_OPAL). For each identified peak the error is calculated by subtracting the value of the two peaks (stereophotogrammetry and Opal sensors). The absolute value of this difference was analysed. Then, the mean of all errors obtained is calculated to obtain an average error value for each test carried out.

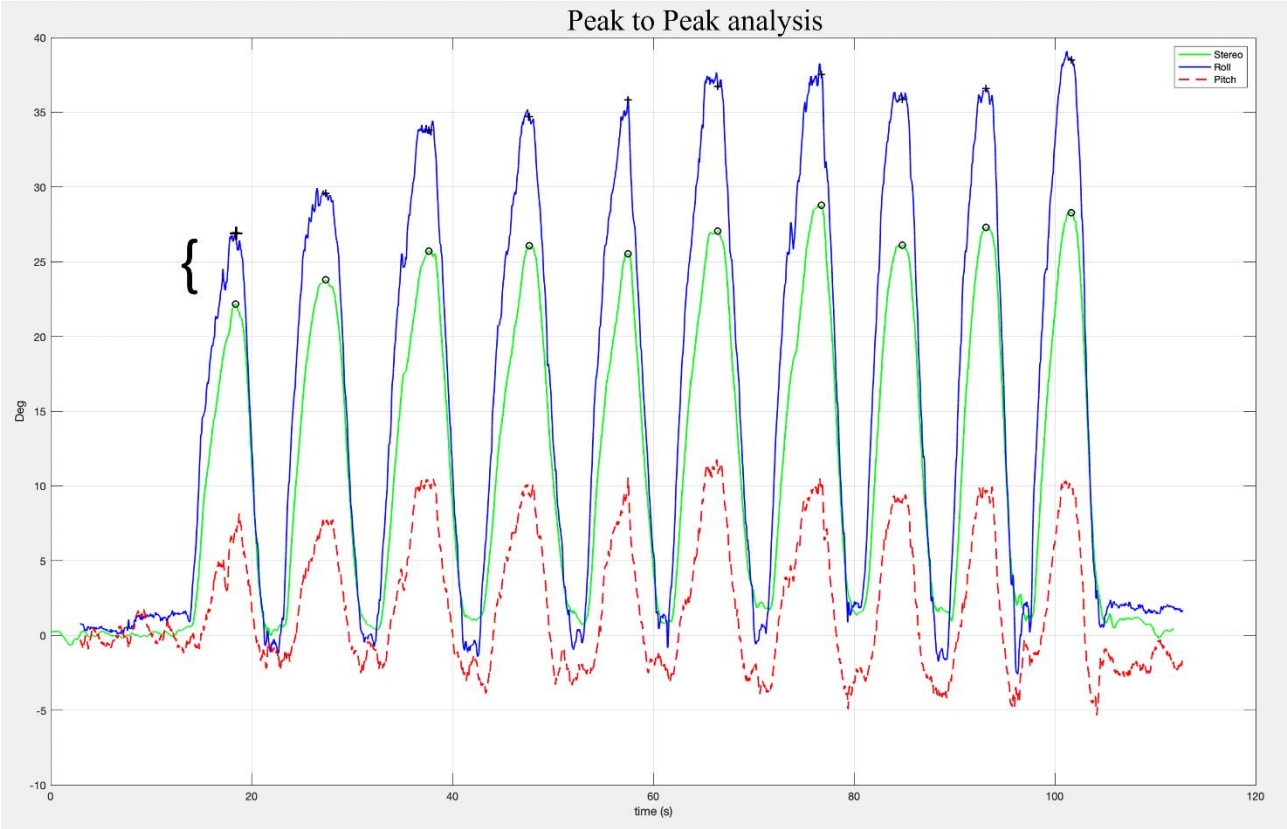

Figure 52 Example of the difference between Opal sensor peaks and stereophotogrammetry peaks.

Opal sensors vs MetaMotion sensors

As described above, OPAL sensors were used during the validation process due to the higher number of available sensors, despite the developed biofeedback rehabilitation system included a single MetaMotion sensor. To determine the comparability of data recorded by the two different system (OPAL and MetaMotion), an additional validation process was conducted between them,

To achieve this, three tests were performed:

1) Right lateral bending with the sensor placed on the left shoulder.
2) Left lateral bending with the sensor placed on the right shoulder (Figure 43)
3) 5 min of static acquisition with sensors placed on a table in a resting condition (Figure 44).

To perform test 1 and 2, the two IMU sensors were placed on the shoulder in a stacked manner using tape scotch (Figure 55) and the following protocol was performed:

- Static position looking forward for 15 seconds.
- 10 lateral bending (pause for a few seconds before each inclination)
- Static position looking forward for 15 seconds.

Figure 55 MetaMotion and Opal sensors' position

As for the previous validation process between OPAL and stereophotogrammetry, before each test three tappings were performed with a forefinger on the stacked IMUs to synchronize post-processing the two different systems.

Figure 56 Two sensors place on a table.

In order to compare the values obtained by the two IMU sensors, the root-mean-square-error was calculated for all three tests in order to evaluate the discrepancy between the two different acquisition systems.

$$E = \sqrt{\frac{1}{n}\sum_{i=1}^{n} |A_i - F_i|^2}$$

Equation 6 Root mean square error formula. In our case, variable A represents MetaMotionRL data and variable F represents Opal sensor data.

3.3 Results

3.3.1 Prototype Test and subject feedback

Three participants were recruited for the evaluation of the developed biofeedback system consisting of a band, a sensor, and a smartphone. Assisted by the clinician (Figure 57), the participant wore the band with the sensor. A vibrotactile biofeedback was sent during a static position to evaluate the subject' perception of the feedback by the subjects. Then, participants were instructed to bend laterally or to assume a resting position. At the end of the test, each participant was invited to complete a defined questionnaire (cap 3.2.2)

Figure 57 Correct positioning of band and sensor.

Depending on the requirements of each subject, the sensor was placed in the most effective location for providing feedback (e.g., Figure 58). Furthermore, we tested other placements to evaluate if the feedback could be perceived accurately.

Figure 58 Sensor position.

Below is reported the questionnaire including responses from the three recruited subjects.

QUESTIONNAIRE:

1)Would you be wearing the home training device?

- Yes [3/3, 100%]
- No

2)How long would you use the device per day?

- 10 minutes
- 20 minutes
- 30 minutes [2/3, 66,6%]
- More than 30 minutes [1/3, 33%]

3)How many times a week?

- 1 time
- 2 times
- 3 times [2/3, 66,6%]
- More than 3 times [1/3, 33%]

5) How intense was the feedback from 1 (not perceived) to 5 (perceived with maximum intensity)? The answer to this question pertains the position of the sensor on acromial processs.
   - 1
   - 2
   - 3
   - 4 [1/3, 33%]
   - 5 [2/3, 66,6%]

6) Did vibration annoy you during the test?
   - Yes
   - No [3/3, 100%]

7) If yes, how annoying was it from 1 (no hassle) to 5 (maximum annoyance)?

1	2	3	4	5

8) During the test:

- The band has guaranteed a more stable and correct posture.
  - Yes [3/3, 100%]
  - No
- The band was comfortable (eg: not too narrow/wide)
  - Yes [3/3, 100%]
  - No

9) Did you find the system easy to use? (1 = not at all simple, 5 = very easy)

- 1
- 2
- 3
- 4
- 5 [3/3, 100%]

10) Were you able to wear the band independently?

- Yes [3/3, 100%]
- No

11) There is something that would change about the design band?

c. Yes [1/3, 33,3%]

d. No [2/3, 66,6%]

12) In general, do you think that the system can be helpful and applicable for posture correction in a home rehabilitation program?

- Yes [3/3, 100%]
- No

13) If so, to what extent from 1 (not applicable and not aid) to 5 (highly applicable and very helpful)?

- 1
- 2
- 3 [1/3, 33,%]
- 4 [1/3, 33,%]
- 5 [1/3, 33,%]

As noted in the answer to question 4, there was a clear perception of the vibration feedback when the sensor was placed on the acromial process. However, further tests were conducted to assess the perception of the sensor vibration in other locations.

For example, the perception was very low (average vote 2) when the sensor was placed in the middle of the back (between the shoulder blades). In this particular position, patients reported perceiving the noise generated by the sensor more than the vibration feedback itself. This issue may lead to discomfort outside a clinical setting (e.g., home rehabilitation training). One possible solution could be designing a new sensor case that amplified vibration propagation, ensuring optimal perception without generating noise. Alternatively, using two sensors on each shoulder blade could also be another possible solution as this position is supposed to be more sensitive.

Regarding the comments and suggestions received from the participants (question 16), there are some important considerations to take into account. Firstly, patients would like to have a system easy to set up: it is necessary to have a designated pocket fixed in the band to guarantee the proper placement of the sensor. Furthermore, the lack of optimal and custom calibration was highlighted, allowing each subject to have a dedicated initial configuration (e.g., initial tilt angle). In this way, the rehabilitation system would only provide feedback when a specific inclination established by the clinician is exceeded.

One case that is important to focus on is related to a person suffering from lumbar scoliosis who tested the biofeedback system (Figure 59).

Figure 59 Subject suffering from lumbar scoliosis

Initially, the sensor was placed on the shoulder to assess if the patient's ability to understand the movement required to adopt a correct posture. However, the patient experienced difficulty in evaluating the required movement. In contrast, when the sensor was placed manually on the iliac ridge(where scoliosis is present at the pelvis), the movement to achieve a correct posture was performed without difficulty. To improve system accessibility for various pathologies (e.g such as scoliosis patients), it may be more beneficial to explore alternatives bands suitable for particular sensors positions (e.g., waist). Regarding to the patient with lumbar scoliosis, it would be appropriate to use a longer band that can reach the iliac ridges, allowing for proper placement of the sensor.

3.3.2 Algorithm validation

OPAL sensors vs stereophotogrammetric system

To test the reliability of the implemented algorithm, Matlab software was used to conduct the analyses. Initially, the signal obtained from stereophotogrammetry was superimposed on the signal recorded through Opal sensors, obtained through the processing of the complementary filter that was put into action. This process allows to compare and validate the accuracy of the data obtained by the two different monitoring systems.

In addition, it is important to note that the signal from the Opal sensor has been divided into two angular components: pitch and roll.

As defined in the previous chapter (3.2.3), three different Opal sensor positions were evaluated to determine the optimal configuration for data logging.

The following plots show on the x-axis the acquisition time of the signal, expressed in seconds (s) and on the y-axis the degrees of inclination, expressed in degree (°). The green curve represents the signal obtained by stereophotogrammetry, while the blue and red curves indicate respectively the roll and pitch components of the signal acquired with Opal sensors.

Before analysing the data obtained from the different tests, it is important to focus attention on the graph (Figure 60) that illustrates the tapping as defined in paragraph 3.2.3. Graphs are helpful in analysing data since they help to understand when the moment of interest was started, without considering the previous phase that is usually characterized by noise or signals that are not of our interest.

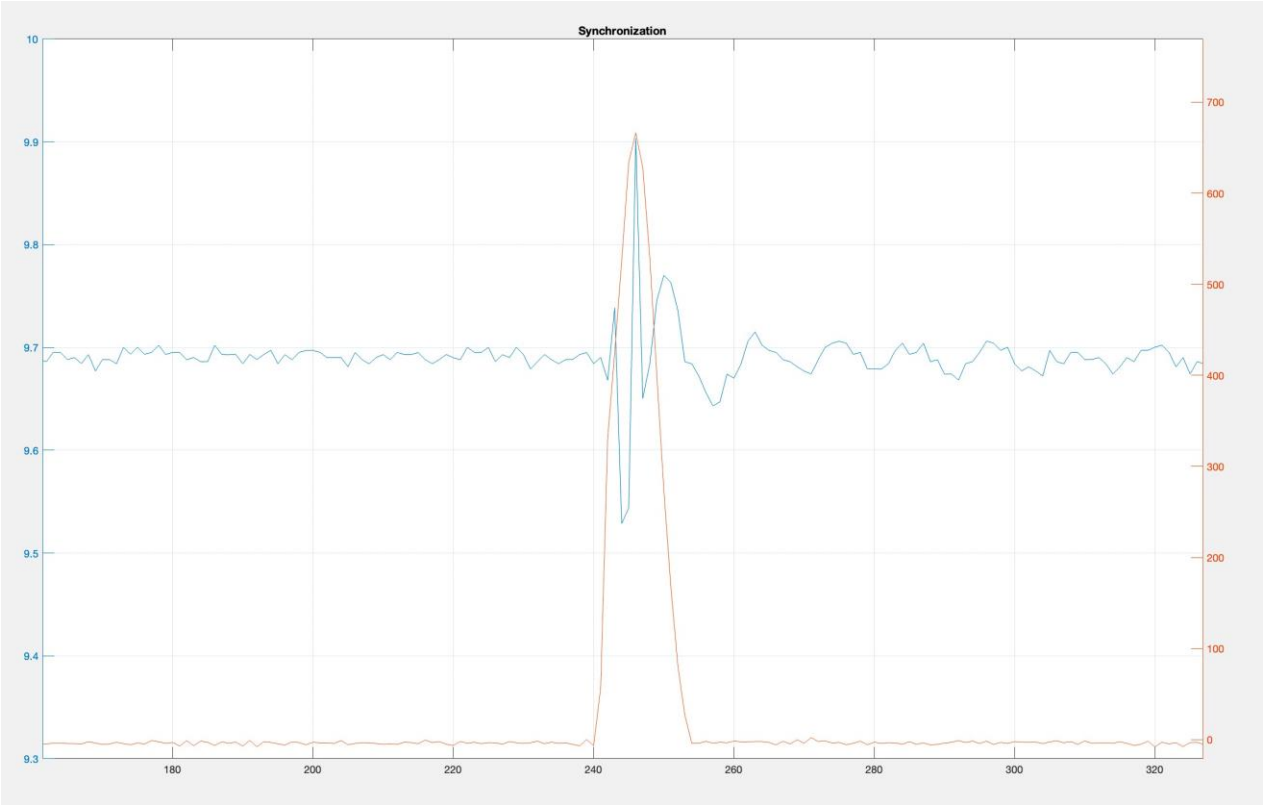

Figure 60 Representation of a tapping signal, which we can identify the synchronization between the two different source signals (Opal IMU and force plate).

The first three pairs of plots represent the data obtained from stereophotogrammetry and Opal sensors positioned in the central shoulder position.

Static 1: sensor placed on the acromial process

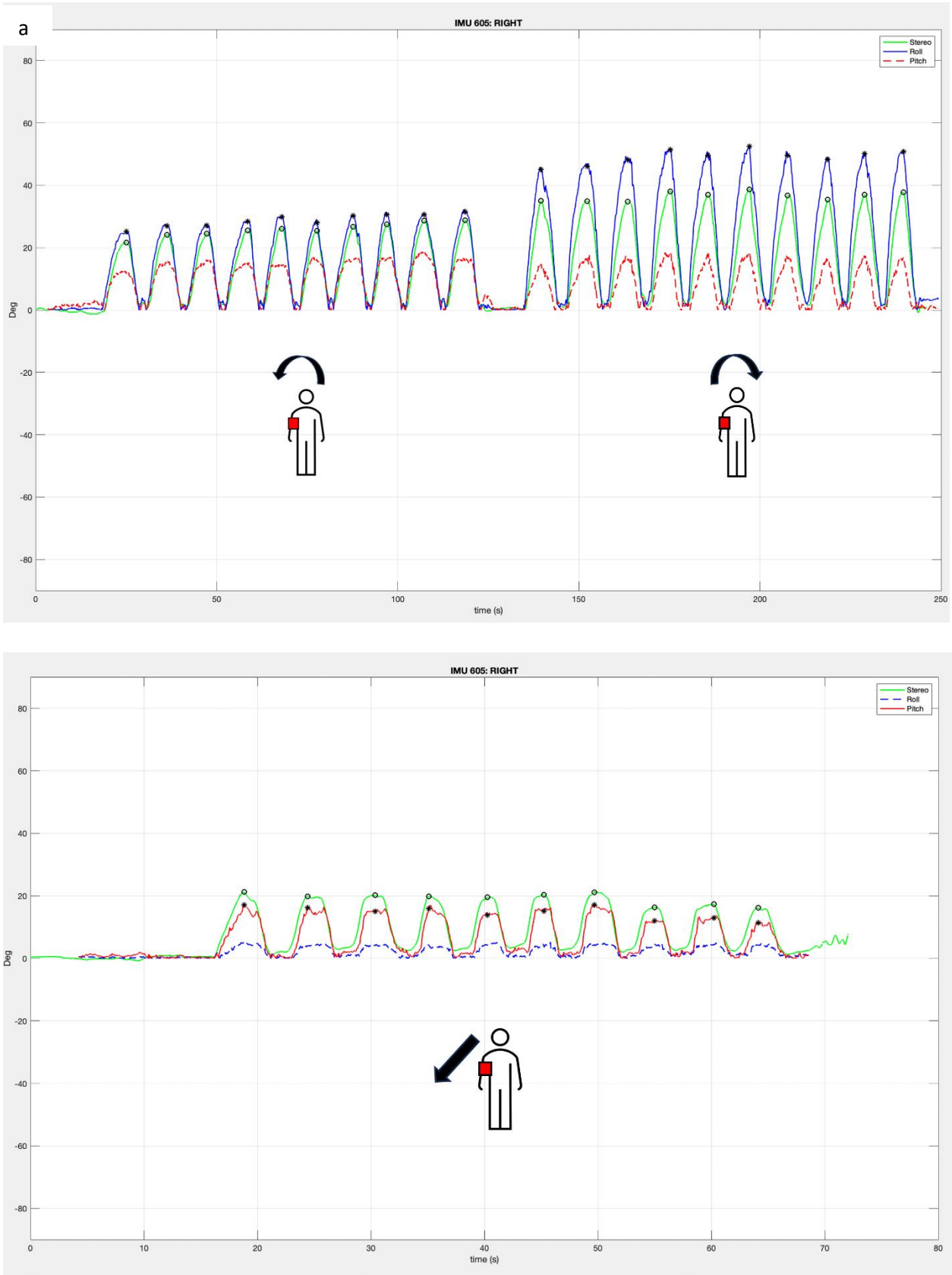

Figure 61 Graphs of Opal 605 positioned on the right shoulder. In part a the lateral bending is shown, with the first 10 right inclinations and after 10 inclinations to the left. Part b of the figure represents the 10 forward trunk inclination.

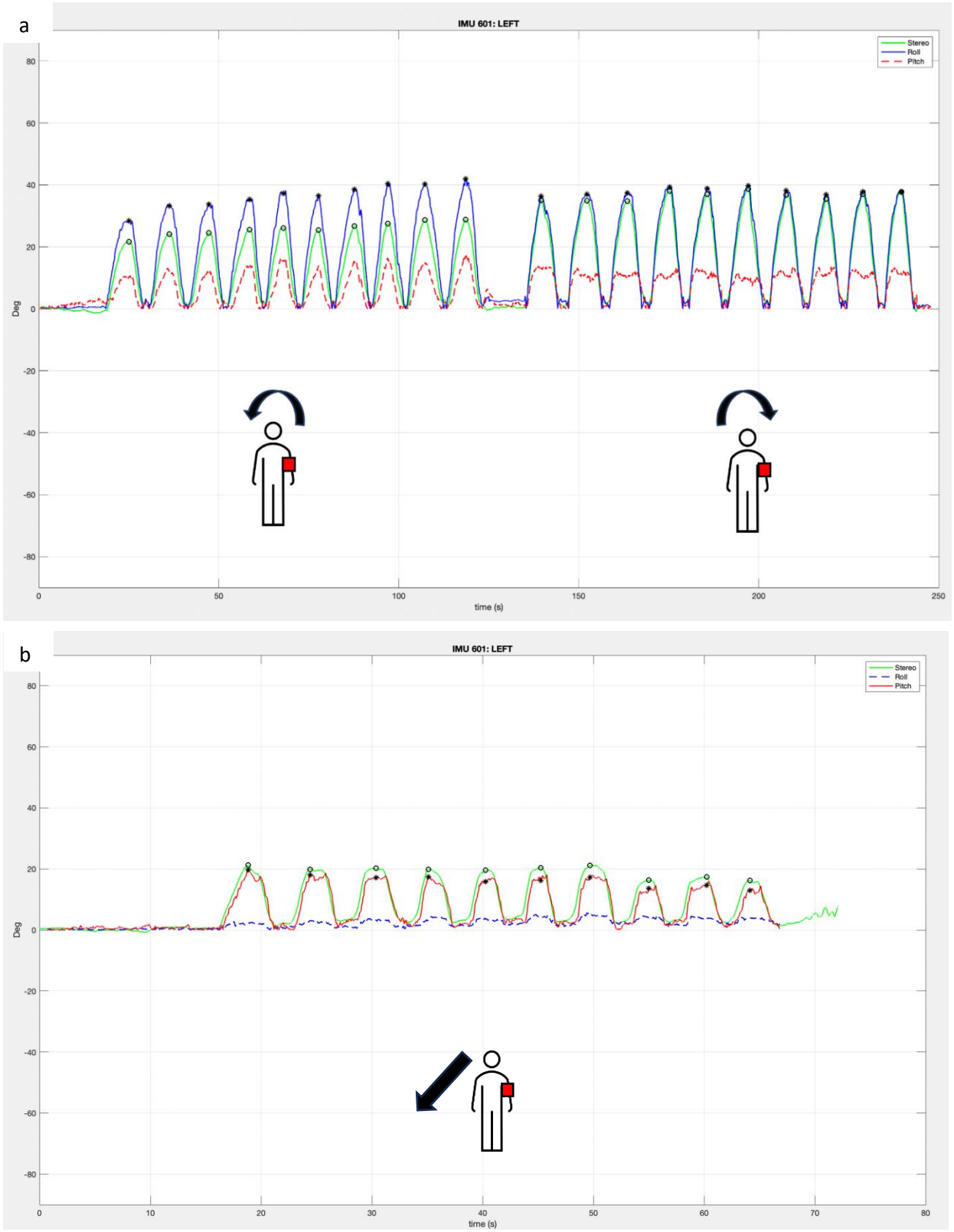

Figure 62 Graphs of Opal 601 positioned on the left shoulder. In part a the lateral bending is shown, with the first 10 right inclinations and after 10 inclinations to the left. Part b of the figure represents the 10 forward trunk inclination.

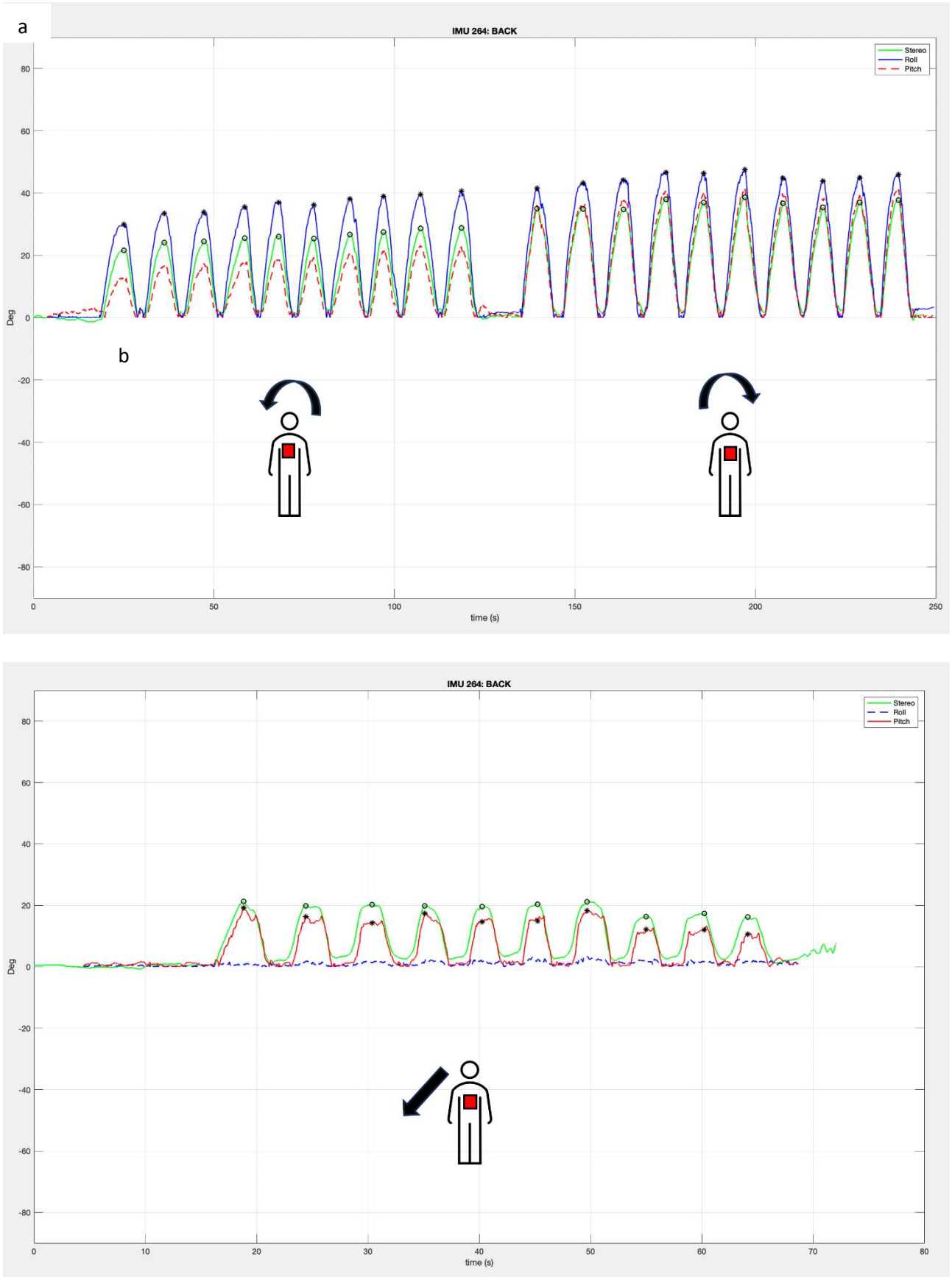

Figure 63 Graphs of Opal 264 positioned on the upper back. In part a the lateral bending is shown, with the first 10 right inclinations and after 10 inclinations to the left. Part b of the figure represents the 10 forward trunk inclination.

Subsequently, the same procedure was carried out by placing the sensors in the anterior position of the shoulder. The following three plots represent the data obtained from stereophotogrammetry and Opal sensors positioned in the anterior shoulder position.

Static 2: sensor placed forward the acromial process

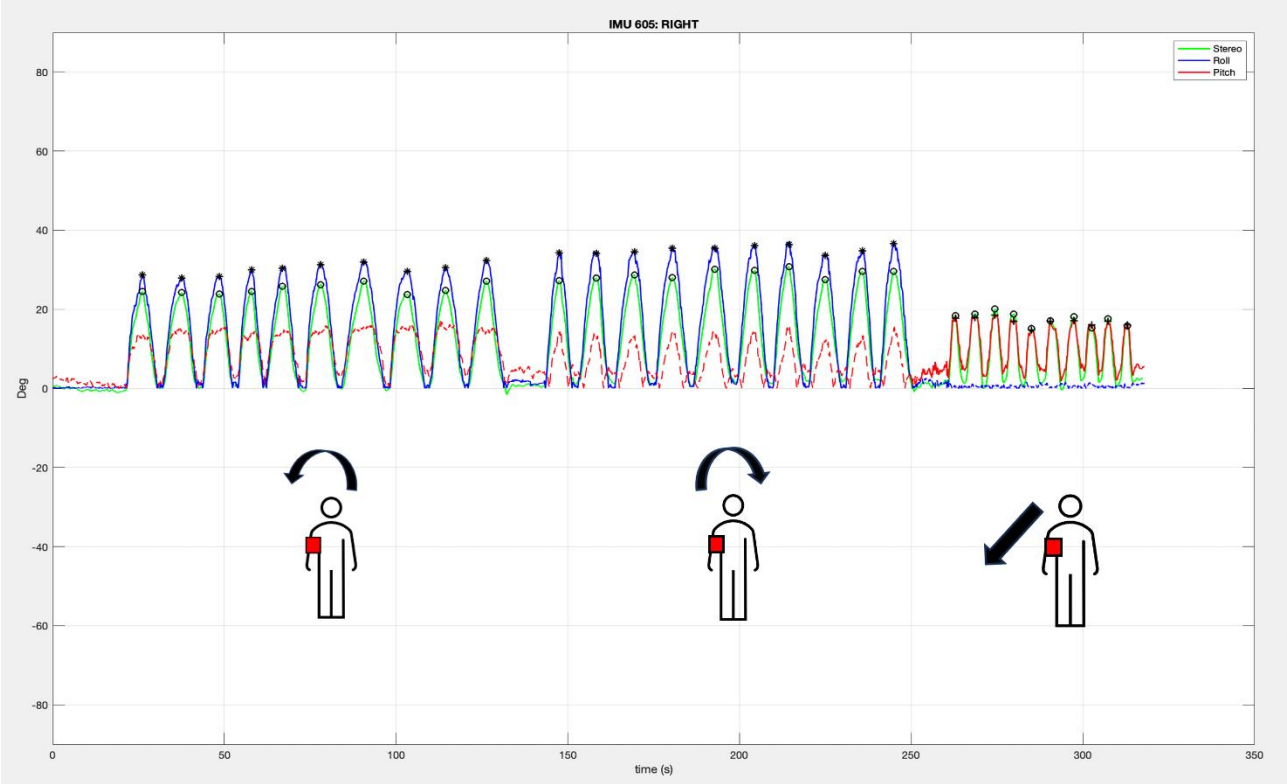

Figure 64 Graphs of Opal 605 positioned on the right shoulder. It is represented: the first 10 right inclinations, 10 inclinations to the left and finally the 10 forward trunk inclination.

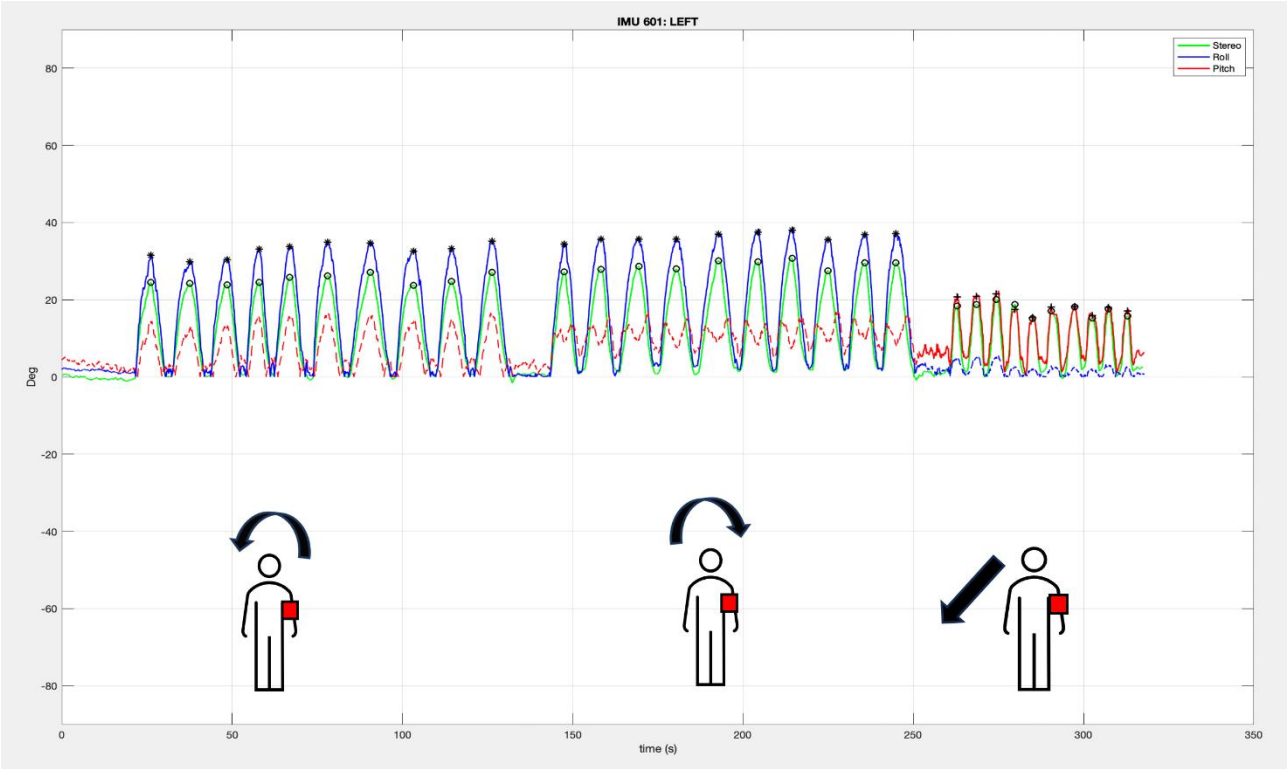

Figure 65 Graphs of Opal 601 positioned on the left shoulder. It is represented: the first 10 right inclinations, 10 inclinations to the left and finally the 10 forward trunk inclination.

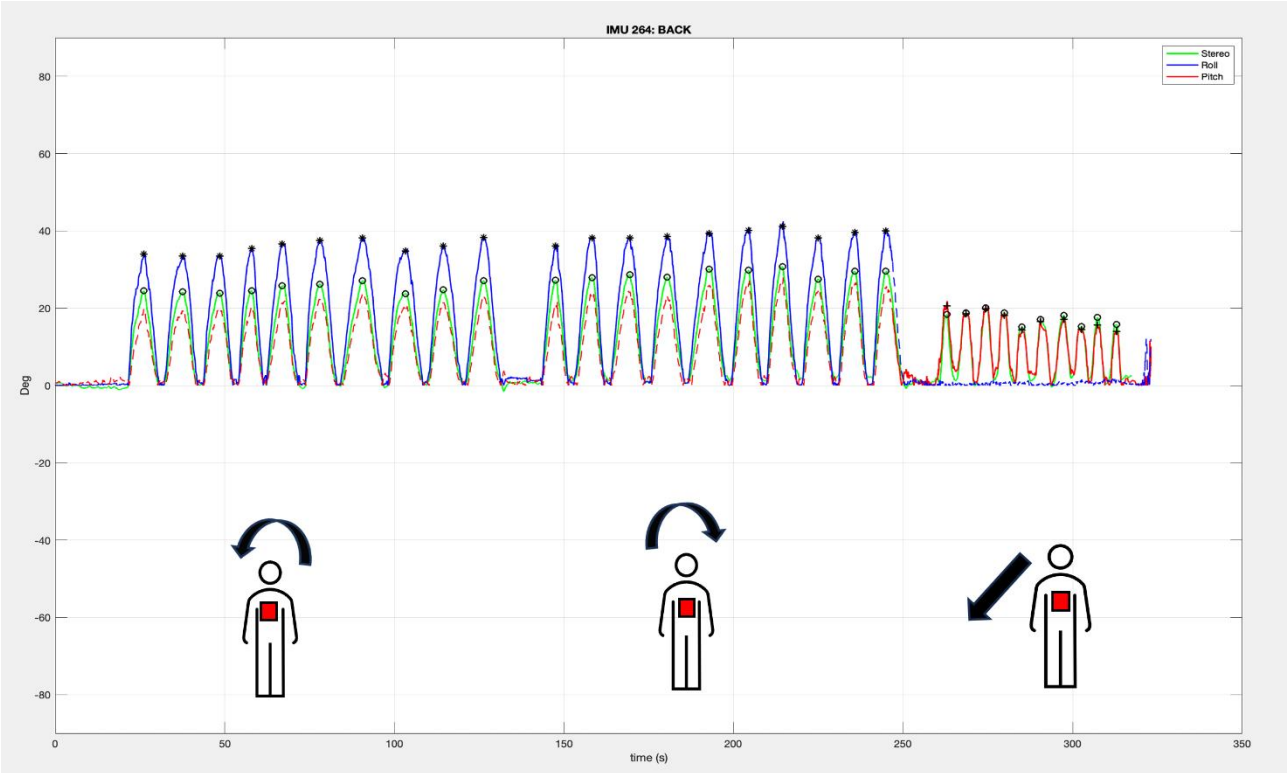

Figure 66 Graphs of Opal 264 positioned on the upper back. It is represented: the first 10 right inclinations, 10 inclinations to the left and finally the 10 forward trunk inclination.

Finally, the same procedure was carried out by placing the sensors in the posterior position of the shoulder. The following three plots represent the data obtained from stereophotogrammetry and Opal sensors positioned in the posterior shoulder position.

Static 3: sensor placed backward the acromial process

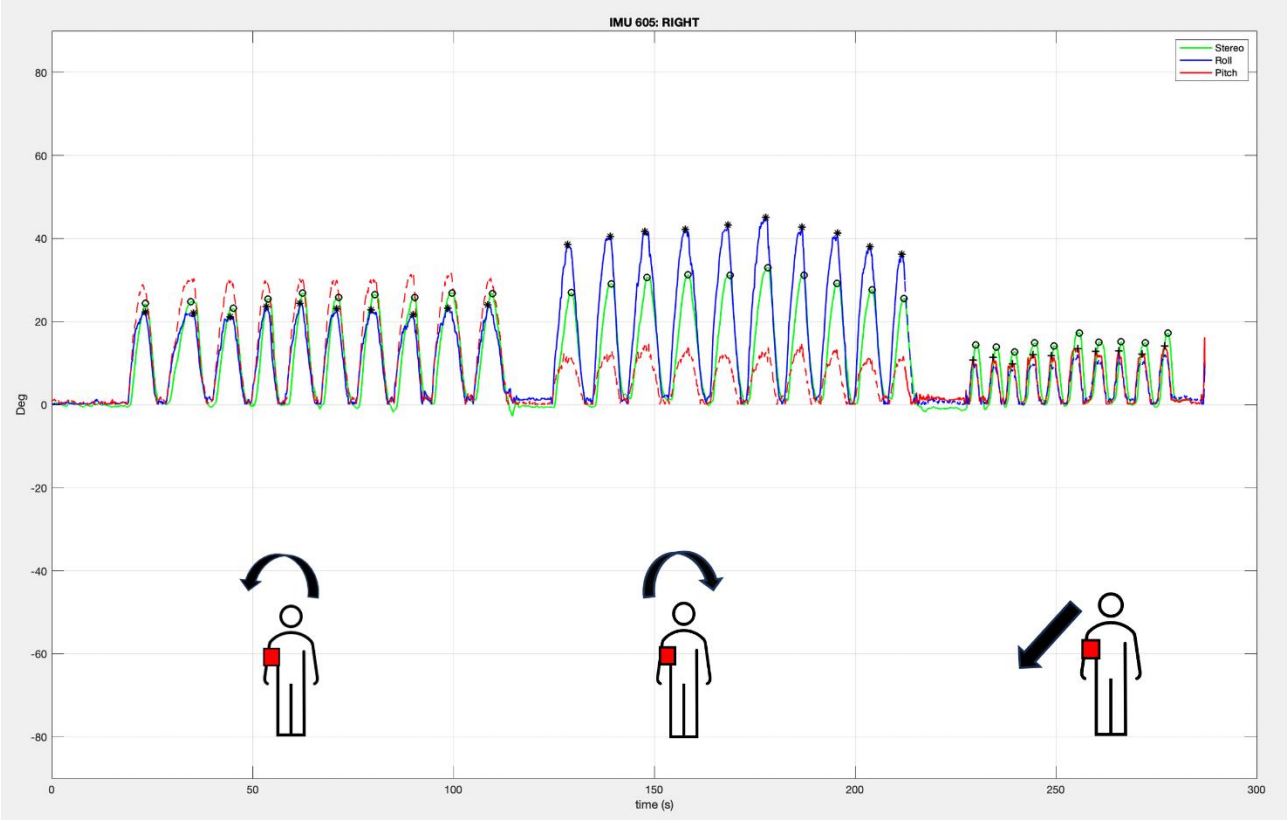

Figure 67 Graphs of Opal 605 positioned on the right shoulder. It is represented: the first 10 right inclinations, 10 inclinations to the left and finally the 10 forward trunk inclination.

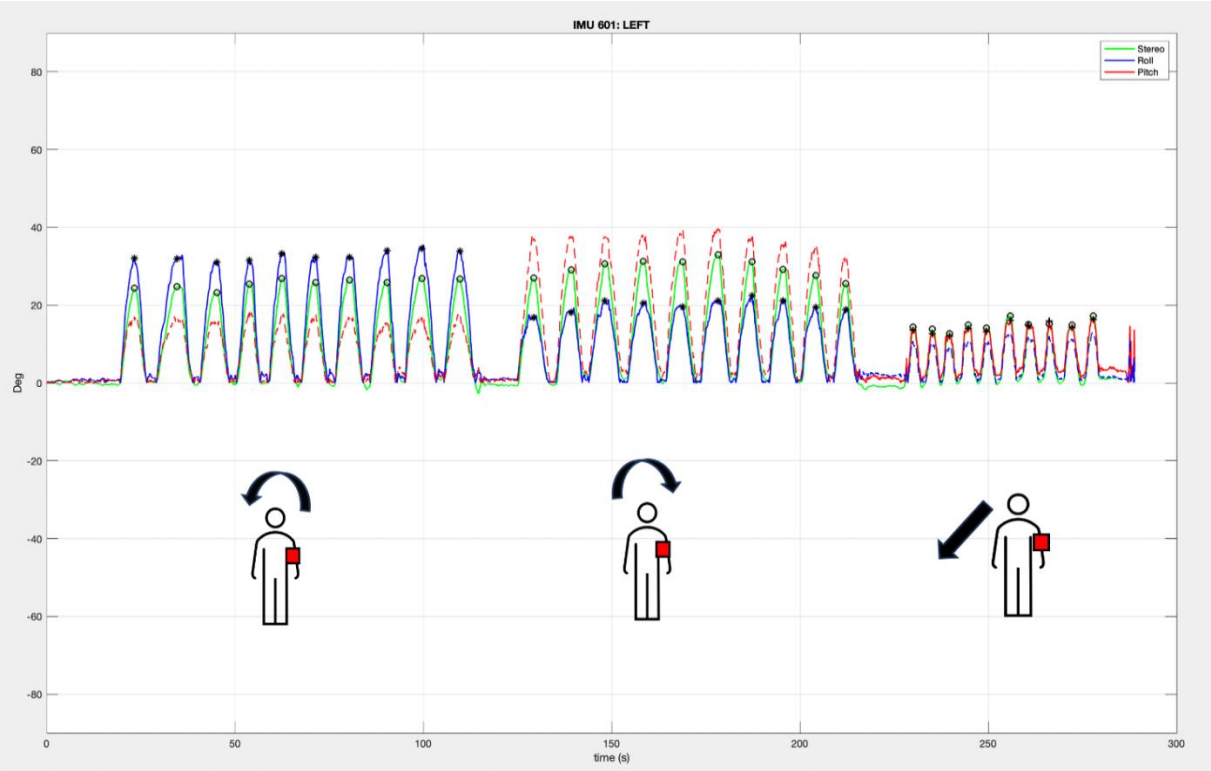

Figure 68 Graphs of Opal 601 positioned on the left shoulder. It is represented: the first 10 right inclinations, 10 inclinations to the left and finally the 10 forward trunk inclination.

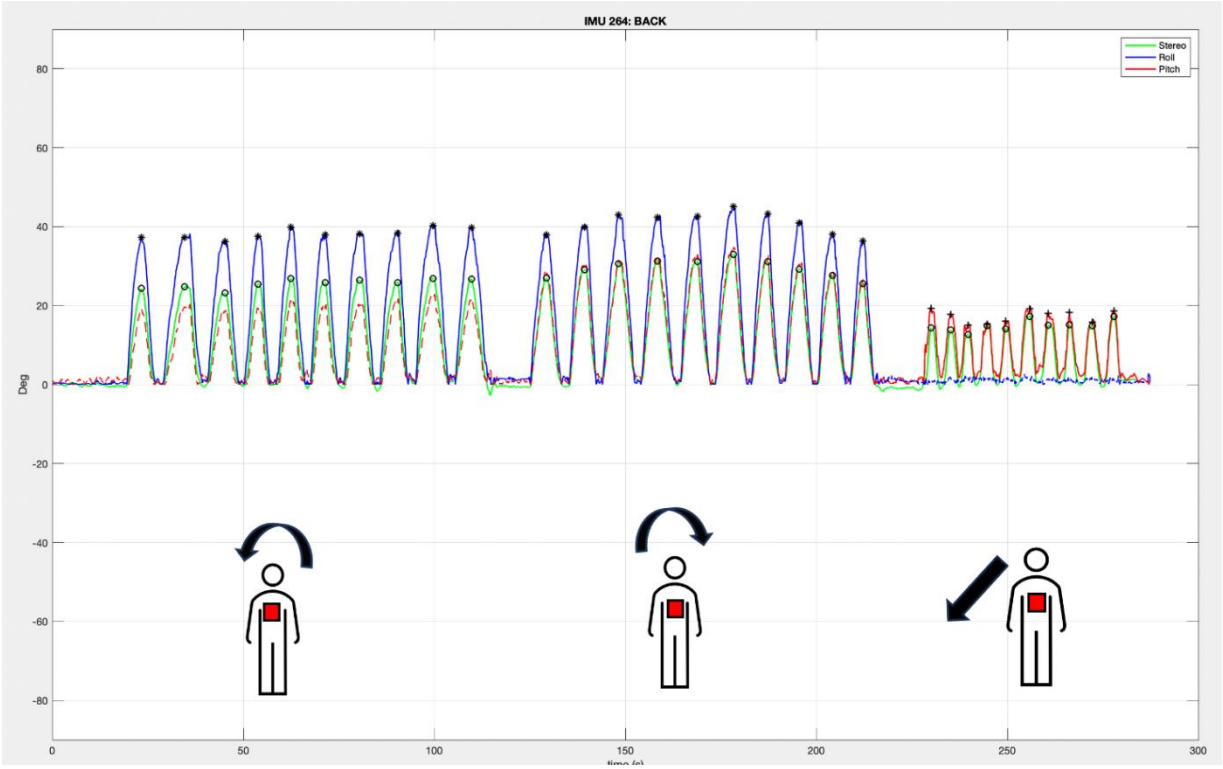

Figure 69 Graphs of Opal 605 positioned on the right shoulder. It is represented: the first 10 right inclinations, 10 inclinations to the left and finally the 10 forward trunk inclination.

From all the graphs becomes evident a gap between the peak of the stereophotogrammetry signals and the signals obtained through the complementary algorithm. Moreover, it is observed that the trends of pitch and roll angles are in accordance with the theory. When forward flexion, the roll angle remains close to the zero-degree value (or with a minimum deviation), while the pitch angle reaches its maximum width. On the other hand, when lateral bending (to the right and left), the roll angle reaches its maximum, while the pitch angle shows a smaller width.

In the last analysis, the three sensors were placed on the left shoulder to determine the optimal location for Opal sensor data collection.

Static 4: three sensors placed on the same shoulder

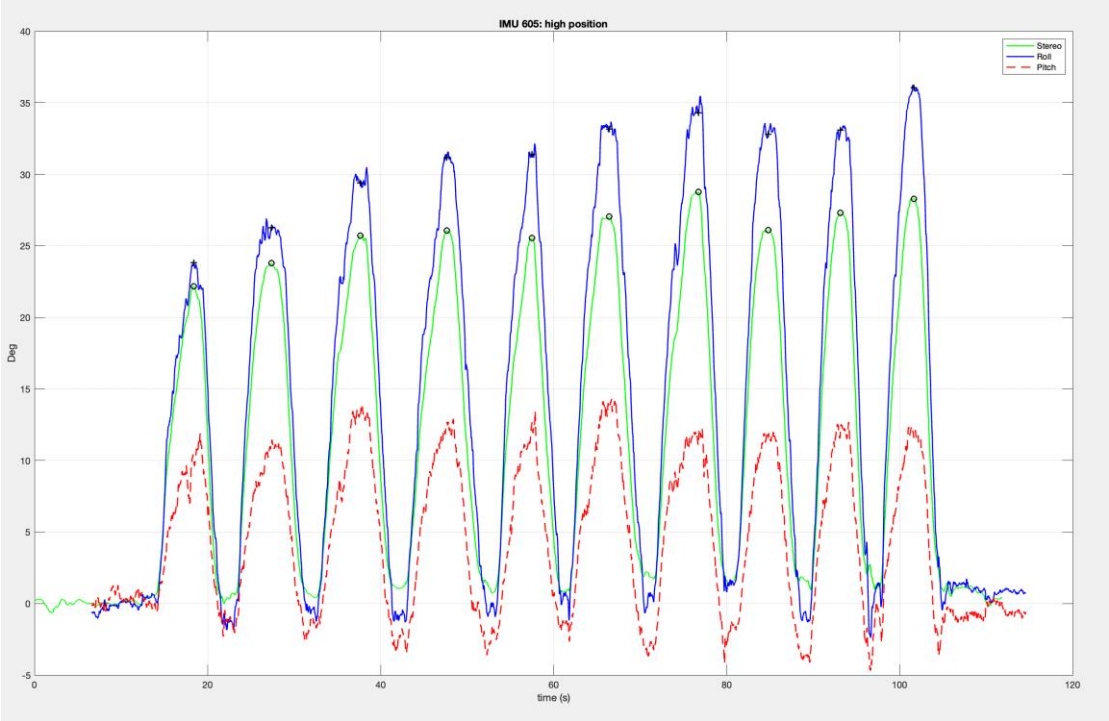

Figure 70 Graph of the 10 left inclinations recorded by the Opal 605 sensor, positioned forward acromial process.

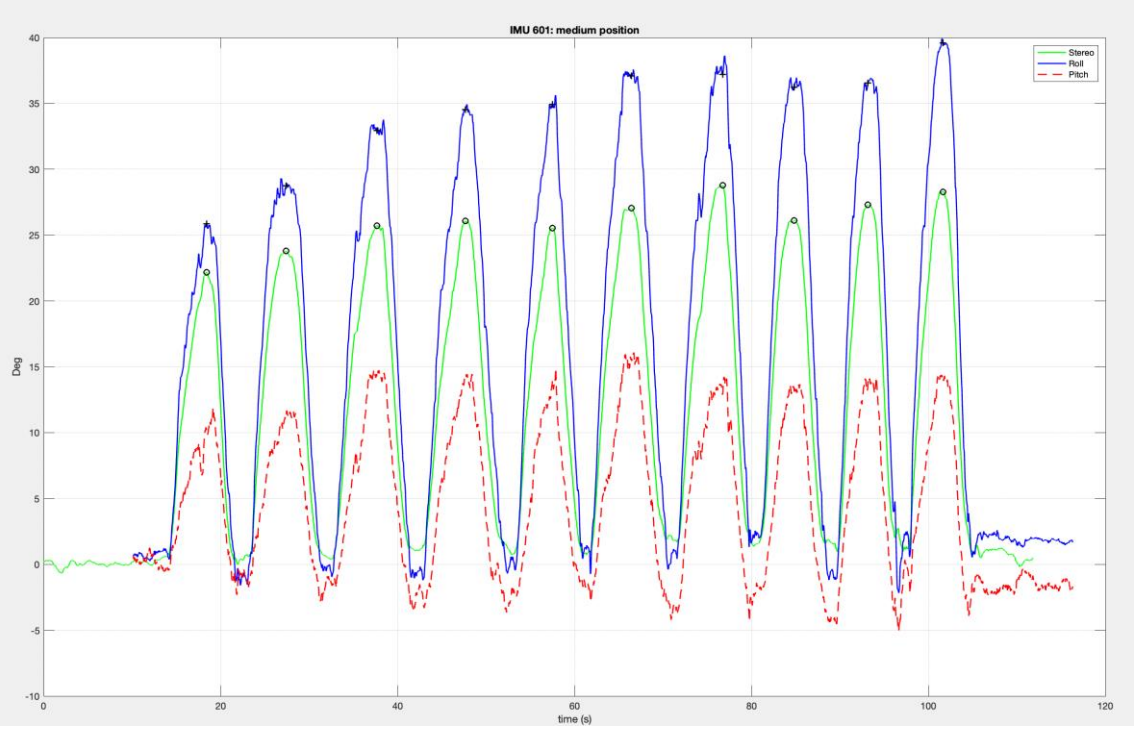

Figure 71 Graph of the 10 left inclinations recorded by the Opal 601 sensor, positioned on acromial process.

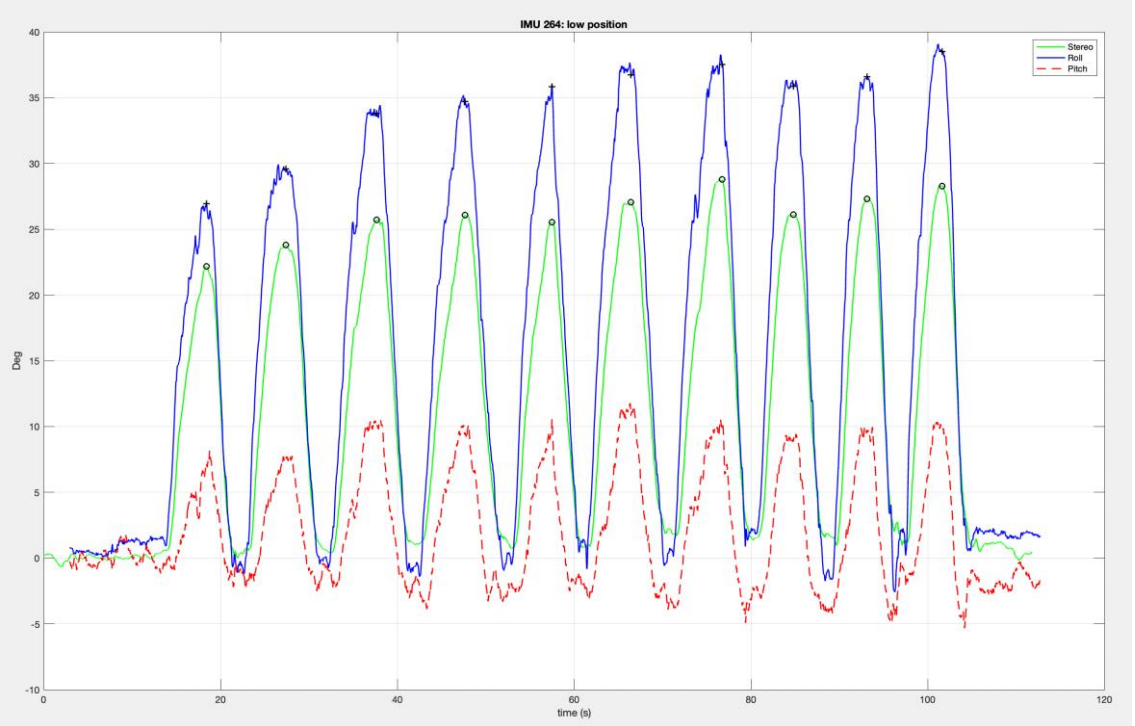

Figure 72 Graph of the 10 left inclinations recorded by the Opal 264 sensor, positioned backward acromial process.

Test	Sensor position	Right inclination		Left inclination		Forward inclination
		Right Sensor	Left Sensor	Right Sensor	Left Sensor	Back Sensor
Static 1	On Ac	2.9608	10.6603	12.6421	1.3872	4.2540
Static 2	Forward Ac	4.8979	7.7343	6.2103	7.4583	1.0232
Static 3	Backward Ac	4.201	7.0382	8.2332	9.6733	2.4060
Static 4	On Ac	-	8.2842	-	-	-
	Forward Ac	-	8.5281	-	-	-
	Backward Ac	-	5.0625	-	-	-

Table 7 Diagram of Static Tests based on sensor position and value error. Abbreviation definition: Ac is the acromial process.

In the second analysis, it was considered a range of values that precede and follow the peak to analyse the variations between the two signals around the peak.

As in the previous analysis, the error was calculated, and the values are presented in the following table:

Test	Sensor position	Right inclination		Left inclination		Forward inclination
		Right Sensor	Left Sensor	Right Sensor	Left Sensor	Back Sensor
Static 1	On Ac	2.9730	6.9918	8.8945	2.0512	3.6747
Static 2	Forward Ac	4.3718	5.6806	4.9728	6.8909	1.1813
Static 3	Backward Ac	2.7742	4.9165	7.3625	4.0939	2.3662
Static 4	On Ac	-	6.1571	-	-	-
	Forward Ac	-	5.9802	-	-	-
	Backward Ac	-	4.0879	-	-	-

Table 8 Diagram of Static Tests based on sensor position and value error. Abbreviation definition: Ac is the acromial process.

From the values relative to the errors, it can be said that the sensor positioned on the side of the inclination offers a better acquisition than the other positions (e.g., opposite side). In the static test 4, where all three sensors were placed on the same shoulder, the best result is when the sensor is slightly backward the shoulder position.

OPAL sensors vs MetaMotion sensor

A further analysis was carried out to compare the acquired data of the Opal sensor and the MetaMotion sensor and evaluate the root mean square. From the output signals, the norms of acceleration and gyroscope were calculated.

In the first test, the Opal 601 and MetaMotionRL sensors are stick together, one above the other, and placed on the left shoulder. The bending is performed to the right.

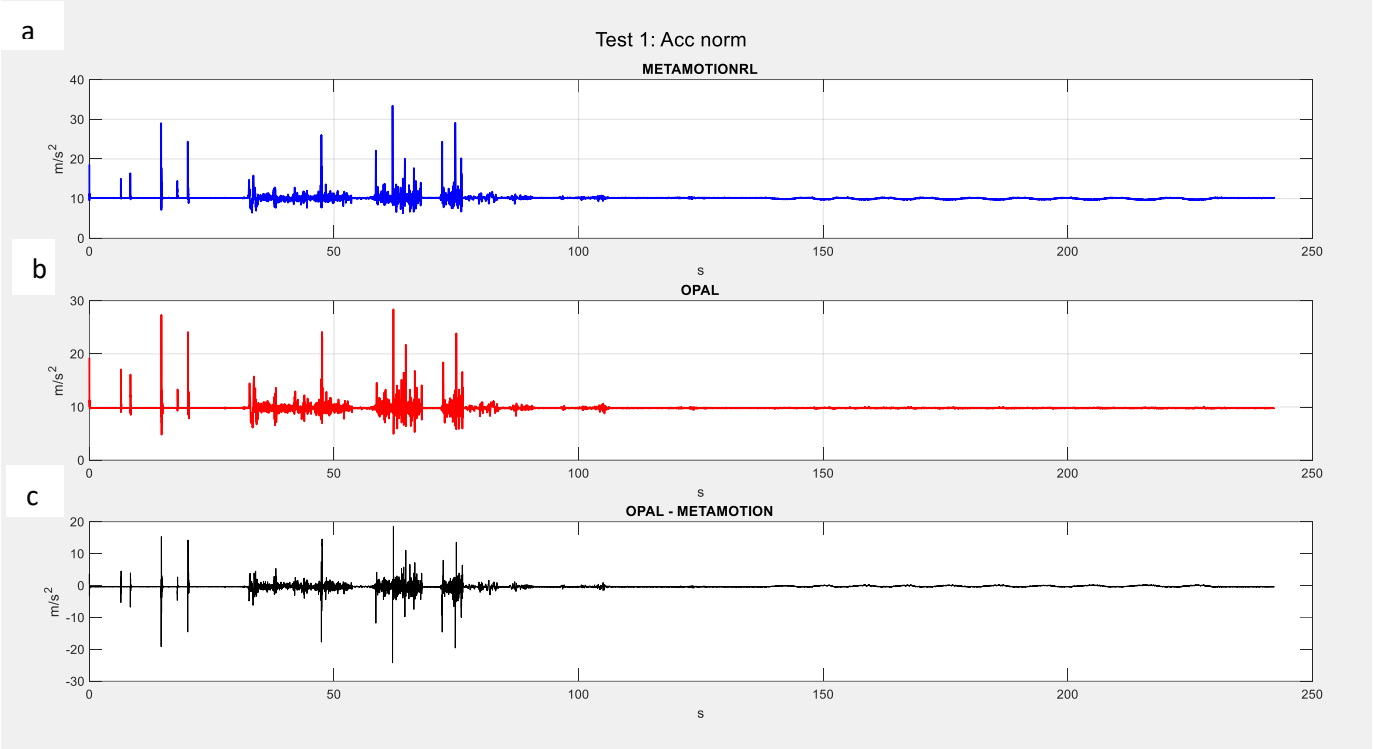

Figure 73Part a, acceleration graph of MetaMotionRL sensor; part B, acceleration graph of Opal sensor; part c, difference between the two previously defined signals.

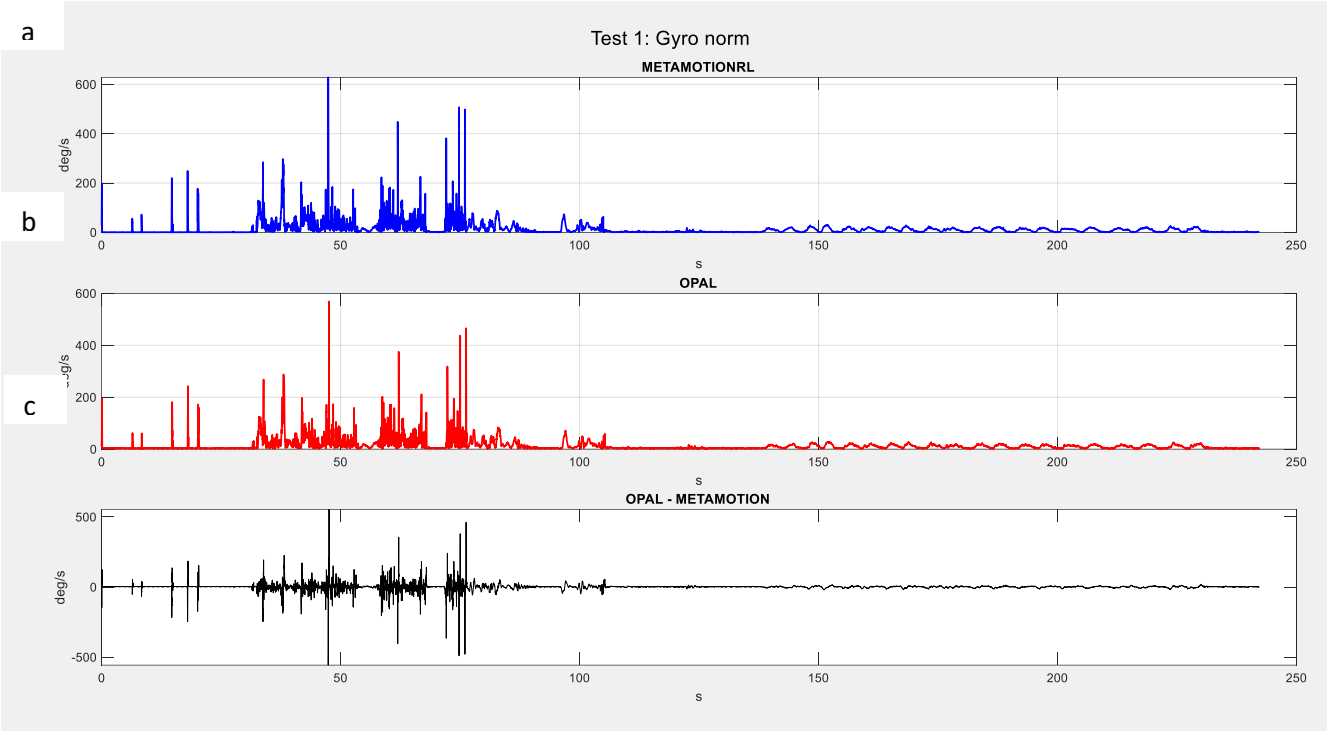

Figure 74 Part a, gyroscope graph of MetaMotionRL sensor; part B, gyroscope graph of Opal sensor; part c, difference between the two previously defined signals.

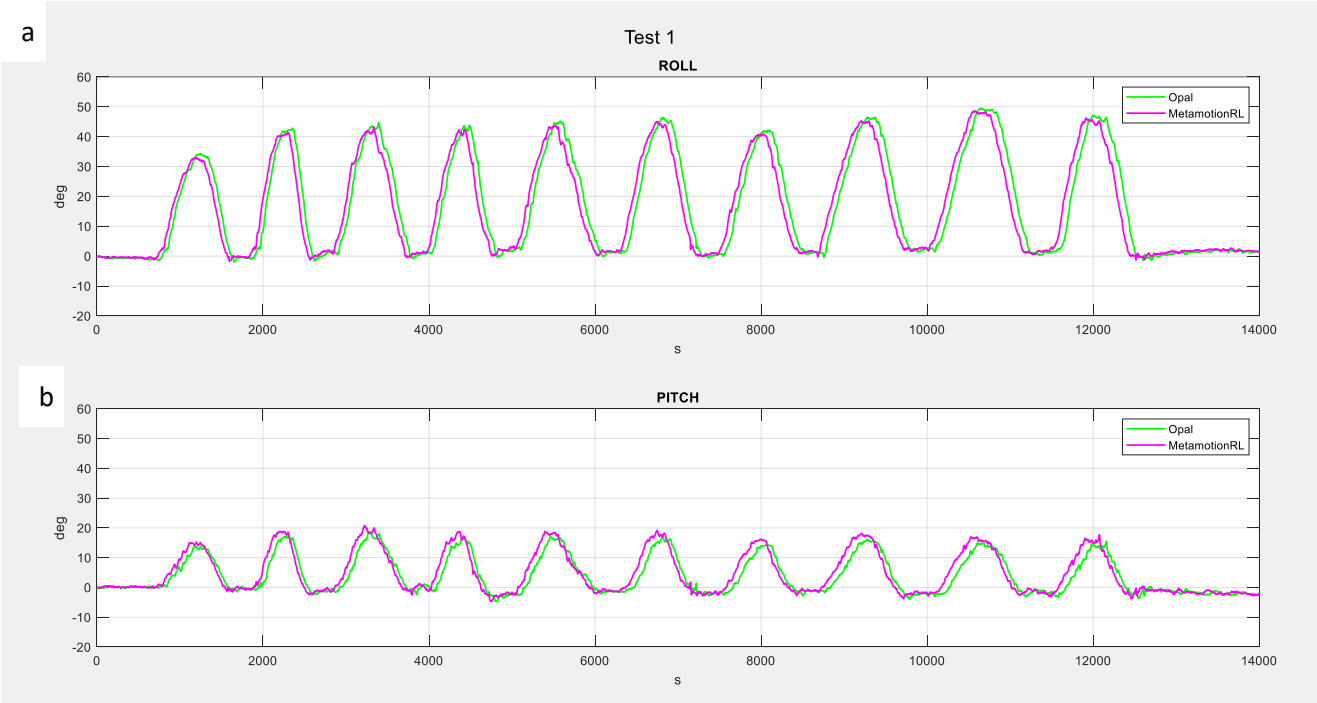

Figure 75 Part a represents the roll angle, part b the pitch angle. The two signals obtained by the two sensors have been superimposed to compare the values.

In test two between the two IMU sensors, they were kept together and were left stationary on the table for 5 minutes.

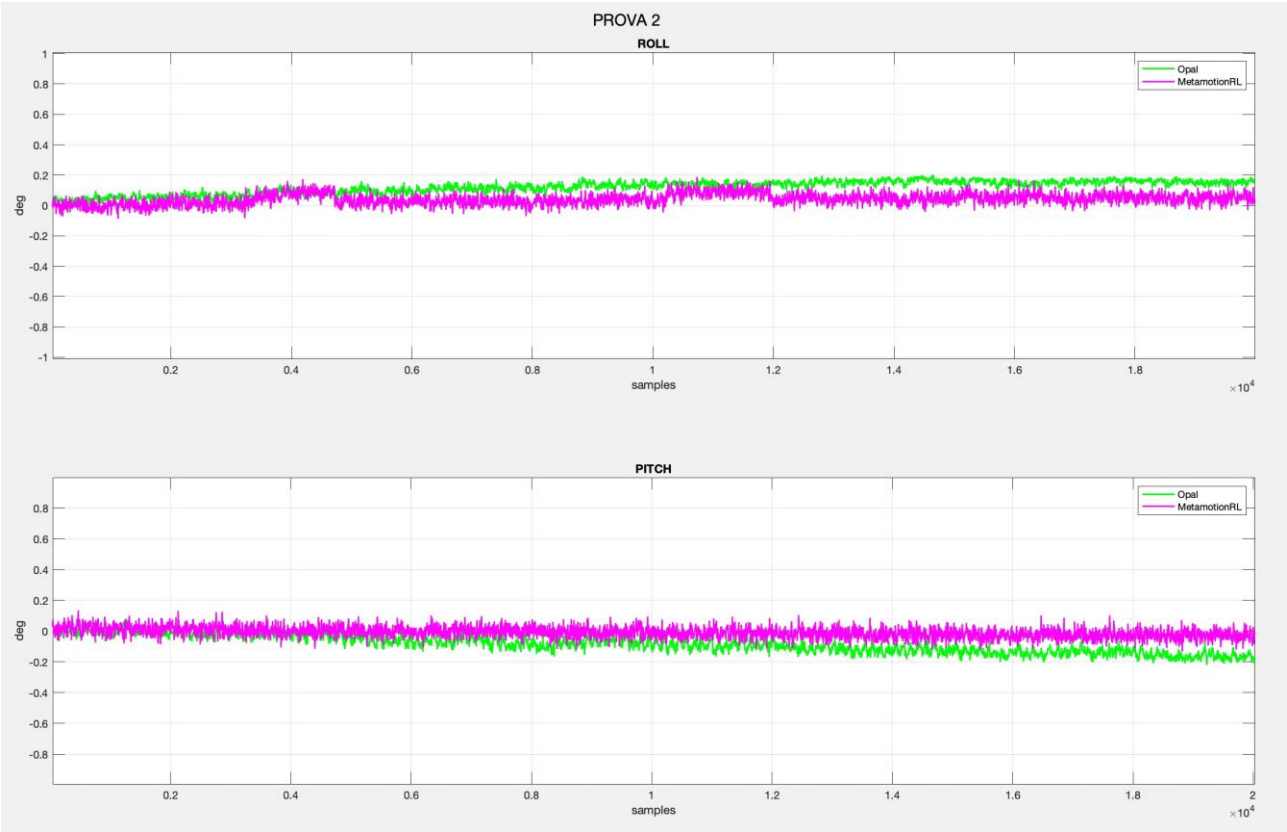

Figure 76 Static registration acquisition.

The last test is symmetrical to the first one, the Opal 601 and MetaMotionRL sensors are stick together, one above the other, and placed on the left shoulder. However, the bending is performed to the left direction.

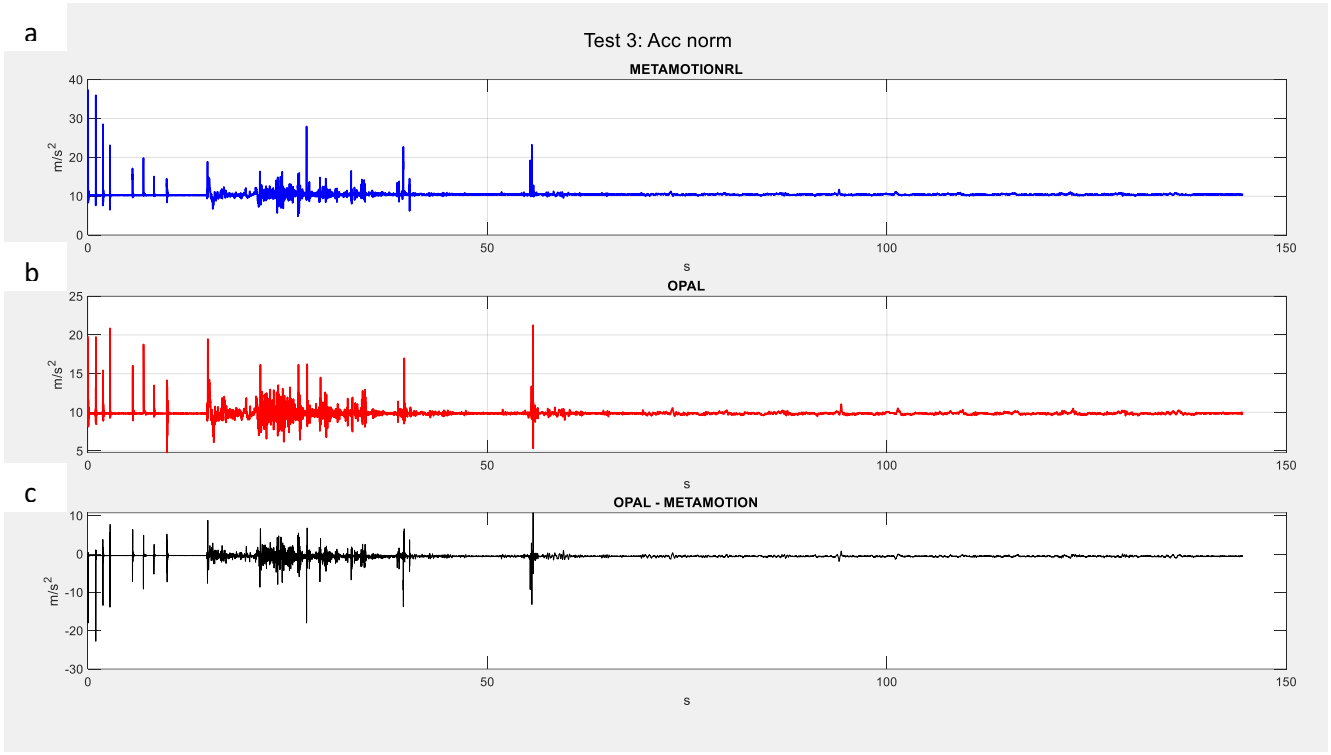

Figure 77 Part a, acceleration graph of MetaMotionRL sensor; part B, acceleration graph of Opal sensor; part c, difference between the two previously defined signals.

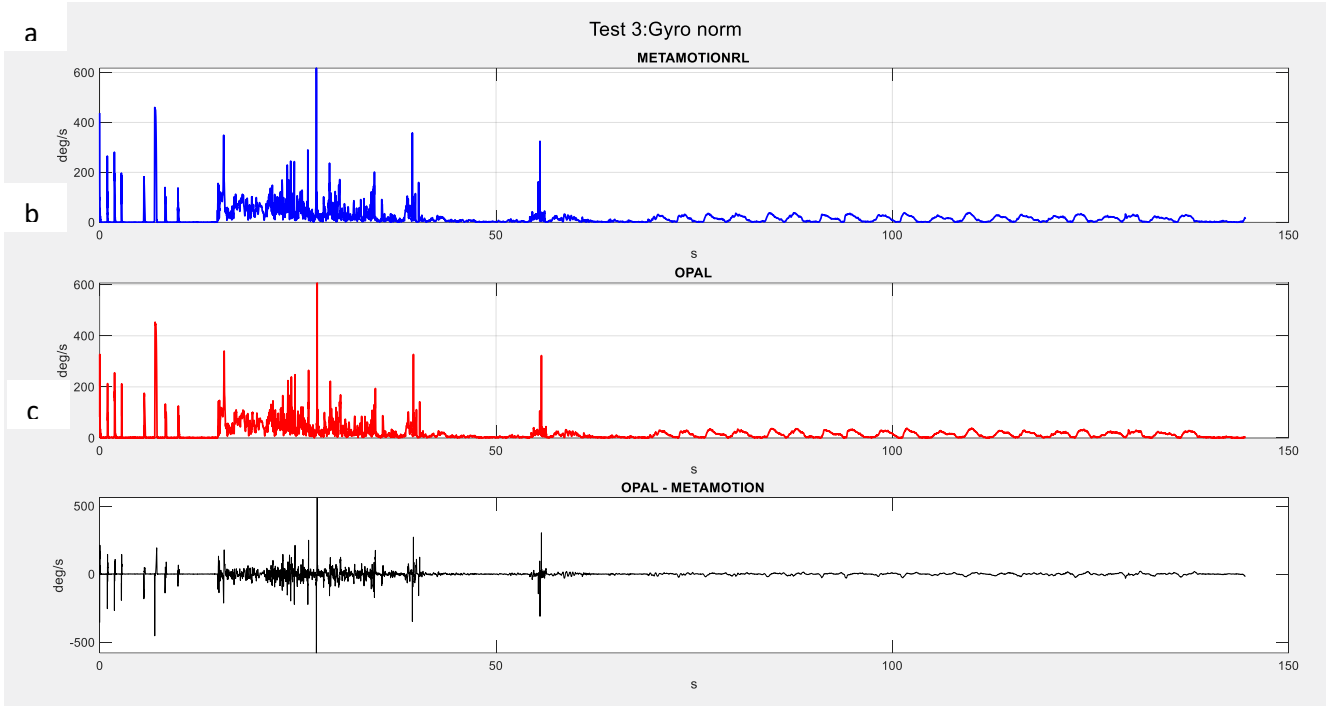

Figure 78 Part a, gyroscope graph of MetaMotionRL sensor; part B, gyroscope graph of Opal sensor; part c, difference between the two previously defined signals

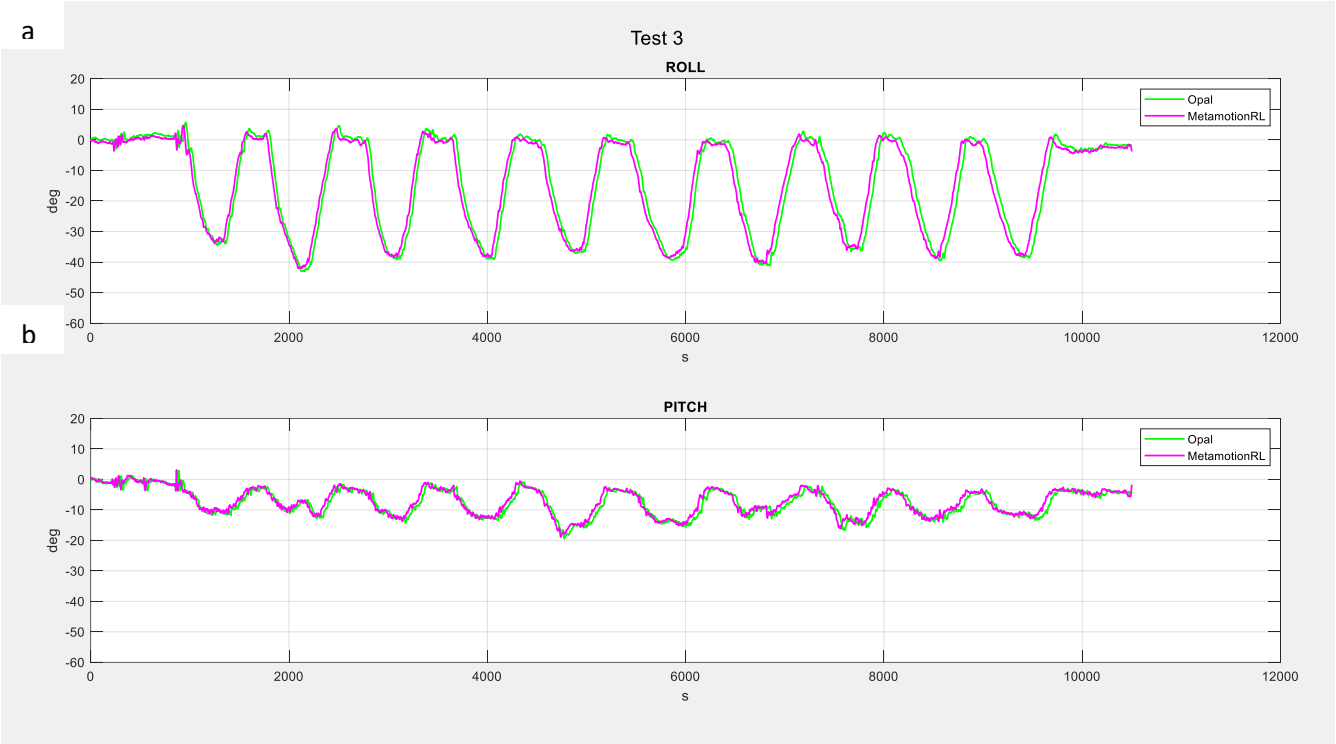

Figure 79 Part a represents the roll angle, part b the pitch angle. The two signals obtained by the two sensors have been superimposed to compare the values.

Test	Inclination	Sensor's position	Norm Acc (m/s^2)	Norm Gyro (deg/s)	Roll	Pitch
1	Right	Left	0.7398	22.3048	5.6699	2.7146
2	-	-	0.5042	17.7823	0.0960	0.1288
3	Left	Left	0.8831	22.0541	4.1169	1.4939

Table 9 Diagram of Static Tests based on sensor position and root mean square.

The results from the Root Mean Square Error (RMSE) analysis represent the discrepancies in the signals acquired between the two sensors, Opal and MetaMotion. It is possible to notice a certain phase shift, as also observable from the figures presented. This discrepancy could be attributed to the synchronization method adopted between the two sensors.

CHAPTER 4 - CONCLUSION AND FUTURE DEVELOPMENT

For this thesis project, an internship was carried out at the Bellaria Hospital for the clinical evaluation of Parkinson's using inertial wearable devices, which are becoming increasingly important and used in clinical and rehabilitation settings.

This thesis was aimed at analysing the posture of Parkinson's patients during pre-DBS monitoring. The signals collected by wearable sensors were examined to compare the motor parameters of interest. The study involved 45 patients who performed the motor activities of monitoring at the Bellaria Hospital in Bologna. Among the different activities, the Quiet Standing task has been of particular interest for this research. This test allows to analyse the Sway, that is the characteristic oscillations of the syndrome itself. The test was performed under two conditions: MED OFF (before taking Levodopa) and MED ON (60-75 minutes after taking Levodopa), both with open and closed eyes. In the first analysis, we focused on the difference between the two conditions under which the test was performed, conducting a statistical analysis. An increasing trend of the Sway in the MED ON condition was shown, in agreement with literature indicating an increase in Sway after drug therapy.

Secondly, in collaboration with Chiara Pirini (master student), the PASSO project was considered. For this purpose, a prototype of a posture rehabilitation device has been developed for people with PISA syndrome and camptocormia. Compared to the PASSO project, two components have been modified: the smartwatch has been replaced with the IMU MetaMotionRL sensor and making changes to the design of the band that houses the sensor. In order to evaluate and analyse the inclinations that the group of subjects analysed should perform, an algorithm based on a complementary filter has been implemented. Tests were carried out to evaluate the validity of this algorithm, comparing data from Opal sensors with Stereophotogrammetry and then with Opal-MetaMotion.

Different sensor positions were evaluated to determine the most effective signal acquisition during flexion. It is important to remember that the sensor should be placed on the side opposite to the subject's involuntary inclination, to guide the patient in making the corrective movement. A possible solution would be to place the sensor on the same side of the subject's tilt for more accurate data and transmit vibration feedback on the opposite side to facilitate corrective movement.

However, the results suggest that acquiring with the sensor positioned on the same side of the inclination leads to enhanced accuracy. In addition, the implemented algorithm presents a deviation from the data acquired by the Gold Standard. In future research, the complementary algorithm can be improved to produce more accurate results with less deviation from the gold standard. This can be achieved by optimizing the parameters of the complementary filter performing further acquisition.

The prototype has been tested on three subjects. To assess the tester's perceptions, a questionnaire was distributed to them to investigate some crucial aspects of the system, such as vibration intensity and design comfort.

The questionnaire's results indicated a good level of satisfaction from the subjects. They expressed the intention to use the device for a home rehabilitation, at least 3 times a week, with 30-minute sessions. The band was considered comfortable. However, some points to improve emerged:

1. Calibration shall be refined and customized for each subject to ensure specific training and avoid false vibration signals caused by incorrect calibration settings, or on the contrary do not have any feedback signal during incorrect posture.
2. Vibration is perceived effectively on bone prominences. For subjects with PISA syndrome, which requires the placement of the sensor on the acromial process, feedback was well perceived. However, vibration was not sufficiently felt in the dorsal region between the two shoulder blades and was associated with a noise. In order to solve this problem, it might be useful to consider alternative solutions, such as the use of two sensors on the shoulder blades or the design of a new sensor case that ensures optimal vibration transmission.
3. For subjects with other pathologies (e.g., scoliosis), to adapt the rehabilitation context, it may be necessary to acquire bands that allow the position of the sensor in different positions for training aimed at specific individual needs.

The prototype demonstrates a potential for rehabilitation. Initially, it will be utilized in the clinical environment to identify any issues and define any necessary improvements. In the future, it could be extended as a home training rehabilitation. A companion of one of the subjects commented: "This system does what I do, that is to note that the shoulder is too low".

This thesis work provides several suggestions for future developments and improvements. For the rehabilitation prototype proposed in the context of the PASSO project, we could consider the implementation of a more advanced graphical interface that allows the users to have their own rehabilitation training program. This may include the ability to perform specific exercises according

to the patient's needs. The interface could also offer the examination of the patient's weekly or monthly progress.

In addition, further improvements could be made to ensure a better perception of the feedback provided in upper back and to identify other locations where the patient can receive this signal efficiently. It has been observed that the prototype has the potential to assist not only patients with PISA syndrome and camptocormia, but also individuals with other pathologies. However, to implement this, an assessment of sensor placement and further evaluation would be necessary.

Bibliography

[1] J. S. Hawley, M. J. Armstrong e W. J. Weiner, Parkinson's Disase: Improving Patient Care, Oxford University Press.

[2] «SanRaffaele.it,» [Online]. Available: https://www.sanraffaele.it/comunicazione/SRpedia/11746/parkinson-dietro-ogni-scoperta-si-cela-un-grande-uomo.

[3] A. Kouli, K. M. Torsney e W.-L. Kuan, «Parkinson's Disease: Etiology, Neuropathology, and Pathogenesis,» 2018.

[4] C. Punin, B. Barzallo e R. Clotet, «A Non-Invasive Medical Device for Parkinson's Patients with Episodes of Freezing of Gait,» *Sensors,* 2019.

[5] A. Samà, C. Pèrez-Lopez e J. Romagosa, «Dyskinesia and motor state detection in Parkinson's Disease patients with a single movement sensor,» 2012.

[6] Z. Ou, J. Pan, S. Tang, D. Duan, D. Yu, H. Nong e Z. Wang, «Global Trends in the Incidence, Prevalence, and Years Lived With Disability of Parkinson's Disease in 204 Countries/Territories From 1990 to 2019,» *Front Public Health,* 2021.

[7] E. Ray e B. R. Bloem, «The Parkinson Pandemic—A Call to Action,» *JAMA Neurology,* 2018.

[8] «Thrive Parkinsons,» [Online]. Available: https://pd-thrive.com/.

[9] J. Jankovic, «Parkinson's disease: clinical features and diagnosis».*BMJ Journals.*

[10] [Online]. Available: https://wemedhealth.com/treatments-programs/parkinsons-disease/.

[11] A. Samii, J. G. Nutt e B. R. Ransom, «Parkinson's disease,» *The Lancet,* 2004.

[12] S. Sveinbjornsdottir, «The clinical symptoms of Parkinson's disease,» *Journal of Neurochemistry,* 2016.

[13] T. Arruda, A. Aquino e L. Medeiros, «Pisa Syndrome and Camptocormia in Parkinson´s Disease: clinical and funcional characterization,» *Revista Neurociências.*

[14] P. Barone, G. Santangelo e M. Amboni, «Pisa syndrome in Parkinson's disease and parkinsonism: clinical features, pathophysiology, and treatment,» *The Lancet,* 2016.

[15] H. Akiyama, S. Nukui e M. Akamatu, «Effectiveness of spinal cord stimulation for painful camptocormia with Pisa syndrome in Parkinson's disease: a case report,» *BMC Neurology,* 2017.

[16] «Cleveland Clinic,» [Online]. Available: https://my.clevelandclinic.org/health/diseases/8525-parkinsons-disease-an-overview.

[17] M. T. Hayes, «Parkinson's Disease and Parkinsonism,» *The American Journal of Medicine,* 2019.

[18] F. Haddad, M. Sawalha e Y. Khawaja, «Dopamine and Levodopa Prodrugs for the Treatment of Parkinson's Disease,» *Journals,* 2017.

[19] [Online]. Available: https://www.stepwards.com/?page_id=7567.

[20] O. Rascol e D. J. Brooks,, «A Five-Year Study of the Incidence of Dyskinesia in Patients with Early Parkinson's Disease Who Were Treated with Ropinirole or Levodopa,» *The new England journal of medicine,* 2000.

[21] A. Giannoni, *Evaluation of the effects of Deep Brain Stimulation in people with Parkinson's Disease analyzing Local Field Potentials and inertial signals,* 2023.

[22] S. Della Seta, *Local field potentials in deep brain stimulation for Parkinson's disease: assessment of the effects of the intervention and relation with inertial signals,* 2023.

[23] L. D. Wood, «Clinical Review and Treatment of Select Adverse Effects of Dopamine Receptor Agonists in Parkinson's Disease,» *Drugs & Aging.*

[24] J. Nutt, «Effect of COMT inhibition on the pharmacokinetics and pharmacodynamics of levodopa in parkinsonian patients.,» *Neurology,* 2000.

[25] J. Jankovic e M. Stacy, «Medical Management of Levodopa-Associated Motor Complications in Patients with Parkinson's Disease,» *CNS Drugs,* 2007.

[26] G. Galeoto, A. Berardi, F. Colalelli e E. Pelosin, «Correlation between Quality of Life and severity of Parkin-son's Disease by assessing an optimal cut-off point on the Parkinson's Disease questionnaire (PDQ-39) as related to the Hoehn & Yahr (H&Y) scale,» 2022.

[27] «Parkinson's europe,» [Online]. Available: https://www.parkinsonseurope.org/about-parkinsons/symptoms/rating-scales/.

[28] R. B. Postuma, W. Poewe e I. Litvan, «Validation of the MDS clinical diagnostic criteria for Parkinson's disease,» *Movement Disorders,* 2018.

[29] A. Balakrishnan, M. Jeevan, K. Pramod e M. Natarajan, «Role of Wearable Sensors with Machine Learning Approaches in Gait Analysis for Parkinson's Disease Assessment: A Review,» *Engineered Science,* 2022.

[30] M. Hoehn e M. Yahr, «Parkinsonism: onset, progression and mortality,» *Neurology,* 1967.

[31] P. Toro, V. Correa e A. Vergara, «Nonlinear dynamics and Poincaré sections to model gait impairments in different stages of Parkinson's disease,» *Dordrecht,* 2020.

[32] S. A. Factor e W. J. Weiner, Rating Scales in Parkinson's Disease: Clinical Practice and Research, 2008.

[33] C. Goetz, S. Fahn, P. Martinez-Martin e W. Poewe, «Movement Disorder Society-sponsored revision of the Unified Parkinson's Disease Rating Scale (MDS-UPDRS): Process, format, and clinimetric testing plan,» *Movement Disorders,* 2007.

[34] A. Balakrishnan e J. Medikonda, «Eng. Sci., 2022, 19, 5–19 © Engineered Science Publisher LLC 2022 Eng.Role of Wearable Sensors with Machine Learning Approaches in Gait Analysis for Parkinson's Disease Assessment,» *Engineered Science,* 2022.

[35] S. A. Factor e W. J. Weiner, Parkinson's DIsease: diagnosis and clinical management.

[36] R. Romijnders, E. Warmerdam e C. Hansen, «Validation of IMU-based gait event detection during curved walking and turning in older adults and Parkinson's Disease patients,» *Journal of NeuroEngineering and Rehabilitation,* 2021.

[37] R. Begg e M. Palaniswami, «Computational Intelligence for Movement Sciences: Neural Networks and Other Emerging Techinques,» Idea Group Publishing, 2006.

[38] V. Tsakanikas, A. Ntanis e G. Rigas, «Evaluating Gait Impairment in Parkinson's Disease from Instrumented Insole and IMU Sensor Data,» *Sensors,* 2023.

[39] «MathWorks,» [Online].

[40] D.Roetenberg, «Inertial and Magnetic Sensing of Human Motion,» 2006.

[41] B. Milosevic, A. Leardini e E. Farella, «Kinect and wearable inertial sensors for motor rehabilitation programs at home: state of the art and an experimental comparison,» *BioMedical Engineering OnLine,* 2020.

[42] C. Lorenzo, *Course note of "Ageing and Rehabilitation engineering",* 2022.

[43] M. Picardi, V. Redaelli, P. Antoniotti e G. Pintavalle, «Turning and sit-to-walk measures from the instrumented Timed Up and Go test return valid and responsive measures of dynamic balance in Parkinson's disease,» *Clinical Biomechanics,* 2020.

[44] L. Palmerini, S. Mellone, G. Avanzolini, F. Valzania e L. Chiari , «Quantification of Motor Impairment in Parkinson's Disease Using an Instrumented Timed Up and Go Test,» *Journala & Magazine.*

[45] A. Capozzo, U. Della Croce, A. Leardini e L. Chiari, «Human movement analysis using stereophotogrammetry: Part 1: theoretical background».

[46] L. Wade, L. Needham, P. McGuigan e J. Bilzon, «Applications and limitations of current markerless motion capture methods for clinical gait biomechanics,» *SPORTS MEDICINE AND REHABILITATION,* 2022.

[47] L. Mündermann, S. Corazza e T. P. Andriacchi , «The Evolution of Methods For the Capture of Human Movement Leading to Markerless Motion Capture for Biomechanical Applications,» *Journal of NeuroEngineering and Rehabilitation volume,* 2006.

[48] A. Menache, Understanding Motion Capture for Computer Animation and Video Games, Morgan Kaufmann.

[49] L. M. Galantucci, F. Lavecchia e G. Percoco, «A simple photogrammetric system for automatic capture and measurement of facial soft tissues during movement,» in *Innovative Development in Design and Manufacturing*, 2010.

[50] R. Begg, *Computational Intelligence for Movement Sciences: Neural Networks and Other Emerging Techniques,* Idea Group Pub, 2006.

[51] H. Luige, «Inertial Sensing of Human Movement,» 2002.

[52] K. Culhane, M. O'Connor, D. Lyons e G. Lyons, «Accelerometers in rehabilitation medicine for older adults,» *Age and Ageing,* 2005.

[53] L. Palmerini, *Course note of Laboratory of Wearable Sensor and Mobile Health,* 2022/2023.

[54] E. Magosso, *Note of course "Biomedical Instrumentation",* 2021.

[55] F. Aprea , *Tesi di laurea "Analisi del cammino e della corsa con stampelle in soggetti amputati tramite sensori inerziali",* 2015.

[56] M. J. Mathie, A. C. F. Coster, N. H. Lovell e B. G. Celler, «Accelerometry: providing an integrated, pratical method for long-term, ambulatory monitoring of human movement,» *Institute of Physics Publishing,* 2004.

[57] A. Colombo, *Sistema inerziale indossabile upper body per l'ergonomia fisica: analisi e validazione,* 2020.

[58] D. Borra, *Analisi del cammino in acqua tramite sensori inerziali: accuratezza strumentale e fasce di normalità,* 2013-2014.

[59] [Online]. Available: https://www.lboro.ac.uk/microsites/mechman/research/ipm-ktn/pdf/Technology_review/an-introduction-to-mems.pdf.

[60] S. B. Mbarek, . N. Alcheikh e H. M. Ouakad, «Highly sensitive low field Lorentz-force MEMS magnetometer,» *Scientific report,* 2021.

[61] M. Contin, G. Lopane e L. Belotti, «Sex Is the Main Determinant of Levodopa Clinical Pharmacokinetics: Evidence from a Large Series of Levodopa Therapeutic Monitoring,» *Journal of Parkinson's Disease,* 2022.

[62] N. Akram, H. Li, A. Ben-Joseph e C. Budu, «Developing and assessing a new web-based tapping test for measuring distal movement in Parkinson's disease: a Distal Finger Tapping test,» *Scientific reports,* 2022.

[63] G. F. Moretto, F. B. Santinelli e T. Penedo, «Prolonged Standing Task Affects,» *Neurorehabilitation and,* 2021.

[64] J. Spildooren, S. Vercruysse e K. Desloovere, «Freezing of gait in Parkinson's disease: The impact of dual-tasking and turning,» 2010.

[65] A. Ferrari, D. Miletti, P. Palumbo e G. Giannini, «Gait apraxia evaluation in normal pressure hydrocephalus using inertial sensors. Clinical correlates, ventriculoperitoneal shunt outcomes, and tap-test predictive capacity,» *Fluids and Barriers of the CN,* 2022.

[66] M. E. Gago, V. Fernandes, J. Ferreira e H. Silva, «The effect of levodopa on postural stability evaluated by wearable inertial measurement units for idiopathic and vascular Parkinson's disease,» *Gait & Posture,* 2014.

[67] M. Contini, R. Riva e A. Baruzzi, «Postural Stability in Parkinson's Disease: the effects of disease severity and acute levodopa dosing,» *Elsevier,* 1995.

[68] L. Neri e G. e. a. Adorante, «Postural Rehabilitation through Kinect-Based Biofeedback,» *Proceedings of the IEEE.*

[69] B. Yu, M. Funk e e. al, «Biofeedback for Everyday Stress Management: A Systematic Review,» *Frontiers in ICT,* 2018.

[70] T. Bowman, E. Gervasoni, C. Arienti e e. al., «Wearable Devices for Biofeedback Rehabilitation: A Systematic Review and Meta-Analysis to Design Application Rules and Estimate the Effectiveness on Balance and Gait Outcomes in Neurological Diseases,» *Sensors,* 2021.

[71] T. Lu, S. Ji, W. Jin e Q. Yang, «Biocompatible and Long-Term Monitoring Strategies of Wearable, Ingestible and Implantable Biosensors: Reform the Next Generation Healthcare,» *Sensors,* 2023.

[72] A. Santoro, E. Mancini e E. Ferramosca, «I SISTEMI DI CONTROLLO AUTOMATICO E LE LORO APPLICAZIONI,» *Giornale Italiano di Nefrologia,* 2007.

[73] E. L. Petancevski, J. Inns, J. Fransen e F. M. Impellizeri, «The effect of augmented feedback on the performance and learning of gross motor and sport-specific skills: A systematic review,» *Psychology of Sport and Excercise,* 2022.

[74] M. R. Afzal, M.-K. Oh e C.-H. Lee, «A Portable Gait Asymmetry Rehabilitation System for Individuals with Stroke Using a Vibrotactile Feedback,» *BioMed Research International,* 2015.

[75] O. Alvarado Cando, K. Robles Hidalgo e B. Chacòn Palacios, «A low-cost vibratory stimulus system to mitigate freezing of gait in Parkinson's disease,» 2016.

[76] S. Prasanna, J. D'Abbraccio e M. Filosa, «Uneven Terrain Recognition Using Neuromorphic Haptic Feedback,» *Sensors,* 2023.

[77] C. Punin, B. Barzallo e M. Huerta, «Wireless devices to restart walking during an episode of FOG on patients with Parkinson's disease,» 2018.

[78] B.-C. Lee, A. Fung e T. A. Thrasher, «The Effects of Coding Schemes on Vibrotactile Biofeedback for Dynamic Balance Training in Parkinson’s Disease and Healthy Elderly Individuals,» *IEEE.*

[79] P. Ginis, A. Nieuwboer, M. Dorfman e L. Chiari , «Feasibility and effects of home-based smartphone-delivered automated feedback training for gait in people with Parkinson's disease: A pilot randomized controlled trial,» *Parkinsonism and Related Disorders.*

[80] D. Rodriguez-Martìn, C. Pèrez-Lopez e A. Samà , «A Waist-Worn Inertial Measurement Unit for Long-Term Monitoring of Parkinson’s Disease Patients,» *Sensors,* 2017.

[81] A. Triantafyllou, G. Papagiannis e S. Stasi, «Application of Wearable Sensors Technology for Lumbar Spine Kinematic Measurements during Daily Activities following Microdiscectomy Due to Severe Sciatica,» 2022.

[82] «Movella,» [Online]. Available: https://www.movella.com/resources/cases/valedo-back-pain-therapy-xsens-technology.

[83] «Postura corretta,» [Online]. Available: https://posturacorrettablog.it/upright-go-2-opinioni/.

[84] V. Wegen, C. de Goede e G. Kwakkel, «Sensor assisted self-management in Parkinson's disease: A feasibility study of ambulatory posture detection and feedback to treat stooped posture,» *Elsevier,* 2023.

[85] C. Zong-Hao Ma e D. e. a. Wai-Chi Wong, «Balance Improvement Effects of Biofeedback Systems with State-of-the-Art Wearable Sensors: A Systematic Review,» *Sensors,* 2016.

[86] S. Imbesi, M. Corzani, G. Lopane, G. Mincolelli e L. Chiari , «User-Centered Design Methodologies for the Prototype Development of a Smart Harness and Related System to Provide Haptic Cues to Persons with Parkinson's Disease,» *Sensors,* 2022.

[87] «Mbientlab,» [Online]. Available: https://mbientlab.com/metamotions/.

[88] M. Caruso, S. Angelo Maria e D. Laidig, «Analysis of the Accuracy of Ten Algorithms for Orientation Estimation Using Inertial and Magnetic Sensing under Optimal Conditions: One Size Does Not Fit All,» *Sensors,* 2021.

[89] S. Yutong, Z. Yongbo e L. Zhonghan, «IMU/UWB Fusion Method Using a Complementary Filter and a Kalman Filter for Hybrid Upper Limb Motion Estimation,» *Sensors,* 2023.

[90] «Robottini, Little robots,» [Online]. Available: https://robottini.altervista.org/.

[91] M. Benoussaad, B. Sijobert, K. Mombaur e C. Azevedo Coste, «Robust Foot Clearance Estimation Based on the Integration of Foot-Mounted IMU Acceleration Data,» *Sensors,* 2016.

[92] F. Silveri, *Sviluppo di algoritmi di data fusion per piattaforme inerziali basati su filtri complementari,* 2018/2019.

[93] M. Bartolo, M. Serrao e C. Tassorelli, «Four-Week Trunk-Specific Rehabilitation Treatment Improves Lateral Trunk Flexion in Parkinson's disease,» *Movement Disorders,* 2010.

[94] [Online]. Available: https://www.biolegend.com/fr-ch/parkinsons-disease.

[95] A. Kos, A. Umek e e. al, «Suitability of Smartphone Inertial Sensors for Real-Time Biofeedback Applications,» *Sensors,* 2016.

[96]

[97] O. M. Giggins, U. McCarthy Persson e B. Caulfield, *Biofeedback in rehabilitation,* 2013.

[98] P. Toro, V. Correa e A. Vergara, «Nonlinear dynamics and Poincaré sections to model gait impairments in different stages of Parkinson's disease,» *Dordrecht,* 2020.

[99] C. Punin, B. Barzallo e M. Huerta, «Wireless devices to restart walking during an episode of FOG on patients with Parkinson's disease,» *IEEE.*

[100] T. Bao, W. J. Carender e C. Kinnaird, «Effects of long-term balance training with vibrotactile sensory augmentation among community-dwelling healthy older adults: a randomized preliminary study,» *Journal of NeuroEngineering and Rehabilitation,* 2018.

[101] C. M. Lind, J. A. Diaz-Olivares, K. Lindecrantz e J. Eklund, «A Wearable Sensor System for Physical Ergonomics Interventions Using Haptic Feedback,» *Sensors,* 2020.

[102] S. Prasana, J. D'Abbraccio e M. Filosa, «Uneven Terrain Recognition Using Neuromorphic Haptic Feedback,» *Sensors,* 2023.

[103] M. Liu, Y. Cai, L. Zhang e Y. Wang, «Attitude Estimation Algorithm of Portable Mobile Robot Based on Complementary Filter,» *Micromachines,* 2021.